ALMA MATER STUDIORUM UNIVERSITÀ DI BOLOGNA

SCUOLA DI SCIENZE

Corso di Laurea Magistrale in Analisi e Gestione dell'Ambiente

Analysis of chemical degradation of caffeine in aqueous solution using an advanced oxidation process: Fenton's reagent and UV radiation

Tesi di Laurea in Chimica Fisica

Relatore

Prof. Alberto Modelli

Presentata da

Irene Coralli

Correlatore

Prof.ssa Natalia Villota Salazar

Sessione unica

Anno Accademico 2017/2018

RINGRAZIAMENTI

Primo fra tutti, vorrei ringraziare il relatore di questa tesi, il prof. Alberto Modelli, il quale ha accettato di prendere parte ad un progetto avviato sotto un'altra supervisione e con numerosi problemi. Lo ringrazio per la volontà e l'impegno spesi per inserirsi in una tematica nuova e per il tempo dedicatomi fin dall'inizio. Non è stato solo una guida, ma anche un punto di riferimento nei miei anni universitari, durante le lezioni, il periodo di Erasmus e la preparazione della tesi.

Come altri collaboratori allo studio, ringrazio la prof.ssa Natalia Villota Salazar, correlatrice della tesi, che mi ha permesso di cominciare questo progetto, la Facoltà di Ingegneria di Vitoria Gasteiz (UPV/EHU) che ha messo a disposizione i laboratori e tutti i professori e ragazzi (in particolare Maite) che mi hanno aiutato, nonostante non fossero coinvolti. Inoltre, vorrei ringraziare il prof. Bergamini, per la sua disponibilità in termini di tempo, strumenti e conoscenze e il Dipartimento di Chimica dell'Università di Bologna.

Ringrazio i miei genitori, per avermi trasmesso l'entusiasmo e la tenacia di battermi per ottenere ciò che voglio e per il loro continuo sostegno alle mie scelte. Ringrazio i miei fratelli, Marta che è la mia più grande ispirazione e Federico che, a modo suo, ha sempre creduto in me.

Ringrazio Andrea, perché ha rispettato le mie decisioni, supportandomi nonostante le mie idee contrastassero le sue e perché ha condiviso soddisfazioni e preoccupazioni, esaltando ogni traguardo e prendendosi cura dei miei momenti bui.

Grazie a tutti i miei amici per avermi alleggerito il carico, in un modo o in un altro, portando un po' di aria pulita nelle mie giornate nere. In particolare, grazie a Federica e Valentina perché da quasi tutta la vita mi sono vicine e, nonostante le nostre strade siano un po' diverse, sono un mio punto fermo.

Grazie anche alle persone che ho conosciuto durante questo percorso, i compagni di Erasmus che hanno reso ineguagliabile l'esperienza che più mi ha formato nella vita e i miei colleghi di corso. Soprattutto ringrazio Giuliana per le nostre colazioni o le chiacchierate fino alle 5 di mattina e Federico, Piero, Marco, Matteo, Enrico, Gianluca per aver condiviso alti e bassi di questi anni.

CONTENTS

ABSTRACT

The present study is aimed to analyse the degradation of caffeine in water employing an advanced oxidation process, the photo-Fenton reaction ($H_2O_2/Fe^{2+}/UV$). Different concentrations of H_2O_2 and Fe^{2+} are used to evaluate the effects of the two reagents on the quality of the water after the reaction and on the kinetics of degradation. The quality of the water is estimated in terms of conductivity, turbidity, colour and aromaticity. These quantities were found to be not dependent on H_2O_2 concentrations, whereas the Fe^{2+} concentration affects them in a proportional way. Compared to the limits of European Directives, the resulting conductivity is acceptable. Turbidity and colour exceed the limits, and the observed influence of the catalyst suggests that they are due to iron species, not to reaction products. Finally, the method employed to evaluate the aromaticity, based on absorbance at 254 nm, does not seem to be reliable. The kinetics of degradation are elaborated through measurements of the absorbance at 272 nm as a function of time. The dependence of the reaction rate on H_2O_2 concentration observed here is small, but even the lowest concentration employed is 16 times larger than that of caffeine. When the H_2O_2 concentration is kept constant, a nearly direct proportionality results between reaction rates and Fe^{2+} doses. Further analyses have shown that caffeine can also be degraded only under UV-visible irradiation (no reagents), but the reaction would need a very long time (6% in 45 minutes). With the addition of Fe^{2+} (without H_2O_2) the reaction rate was found somewhat higher, while with the addition of only H_2O_2 (without Fe^{2+}) the photo-degradation rate was found to be 2/3 of that measured using both reagents. Therefore, the Fe^{2+} catalyst contributes to the degradation, but dissociation of the perossidic O-O bond of H_2O_2 to give $OH^{\bullet}$ radicals can also be directly caused by UV irradiation.

INTRODUCTION

Water is an essential natural resource for life, not only in terms of drinking water for human life, but for every life aspect, including, agricultural and industrial development [1]. Two important factors concern drinking water supply in future scenarios. The first is population growth and the second is connected to the inescapable effects that climate changes could produce: temperature increase, short rains, seasonal changes, etc. [2]. Over the last years, there has been a growing attention to the problem of water supply, and methods for water optimization and reuse have been developed [3].

Human civilizations always developed close to water courses, thus being the first cause of degradation of this habitat, due to water use, exploitation of aquatic animals, use of rivers for transports and dumping [1]. River ecosystems are highly vulnerable, river beds support constant material flows with rapid changes in weight and closed system, such as lake and ponds, have slow natural cycles to remove contaminants [4]. Water contamination is still one of the biggest problems in our current civilization [2]. Acid rains, wastewaters, pesticides used in agriculture, etc, flow into rivers. This is a big problem in both industrialised nations, due to the amount and the variety of contaminants produced, and in developing countries, due to inadequate technologies for water depuration and wastewater reuse [1]. As reported in the World Water Development Report (2017) actual technologies can eliminate only ≈20% of sewage production, so the remaining 80% is released untreated. “On average, high-income countries treat about 70% of the municipal and industrial wastewater they generate. That percentage drops to 38% in upper middle-income countries and to 28% in lower middle-income countries. In low-income countries, only 8% undergoes treatment of any kind” [5].

1. CONTAMINANTS OF EMERGING CONCERN

The diagram of Figure 1.1 shows the variety of environmental compartments impacted by human activities, how water pollution takes place or water quality alteration occurs. According to Figure 1.1, the principal source of pollutants which reach aquatic environments are wastewaters, which include wastes of urban, industrial, agricultural and cattle origin.

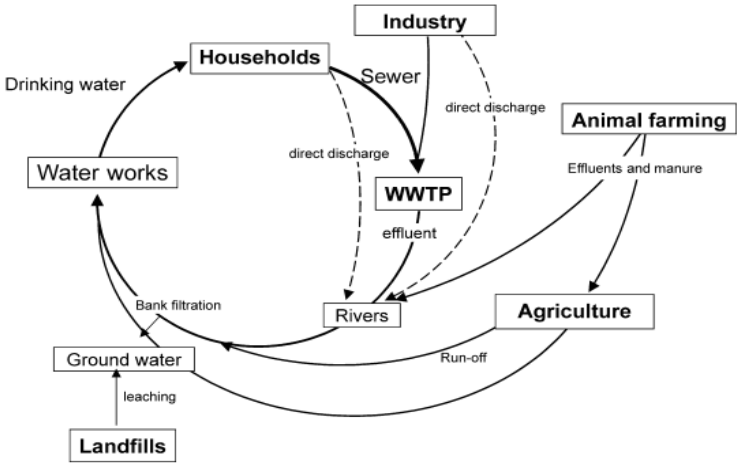

Figure 1.1. Components of a (partially) closed water cycle with indirect potable re-use [3]

Sometimes chemicals not previously detected (or found in far lesser concentrations) are discovered in a water supply [3]. These chemicals are known as "contaminants of emerging concern" (CECs) or simply "emerging contaminants". They are important because the risk they pose to human health and the environment is not yet fully understood [6]. CECs are increasingly being detected [7] at low levels in surface water, thus stimulating researches to get deeper insight into the impact that these compounds can have on organisms which benefit from water resources [8]. Investigations on CECs are therefore important for evaluating their potential impact on terrestrial and aquatic life and making decisions to prevent it [9]. CECs are chemicals designed to generate adverse or beneficial effects on living organisms (for instance: pesticides, pharmaceuticals, etc). These compounds are generally not degraded by the current processes for water depuration, so that they are reintroduced in the environment and act on different targets [10].

Many CECs are as called endocrine disruptors (EDCs) because they alter the normal functions of hormones, giving rise to a variety of health effects. EDCs can alter hormone levels leading to adverse effects on the reproductive apparatus of organisms which live in water or benefit from it [11]. Evaluation of these effects may require analytical methodologies not typical. Moreover, the concentration limits are not totally defined yet [12]. The effects on the reproductive apparatus seem to be significant even at low concentration levels. In addition, the effects caused on aquatic organisms during the early stages of life may not be observed until their adulthood. Therefore, traditional toxicity test may be not adequate for detection of these chemicals, and this family of chemicals may have modes of action which affect only specific types of animals [12].

Emerging contaminants are different compounds which are part of a wide group. The most important and dangerous features which make them part of this new group are listed below [3]:

- **Persistence:** CECs are continuously introduced in environment. That makes them considered as "pseudo-persistent" pollutants, which may be able to cause the same exposure potential as regulated persistent pollutants
- **Bioconcentration:** their affinity for organic matter is greater than that for water, so they can easily enter the organism
- **Bioaccumulation:** due to their persistence and bioconcentration, they tend to accumulate in organic matter
- **Biomagnification:** some of them can undergo biomagnification. This means that their concentration tends to increase through the feed chain
- **Toxicity:** CECs cause toxic effects (acute or chronic) on humans and/or animals
- **Mobility:** CECs can move among environmental compartments, thus fitting different cycles
- **Transformation:** some of them can transform into more dangerous substances

In the following paragraphs, the main CECs are classified and some information about them are provided.

1.1. Classification of contaminants of emerging concern

Among CECs, more importance must be given to the following groups:

- Flame retardants
- Chlorinated paraffins
- Pesticides
- Perfluorinated compounds
- Drugs
- Pharmaceutical products

1.1.1. Flame retardants

Flame retardants are chemical compounds widely used as additives to commercial and consumer products, such as plastics, textiles and surface coatings, due to their ability to prevent or slow down ignition. They are mainly used in electronic products to insulate components exposed to possible overheating and remain below flammability standards [13]. They are also used in polyurethane foam, in wires and cables, etc. Not all flame retardants present concerns, but halogenated and organophosphorus flame retardants often do [14]. Among these the most used are brominated flame retardants (BFRs), as shown in Figure 1.2. Due to the increasing usage of polymeric materials in construction and electronic equipment, the global market demand for BFRs continues to grow substantially; for example, the global market demand in 1990 was 145000 tonnes [15], and grew to over 310000 tonnes [16] in 2000, which represents a growth of over 100% [17].

In general, halogen substituents characterise the chemical reactivity and toxicity of a compound, their presence increases molecular lipid solubility and reduces molecular water solubility [18]. Both characteristics determine higher bio-accumulative behaviour. In addition, halogen substituents and their potential organohalide metabolites may increase the inherent toxicity of a compound. So BFRs are toxic (acute and chronic), persistent and bioaccumulate in the environment. Their presence has been observed in indoor and outdoor air and dust samples [19], in water [20], in soil and sediment and in sewage sludge [21]. Toxic and ecotoxic effects of some BRFs have been observed such as cytotoxicity, neurotoxicity, endocrine disruption, genotoxicity, mutagenicity, carcinogenicity

and teratogenicity [21]. It is important to highlight that despite these observations, information about BFRs is limited.

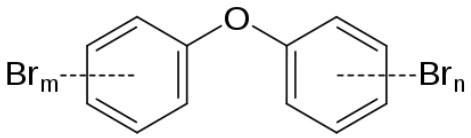

Figure 1.2. Brominated flame retardants structure

1.1.2. Chlorinated paraffins

Chlorinated paraffins (CPs) are complex mixtures of polychlorinated n-alkanes (see Figure 1.3), which can be divided into short-chain chlorinated paraffins (SCCPs), medium-chain chlorinated paraffins (MCCPs) and long-chain chlorinated paraffins (LCCPs) [22]. Chlorinated paraffins are insoluble in water or lower alcohols, can form emulsions or suspensions, but with low (<35%) chlorine contents are usually mobile liquids. Chlorinated paraffins with higher degrees (40–60%) of chlorination are viscous oils, while higher chlorination of n-paraffins results in a waxy solid with a glassy sheen [23].

About CPs consume, approximately 70 million pounds of chlorinated paraffins were produced in the U.S. in 1998 [24] and half of all CPs consumed in the U.S. are used as extreme-pressure lubricant additives in the metal working industry [25]. Chlorinated paraffins carcinogenicity on animals depends on chains length, but there are no data available from studies in humans [26].

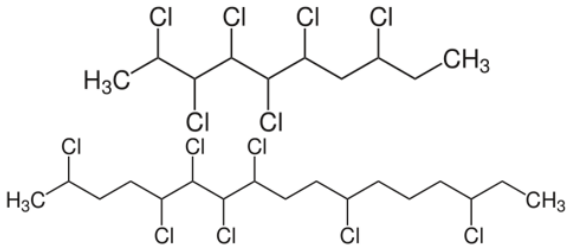

Figure 1.3. Structures of 2,3,4,5,6,8-hexachlorodecane (an SCCP) and 2,5,6,7,8,11,15-heptachloroheptadecane (an MCCP).

1.1.3. Pesticides

Pesticides are compounds which contain both “active” and “inert” ingredients: the former act to control the pests (destroy, repel, mitigate a pest, are plant regulators, defoliant, desiccant, or nitrogen stabilizers), the latter improve the product performance and usability [27]. Active ingredients determine severe environmental impacts. It has been estimated that less than 0.1% of the pesticide used in agricolture reaches the target pest [28]; the rest enters the environment and affects nontarget organisms. Pesticides are widely employed and their use lead to agricultural improvement, but with runoff water they can move and reach rivers and others ecosystem, thus creating impact on soil, water, vegetation [29]. They kill dangerous pests or weeds, but can be toxic to other organisms including birds, fishes, beneficial insects and non-target plants. Insecticides are generally the most acutely toxic class of pesticides, but herbicides can also pose risks to non-target organisms [30]. This means that there is no part of population which is completely protected against exposure to pesticides and the potentially serious health effects [31]. The world-wide deaths and chronic diseases due to pesticide poisoning is evaluated to be about 1 million per year [32].

1.1.4. Perfluorinated compounds

Perfluorinated compounds (PFCs) are a wide class of fluorinated chemicals used in many industry sectors for several applications. They are produced since 1940s, for their surfactant qualities, as oil and water repellent. In the following years they have found several applications in production for packaging material, soap, shampoo, teflon, etc [33]. PFCs are persistent thanks to the high dissociation energy of C-F bonds and resistant to many processes of environmental transformation, such as hydrolysis, photolysis, bio-degradation [34]. Moreover, PFCs with chains longer than 6-carbon atoms are bio-accumulated, leading to biomagnification in some fish species [35]. In environment they are ubiquitous, and were detected in superficial waters, remote areas, indoor and outdoor airs [35].

The most prevalent PFCs in the environment are the perfluorooctanoic acid (PFOA) and perfluorooctane sulfonate acid (PFOS) (Figures 1.4 and 1.5) [36]. These two compounds were widely used thanks to their good performance as

surfactants, thermal/chemical stability, action in low concentration, resistance to strong acids and bases [35]. Because both PFOS and PFOA are persistent, bioaccumulative and potentially toxic, they are being proposed as candidates for a new class of POP (Persistent Organic Pollutant) [35]. PFOA was the first perfluoroalkyl-derivative identified in human serum and, from other studies, several PFCs has been detected on human serum, blood, plasma and tissues [37, 35, 38]. Between 2000 and 2002, PFOS was phased out of production in the U. S. by its primary manufacturer and in 2006 eight major companies voluntary agreed to stop the production of PFOA and PFOA-related chemicals [34]. It is important to mentioned that PFOA and PFOS can not be generated in nature, they only can be synthesized or be originated from PFCs degradation.

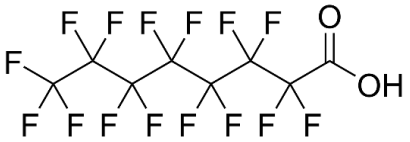

Figure 1.4. Perfluorooctanoic acid

Figure 1.5. Perfluorooctanesulfonic acid

1.1.5. Drugs

Illicit drugs were recently indicated as emerging contaminants since they have been detected in waste, surface and drinking water and in airborne particulates in several European countries and USA [39]. The presence of drugs in the environment is mainly due to the human consumption, because of residues persisting in consumers' urine. In 2004 the first investigation about illicit drugs in environment was carried out in USA for amphetamines [40], and several other compounds were later found in many environmental compartments, such as rivers, lakes, sea surface water, and air [41, 42]. Traces of illicit drugs were also detected in the airborne particulate of several cities [39]. This means that these substances can reach the air compartment despite their polarity and high-water solubility.

Amphetamine, cocaine and its metabolites, methamphetamine, heroine, 3,4-metilenediossimetanfetamina (MDMA), also known as ecstasy, and morphine are the main illicit drugs studied as contaminants. Despite low concentrations of illicit drugs in environment (ng/L in wastewater [43]), these substances can impact on wildlife and humans, mainly on the most vulnerable population. The effects they can produce are linked to the purpose for which they are made, and they can produce severe damages to the nervous system [44].

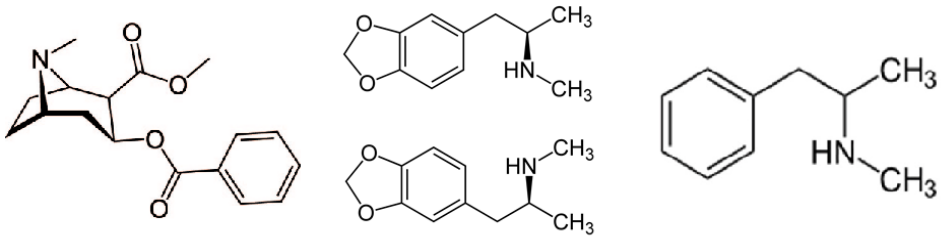

Figure 1.6. Heroine, MDMA and methamphetamine

1.1.6. Pharmaceutical products

Pharmaceutical products are a large and diverse group of organic compounds used for prevention and treatment of diseases in human and animals. They have been detected at trace concentrations (ng/L levels) in a wide variety of environmental water samples including sewage flows, rivers, lakes, groundwater aquifers and drinking water [45]. Pharmaceutical compounds are considered as emerging contaminants due to their presence in a still active form that may determine effects on plants and humans. Given that their effects have not sufficiently been studied yet, they remain unregulated. Since these compounds are not tested at low doses and long-term exposures or when present in mixtures, adverse effects are largely unknown [46]. Pharmaceuticals can not be completely removed using wastewater treatments, because they are usually water soluble and poorly degradable [47, 48]. Pharmaceutical consumption is large in all the world, specific types and quantities per year depending on the country. In 2004, 100000 tonnes of pharmaceuticals for human medicine were consumed, corresponding to an average annual consumption of 15 g per capita, but this value is estimated to be between 50 and 150 g in developed countries [49]. Currently in the European Union more than 3000 different active pharmaceutical substances are available as analgesics, anti-inflammatories, contraceptives, antibiotics, neuroactive compounds, etc [50].

Table 1.1 shows average annual consumptions (in g per person per year) of common pharmaceutical compounds in France, Germany, Poland, Spain and the UK between 1999 and 2006.

Table 1.1. Main pharmaceutical products and their consumption (g per person per year) in France, Germany, Spain, UK and Poland [51]

Class	**Compound**	**Annual per capita consumption of pharmaceutical [g/cap/y]**				
		France	**Germany**	**Spain**	**UK**	**Poland**
Antibiotic	Amoxicillin	6.50	1.20	-	1.54	-
	Ciprofloxacin	0.21	0.17	0.09	0.12	0.13
	Clarithromycin	0.25	0.12	0.13	0.08	0.27
	Sulfamethoxazole	0.34	0.65	-	0.02	0.17
Mood stabilizer	Carbamazepine	0.61	0.98	-	0.77	0.8
Analgesic	Tramadol	0.44	0.30	-	0.27	-
	Ibuprofen	3.40	3.20	2.60	2.80	5.04
	Paracetamol	47.14	4.46	3.60	15.68	4.84
Antidiabetic agent	Metformin	12.10	6.30	-	5.90	-

In the following paragraphs, the main pharmaceutical products are classified and some information about them is provided.

1.1.6.1. Antibiotics

Antibiotics are powerful medicines which can fight bacterial infections, such as colds, flu, bronchitis and throat sore. The fundamental issue which involves antibiotic consumption is their abuse or improper use. In these conditions, human body can develop antibiotic resistances, due to bacteria changes that make them able to resist antibiotics. In turn, this determines an increase of antibiotic use and an increase of antibiotic concentrations in environments which produce effects on organisms [52]. Between 2000 and 2010, antibiotic consumption increased by 35% [53].

1.1.6.2. Antidepressant

A few years ago, the Organization for Economic Cooperation and Development (OECD) analysed antidepressant consumption in 25 countries between 2000 and 2013. The consumption trend is shown in Figure 1.7 and, in every country monitored by OECD, antidepressant use was on rise. According to OECD [54], this might reflect the reduction of the time period which normally passes between a depression treatment and the next one. There are significant variations in consumption of antidepressants in different countries. Iceland reported the highest level of consumption of antidepressants in 2013, twice the OECD average, followed by Australia, Portugal and Canada. Chile, Korea and Estonia reported low consumption levels [54].

Antidepressants use lead to their presence in environment. U. S. Geological Survey (USGS) scientists published a paper [55] which documents that specific antidepressants and their metabolites found in wastewater, discharged into streams by municipal wastewater treatment plants, are uptaken into the body of fish living downstream of the plants. This research demonstrates that the antidepressant concentration in stream waters does not necessarily correlate with the concentrations found in fish tissues [55]. This study documents that specific antidepressants present with low concentrations in water are selectively up taken into fish brain tissues. There are many reasons why this selective uptake may occur - including differences in octanol/water partition coefficient of the targeted antidepressants - but these results suggest that other mechanisms, not yet unidentified, may also be involved, thus stimulating further studies. Another study [56] indicates that antidepressants cause implications on fish health and population. In particular, this work documents a slowed predator avoidance behaviour in larval fathead minnows exposed to antidepressants. A slower response to predators is dangerous for species that are on the lower end of the food chain, so this exposure can result in a sizeable reduction of this species.

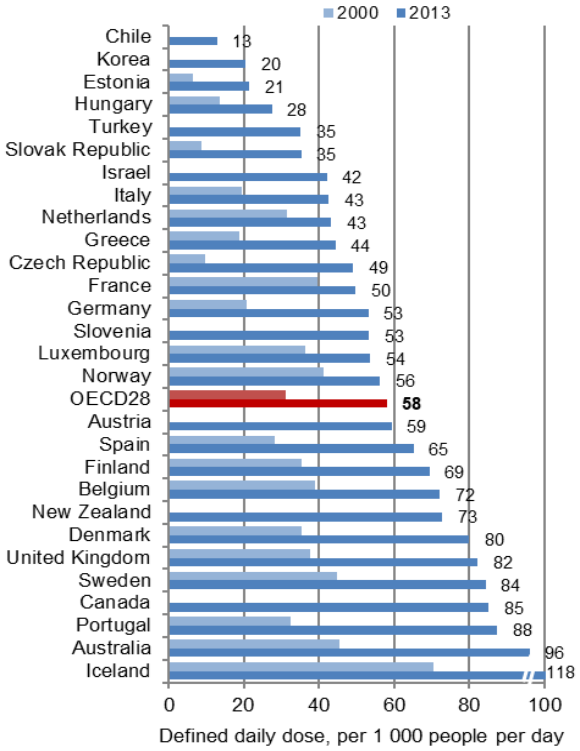

Figure 1.7. Antidepressant consumption, 2000-2013 [57]

1.1.6.3. Analgesics

Analgesics are very popular and common use pharmaceuticals, mainly used to treat the symptoms of colds, aches and pains, or for the treatment of painful diseases mostly of rheumatic origin [58]. Because of this wide use (and often abuse), analgesics are detected in environment. Clot-Faybesse at al. [59] studied a population of 10818 residents in nursing home. They considered as chronic prescription a duration of 28 days (or greater). As result, in 2012, 62% consumed at least one analgesic, 51% had a chronic analgesic consumption, 11% had a short analgesic consumption and 25% had both short and chronic analgesic consumptions. This study revealed an analgesic consumption sometimes inappropriate (overuse), paracetamol being the reference molecule [59].

1.1.6.4. Antidiabetic agents

Antidiabetics are useful medicines to stabilise blood glucose levels in people with diabetes. A few years ago, the OECD analysed antidiabetics consumption in 25 countries between 2000 and 2013 (Figure 1.8). Over that period, the use of antidiabetics has almost doubled. This growth parallels the increase of obesity, a major risk factor for the development of type-2 diabetes. In 2013, the highest

consumption of antidiabetics was observed in Finland, Germany and the United Kingdom.

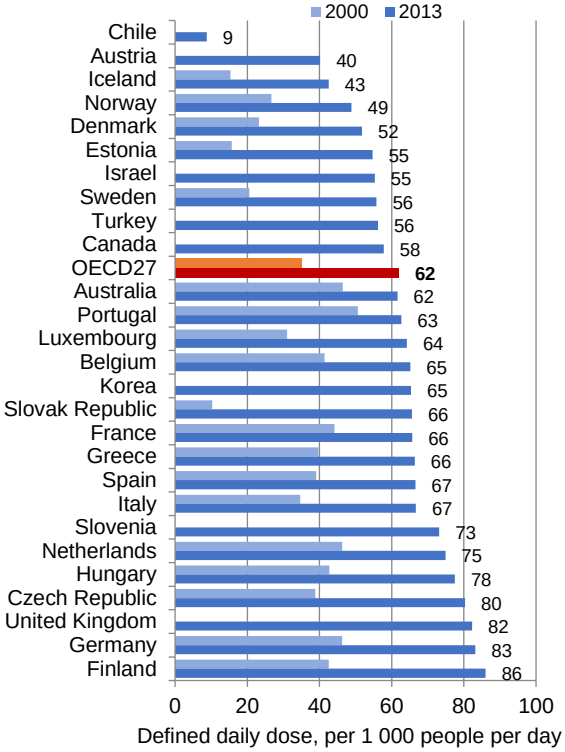

Figure 1.8. Antidiabetic consumption, 2000-2013 [57]

1.2. Caffeine

Caffeine is the most widely consumed central-nervous-system (CNS) stimulant. Stimulants purpose is to temporarily increase alertness and energy. A lot of different substances fall into this category, as drugs (cocaine, amphetamines), pharmaceutical and natural compounds (caffeine, theobromine, etc). Stimulants can be addictive, thus increasing the probability of abuse.

Caffeine is a plant alkaloid and it can be found in numerous plant species where it acts as a natural pesticide by producing endogenous substances (toxins, compounds with pheromone-like activity or bitter-tasting substances [60]) which discourage insect feeding [61, 62]. The most commonly used plants which contain caffeine are coffee, tea, and to some extent cocoa, but other sources of caffeine, less commonly used, include the yerba mate and guarana plants, specially used for preparation of tea, energy drinks or food supplement to improve weight loss or sport performance [63, 64].

Table 1.2. Quantities of caffeine found in common foods and beverages [65]

Product	**Serving size**	**Average caffeine per serving [mg]**
Caffeine tablet	1 tablet	200
Excedrin tablet	1 tablet	65
Brewed coffee	240 mL	135
Decaffeinate coffee	240 mL	5
Coffee espresso	57 mL	100
Italian coffee espresso	30 mL	75
Dark chocolate (Hershey's Special Dark)	1 bar (43 g)	31
Milk chocolate (Hershey Bar)	1 bar (43 g)	10
Red Bull	240 mL	80
Cocaine Energy Drink	250 mL	280
Buck fast Tonic Wine	750 mL	280
Bawls Guarana	296 mL	67
Foosh Energy Mints	1 mint	100
Buzz Bites Chocolate Energy Chews	1 chocolate	100
Soft drink, Coca-Cola Classic	355 mL	34
Atomic Rush	255 mL	100
Green tea	240 mL	15
Leaf or bag tea	240 mL	50

Table 1.2 shows the caffeine content found in most consumed products. The primary caffeine source is the coffee bean, from which coffee is brewed. The content of caffeine in coffee depends on the type of coffee bean and preparation method. Another common caffeine source is tea, which usually contains about half as much caffeine per serving as coffee [66], but even in this case, concentrations depend on plants and method of preparation. Others caffeine sources are chocolate, beverages as energy drinks or soft drinks, pharmaceuticals, drugs and pesticides [67, 64]. Over the last years, caffeine has been widely used in the pharmaceutical field because it enhances the effect of some analgesics and it is a stimulant for cardiac, cerebral and respiratory diseases [68]. Due to its introduction in so many products, caffeine is included on the list of High Production Volume Chemicals [69].

After its consumption, caffeine is metabolized in human body, but 5% is excreted unchanged in urine [70].

In addition to caffeine, these products in Table 1.2 usually contain theobromine and theophylline, which are stimulants included in the same chemical group of

xanthine (Figure 1.9). Xanthine is a purine base found in many body tissues and fluids, some plants and urinary calculi. The xanthine derivatives methylated on the various nitrogen atoms are found in nature. Methylxanthines constitute a class of drugs called alkaloids, which include caffeine, aminophylline, paraxanthine, pentoxifylline, theobromine, and theophylline [61].

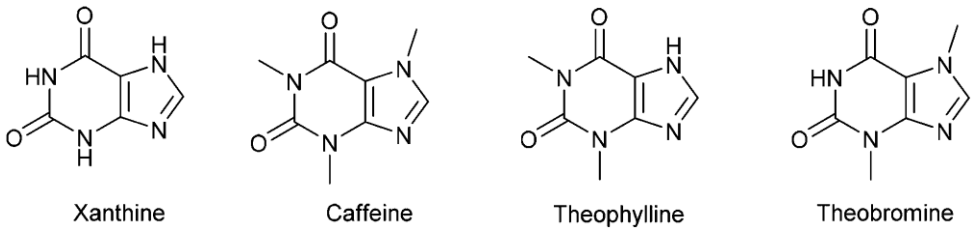

Figure 1.9. Molecular structures of xanthine, caffeine (1,3,7-trimethylxanthine), theophylline (1,3-dimethylxanthine) and theobromine (3,7-dimethylxanthine)

Theobromine, the principle alkaloid in theobroma cacao beans and other plants, is the main responsible for the mood-elevating effects of chocolate [71]. The amount found in chocolate is small enough that chocolate can be safely consumed by humans in large quantities, but animals that metabolize theobromine more slowly, such as cats and dogs, can easily consume enough chocolate to cause chocolate poisoning [72]. Theobromine is a stimulant frequently confused with caffeine, but its effects on the human body are quite different from those of caffeine; it is a mild, lasting stimulant with a mood improving effect. In medicine, it is used as a diuretic, vasodilator, bronchodilator and myocardial stimulant, but it has practically no stimulant effect on the central nervous system [73, 71].

Theophylline is a natural alkaloid derivative of xanthine isolated from the plants camellia o tea sinensis and coffee arabica [71]. Physiologically, this agent relaxes bronchial smooth muscle, produces vasodilation (except in cerebral vessels), stimulates the CNS and cardiac muscles, induces diuresis, and increases gastric acid secretion; it may also suppress inflammation and improve contractility of the diaphragm [73].

Caffeine produces stronger effects than theophylline and theobromine, for this reason it is the most widely consumed CNS stimulant [71]. Its effects are explained in the following paragraph.

1.2.1. Effects and toxicity on humans

Humans consume caffeine by assuming food, pharmaceuticals, energy drinks and drugs. According to EFSA [74], caffeine consumption by food and beverage is reported in Table 1.3.

Table 1.3. Summary of dietary exposure to caffeine [mg/kg of body weight per day] [74]

	Toddlers	**Children**	**Adolescents**	**Adults**	**The elderly**	**Very elderly**
	12-35 months	3-9 years	10-17 years	18-64 years	64-74 years	>75 years
Mean	0-1.5	0.2-2.0	0.5-1.4	0.5-4.3	0.3-4.9	0.3-6.0
95^{th} percentile	0.1-3.5	1.5-4.5	1.5-4.3	1.6-10	1.5-10	2.3-6.3

Daily exposure from all sources in food ranged from 0 to 10 mg/kg of body weight across all the population groups. EFSA recently come at the conclusion that caffeine intake up to 400 mg/day (about 4.5 mg/kg of body weight per day) does not lead to safety concerns for adults. The threshold is lower for pregnant women, children and adolescents (3 mg/kg of bodyweight per day) [64].
Caffeine at moderate doses seems to produce several behavioural effects in humans, among them [75, 64]:

- Increased alertness and reduced fatigue
- Improved performance on tasks that involve vigilance or long-lasting response when the alertness has been reduces
- Improved mental performance and fatigue

For these reasons, in activities involving operational skills caffeine intake appears to be beneficial [76]. On the other side, the excessive consumption of caffeine can produce negative effects in the organism. Regarding the effects of caffeine abstinence, syndromes have been suggested to be related to the uncontrolled and excessive use of caffeine. This intake seems to produce withdrawal symptoms, which include headache, stress, anxiety, fatigue, decreased alertness, depression anxiety [77, 64].

When ingested in excessive dosage for extended periods, caffeine produces a specific toxidrome (syndrome caused by a dangerous level of toxins in the body) called caffeinism, whose primary characteristics are described below [78, 62]:

- **Central nervous system features:** headache, light-headedness, anxiety, agitation, tremulousness, extremity tingling, confusion, psychosis, seizures
- **Cardiovascular features:** palpitations or racing heart rate, chest pain, tachycardia, hypotension, tachipnea
- **Gastrointestinal features**: nausea and vomiting, abdominal pain, diarrhea, bowel incontinence, anorexia

1.2.2. Effects and toxicity on animals and insects

Caffeine can produce benefits or negative effects on humans as well as on animals. At variance with humans, the exposition to caffeine of animals is involuntary. The benefits that caffeine can produce in some animals are the same as in humans: increase of alertness, decrease of fatigue, improving concentration etc…For example, it was found that in chickens caffeine increases the ability to keep awake or alert, this being considered a positive effect because it expands their period of productivity [79]. Also horses can take advantage of caffeine. For instance, they display exceptional endurance, jumping ability, and speed after assumption of caffeine, as well as reduction in mental and physical fatigue [80]. Studies on bees show that they are statistically much more likely to identify the odour of caffeinated nectar than other nectar types, suggesting a caffeine-influenced improvement in memory [81].

Anyway, caffeine in environment is not present only for animals which benefit from it, and in most cases, caffeine has negative impacts on ecosystems. First of all, caffeine is a natural pesticide and it acts by inhibiting enzymes of the nervous system in herbivorous insects, causing their paralysis or death [62]. This action is useful if caffeine is used as a pesticide to protect plants, but in environment caffeine acts on a non-discriminatory basis, so that spiders, snails and other harmless insects can die or be affected from it, causing ecosystem problems [82] In addition, caffeine impacts not only on insects, but also on little animals. For instance, according to the Hawaiian Department of Agriculture [83], high caffeine

concentrations or chronical exposure can induce heart attacks on coqui-frogs, silencing the amphibians' croaking. Moreover, a post-mortem analysis of a larger animal (a wild parrot) following a 20-g caffeine-laced meal of dark chocolate showed irreparable damage of its liver, kidneys, and brain neurons [84].

There are examples about how caffeine can negatively impact on animals. However, instead of thinking about each single case, it is important to conclude that caffeine can impact on different environmental compartments, producing serious problems on ecosystems.

1.2.3. Caffeine in environment

According to Sections 1.2.1 and 1.2.2 caffeine effects can pose a risk to humans, animals and insects. All the effects listed above are the possible consequences that a subject can report by assuming caffeine. Nevertheless, caffeine is a CEC, so it can be found in environment and can passively enter in organism.

As mentioned in Chapter 1.2, caffeine is a natural product, but it is also a constituent of a lot of food, beverage, pharmaceuticals and drugs; 5% of caffeine consumed is not metabolized, so it is released in environment unchanged [70]. According to EFSA [74], caffeine intake up to 400 mg/day does not lead to health concerns for an adult. Therefore, assuming the right consumption of caffeine, an adult releases in environment 20 mg/day of caffeine. In addition, there is a non-ingested dose of caffeine which enters in environment as domestic or industrial wastes.

Over the last decades, caffeine has been detected in wastewater, surface water, and groundwater worldwide; some results are reported in Tables 1.4, 1.5 and 1.6.

Table 1.4. Caffeine concentrations in groundwater

Country	Location	Caffeine [ng L^{-1}]	Reference
United States	Wells in four valley from 0.5 to 60 m deep	10-80	[85]
	Wells deeper than 10 m – Shallow wells	<40-230	[86]

Table 1.5. Caffeine concentrations in river water

Country	Location	Caffeine [ng L^{-1}]	Reference
Spain	Henares-Jarama-Tajo River	12.2-415.7	[87]
United States	Mississippi river	ND-38	[88]
France	Jalle River	40-75	[89]
Brazil	Rio de Janeiro	174-127092	[90]
South Korea	Han River	28-250	[91]
China	Pearl River	ND-865	[92]
	Xiagjiang River	0.11-49.8	[93]
Indie	Ahar River	66-476	[94]

Table 1.6. Caffeine concentrations in seawater

Country	Location	Caffeine [ng L^{-1}]	Reference
	North Sea	2-16	[95]
United States	Massachusetts Bay	5-71	[96]
	Boston Harbor	140-1600	[96]

Buerge et al. [68] developed a study about using caffeine as a marker of anthropogenic contamination of water. In this study wastewater samples, obtained from municipal WWTPs in Switzerland, have been analysed. These WWTPs operate with three or four stages: mechanical, biological and chemical treatment and in some cases a subsequent sand filtration. Caffeine in effluents has resulted considerably lower than in influents, but technologies were not sufficiently

suitable to completely eliminate it. The 80% of caffeine elimination has been primarily assigned to microbial degradation. In the same study, caffeine has been measured in several lakes located close or far from human settlements. It has been noted that the anthropogenic burden to a lake increased with the ratio population (P) in the catchment area, but it decreased with increasing dilution (throughflow of water, Q). Buerge et al. [68] have defined (see Equation 1.1) the relation which has to be fulfilled to define a marker of anthropogenic contamination:

$$C \propto \frac{P}{Q} = \frac{P\tau}{V} \qquad 1.1$$

where C is the concentration of the contaminant V is the volume of the lake and τ is the mean water residence time. By applying Equation 1.1 to sampled data, caffeine resulted suitable as a quantitative anthropogenic marker.

A study conducted in Basque Country in 2018 [97] shows caffeine effectiveness as a marker of anthropogenic water contamination.

In three estuaries (in Bilbao, Plentzia and Urdaibai) several emerging contaminants have been analysed, including caffeine. In addition to this, the effluents of the main wastewater treatment plants (WWTPs) of each estuary were also monitored. The main results are summarized in Table 1.7.

Table 1.7. Caffeine concentration ranges [ng/L] in estuaries and related WWTPs effluents

Bilbao		**Plentzia**		**Urdaibai**	
WWTP	**Estuary**	**WWTP**	**Estuary**	**WWTP**	**Estuary**
25-99	25-699	71-317	20-362	1752-65999	27-1092

According to Table 1.7, caffeine was found in every WWTP effluent, thus indicating that their technologies can not degrade caffeine. Concentration ranges are different for each WWTP. These differences are due to caffeine concentrations in influents incoming in each WWTP, which depend on human activities. The caffeine concentration in the Bilbao and Plentzia estuaries are larger than those of the corresponding effluents, suggesting that secondary urban inputs are located between WWTPs and estuaries. These secondary inputs have been investigated

and confirmed by the authors. The estuary in Urdaibai presents a concentration range of caffeine shorter and smaller than its related WWTP effluent, thus indicating that no new inputs are present. Therefore, according to Mijangos et al. [97], caffeine concentration in environment primarily depends on the primary urban inputs and the efficiency of WWTPs, in agreement with the use of caffeine as a marker of anthropogenic contamination of water.

To date, only a few studies have been conducted about passive caffeine assumption. One of the most recent study is that of Ondarza et al. [98]. Different tissues (muscle, liver and gills) of fishes have been examined to evaluate the bioaccumulation of CECs. Fishes were sampled from Paranà River and Acaragua River (Argentina), commonly used for drinking water and domestic purposes, which receive untreated wastewater. This research has confirmed that caffeine bioaccumulates. Caffeine was consistently detected in all tissues of all species, with concentrations between 1.2 µg/kg and 13 µg/kg. Caffeine represented up to 91% of the total measured CECs concentrations. Therefore, caffeine undergoes bioaccumulation.

Rodriguez-Gil et al. [99] analysed the global exposure distribution of caffeine and paraxanthine (its first metabolite) with the aim to evaluate the risk which they pose to aquatic ecosystems. The main conclusion of this study was that the risk posed by caffeine was unacceptable, because of the chronic exposure in effluents, surface water and estuary water.

1.2.4. Caffeine degradation pathways

Another issue about caffeine in environment is its transformation. Caffeine degradation does not follow a single pathway. There are several possible pathways, on the basis of the kind of reaction whereby caffeine is involved, which lead to different metabolites and intermediates. The diagram of Figure 1.10 gives an overview of the main caffeine metabolites and intermediates formed along various possible degradation pathways promoted by microorganisms [100].

In chemical terms, caffeine is 1,3,7-trimethylxantine ($C_8H_{10}N_4O_2$), whose molecular weight is 194.9 g mol^{-1}.

According to the diagram of Figure 1.10, caffeine demethylation (which can be naturally promoted by Serratia marcescens, Pseudomonas putidas, Penicillium commune, Aspergillus tamarii and other microorganisms) can produce

theobromine, theophylline or paraxanthine [101]. Paraxanthine is the main product of caffeine metabolism in humans. According to Magkos & Kavouras [70], it represents the 80% of the total caffeine metabolism excretion. In line with its close structure, it is a psychoactive stimulant of the central nervous system [102]. The features of theobromine and theophylline were presented above (see Section 1.2).

Theobromine, paraxanthine and theophylline can also undergo demethylation, producing methylxanthines in the form of structural isomers in which the position of the methyl group changes (1, 3 and 7). Further demethylation leads from methylxantines to xanthine.

Some bacteria (Rhodococcus spp. and Klebsiella spp.) promote caffeine oxidation to 1,3,7-trimethyl uric acid which can undergo urate oxidase to 3,6,8-thrimethylallantoin [103]. This compound dissociates in water to give dimethylurea, methyl urea and glyoxylate.

As mentioned above, these degradation pathways are driven by microorganism. In this study caffeine degradation occurs by chemical oxidation in particular conditions, as described in the following chapters. It is thus not possible to predict which intermediates or products will form during the degradation reaction, and whether they follow the scheme in Figure 1.10.

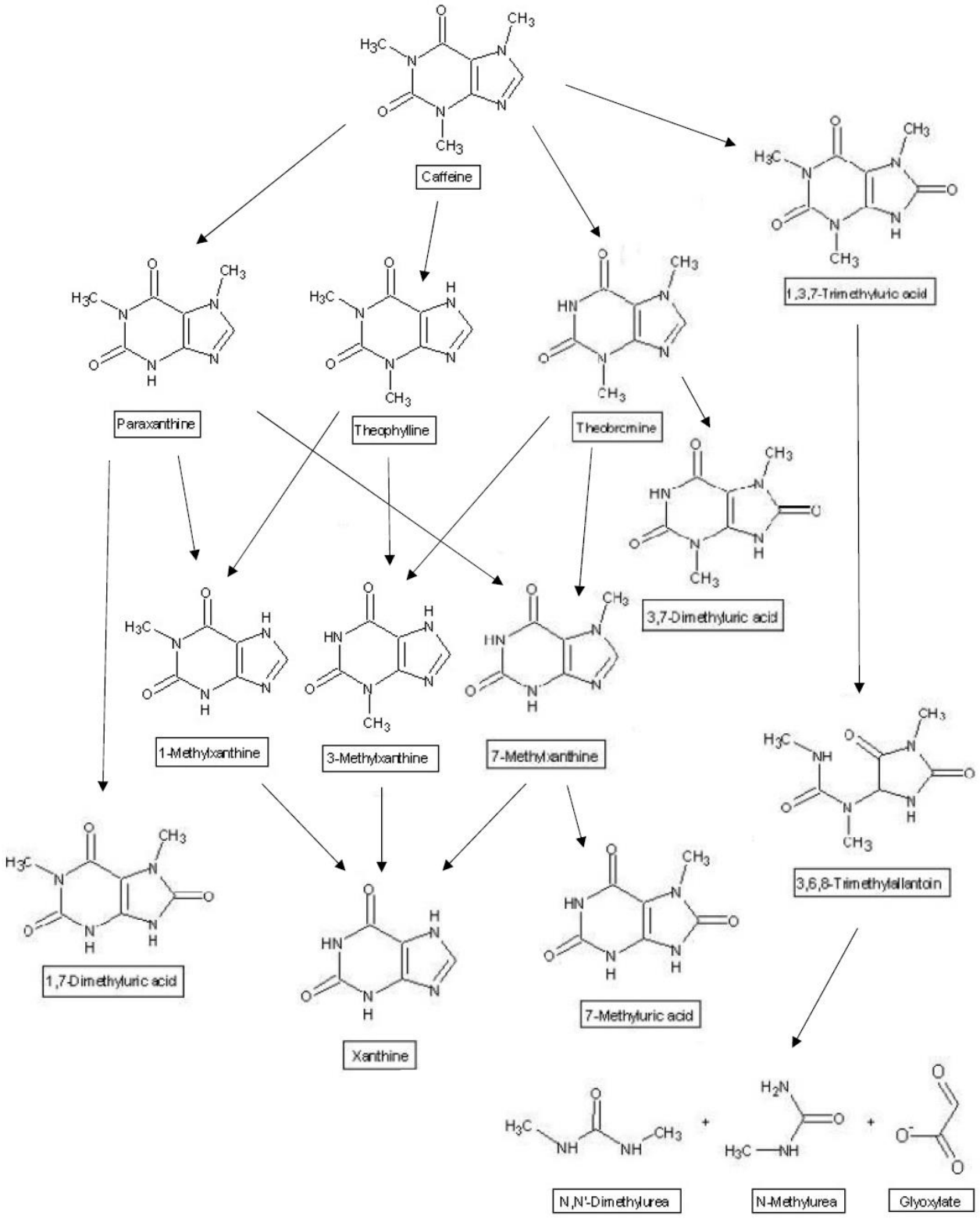

Figure 1.10. Caffeine degradation pathways [100]

2. ADVANCED OXIDATION PROCESSES

As described in Chapter 1, over the last decade, the occurrence of a new generation of contaminants has been detected in wastewater, surface and underground water and even in drinking water [4]. These substances, called "emerging contaminants", are not subject to regulations because the risk they pose to human health and the environment is not yet fully understood [6]. Anyway, their recalcitrant character and their effects as endocrine disruptors suggest that their bio-accumulation will have severe implications for the environment [10].

In general, contaminated waters are purified in treatment plants with physical, biological and conventional chemical processes (thermal oxidation, chlorination, ozonisation, etc.), but in many cases these treatments do not allow to reach the needed decontamination degree, which consists of biodegradable substances or no-toxic species [3]. The main purpose of the oxidation of pollutants in water and wastewater is their mineralization. "To mineralize" means "*to convert the constituents of an organic pollutant in to simple and relatively harmless and inorganic molecules*" [104].

Advanced oxidation processes (AOPs) can be defined as those processes which involve the generation of hydroxyl radicals in sufficient quantity to achieve an efficient oxidization [105]. AOPs have demonstrated to be particularly useful in degrading, and eventually mineralizing, emerging contaminants [3, 106, 107, 108].

The main disadvantages of AOPs consist in the possibility of accumulation of oxidation by-products and occurrence of radical scavenging by interfering compounds which leads to a reduction in the effectiveness of AOPs [104]. At economical and operational levels, AOPs are expensive for the cost of employed reagents and because the application of these processes requires to separate water before the treatment (they can not be carried out in situ) and a continuous control [109, 110, 111, 112].

However, AOPs are the most efficient option for the degradation of emerging contaminants and the main AOPs advantages are listed below [112, 104]:

- Degradation of refractory contaminants
- Full mineralization of contaminant organic matter

- Rapid reaction rate
- Potential reduction of toxicity
- No production of materials that requires further treatments
- No creation of sludges

In general, AOPs involve two stages of oxidation [105]:

Stage 1: Formation of strong oxidant species (mainly hydroxyl radicals)

Stage 2: Reaction of oxidant species with organic contaminants in water

The hydroxyl radical (OH·) is a short lived radical, due to its instability, so it must be generated continuously in situ from chemical or photochemical reactions to complete the oxidation process [113]. As shown in Table 2.1, technologies classified as AOPs fall under two general categories depending on the use (or not) of a light radiation [114]. Another classification of AOPs depends on the status of the reagents which are processed: when they are all in a solution the process is homogeneous, otherwise it is heterogeneous [115].

Table 2.1. Classification of certain advanced oxidation processes [114]

Non-photochemical	**Photochemical**
Ozonation (O_3)	Photocatalytic oxidation, UV/catalyst
Ozonation with hydrogen peroxide (O_3/H_2O_2)	UV/O_3
Processes involving oxygen, temperature and pressure	UV/H_2O_2
Electrochemical oxidation	$UV/O_3/H_2O_2$
Radiolysis	$UV/TiO_2/O_2$
Non-thermal plasma	$UV/TiO_2/H_2O2$
Fenton (Fe^{2+} or Fe^{3+}/H_2O_2)	Photo-Fenton ($Fe^{2+}/H_2O_2/UV$)

2.1. Hydroxyl radical

The first aim AOPs is to produce hydroxyl radicals (HO·) in water [105]. Hydroxyl radicals are reactive species because they present one-electron deficiency which make them extremely unstable [116]. Some features of this species are listed below:

- Very powerful oxidant. It has the second highest thermodynamic reduction potential (Table 2.2)
- Relatively non-selective electrophilic oxidizing agent
- Highly reactive therefore short lived (106-1012 times more rapid than conventional oxidants [113])
- In aqueous media it tends to oxidize organic contaminants and to produce carbon dioxide, water and salt [117]

Table 2.2. Standard reduction potentials of some oxidant species (25° C) [104]

Oxidant	Eh [V]
F_2	3.03
HO·	2.80
O·	2.42
O_3	2.07
HO_2·	1.70
H_2O_2	1.78
HOCl	1.49
Cl_2	1.36

Four types of chemical reactions of the hydroxyl radical in water ca be identified [118, 119]:

1. *Addition*. A hydroxyl radical added to an unsaturated compound, aliphatic or aromatic, forms a free radical product. For instance:

$$HO\cdot + C_6H_6 \rightarrow (OH)C_6H_6\cdot \qquad 2.1$$

2. *Hydrogen Abstraction.* Products of this kind of reaction are organic free radicals and water. For instance:

$$HO\cdot + CH_3OH \rightarrow CH_2OH\cdot + H_2O \qquad 2.2$$

3. *Electron Transfer.* This reaction produces ions of a higher valence or, when a mononegative ion is oxidized, an atom or free radical. For instance:

$$HO\cdot + [Fe(CN)_6]^{4-} \rightarrow [Fe(CN)_6]^{3-} + OH^- \qquad 2.3$$

4. *Radical Interaction.* The hydroxyl radical reacts with another hydroxyl radical or with an unlike radical to combine or to disproportionate, forming a stable product. For instance:

$$HO\cdot + HO\cdot \rightarrow H_2O_2 \qquad 2.4$$

The hydroxyl radical decomposes most organic compounds into CO_2 and H_2O [114], therefore it should be the preferred oxidant in water treatment. The two mechanisms shown in Equation 2.1 and 2.2 are predominant in industrial wastewater treatments [119].

2.2. Non-photochemical advanced oxidation processes

In the processes described below, oxidation occurs without use of light radiation. These types of advanced oxidation processes are based on the generation of strong oxidant species through transformation of particular chemical species or the use of several types of energy other than light radiation.

2.2.1. Ozonation

Ozonation is a homogeneous process (reagents are all in solution) of advanced oxidation [6]. Ozone (O_3) is a very unstable and reactive gas, and a very powerful oxidizing agent, Eh=2.07 V (25 °C) (see Table 2.2). In fact, ozonation is successfully applied for polycyclic aromatic hydrocarbons (PAHs) contaminated

soil remediation, with the purpose to obtain a complete mineralization of recalcitrant organic pollutants or transform them into simpler compounds, more soluble in aqueous phase [120]. Ozonation is also used for pre-treatments in biological processes and in combined processes because ozone can degrade organic compounds to aldehydes, ketones or carboxylic acids and its reactions do not produce colours [113, 121]. Due to its ability to oxidize many organic compounds [113], ozone is widely used in industrial processes to blech waxes, oils and textiles, as a deodorizing agent, as a germicide, and it is also used to sterilize air and drinking water [121].

Ozone is able to oxidize inorganic substances to their highest stable oxidation states and organic compounds to carbon dioxide and water [105]. In aqueous solution, ozone may act in two different ways: direct reaction O_3-molecules or radical-type reactions [122]. Radical-type reactions involve the generation of radical species (by ozone decomposition in water) which react with molecules (Figure 2.1).

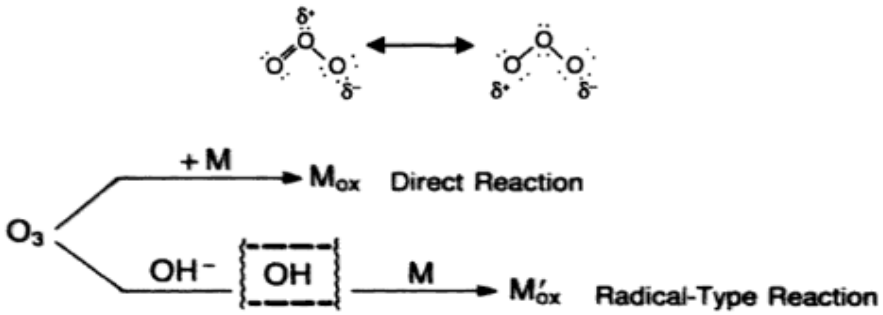

Figure 2.1. Reactivity of ozone in aqueous solution [122]

Direct reactions usually take place in acid media. These are slow and selective reactions in which ozone attacks can act as a dipole, as an electrophilic agent or as a nucleophilic agent [123]. In these types of oxidation only some part of an organic compound can be degraded, so additional treatment may be required to remove by-products [122]. Equation 2.5 shows O_3 which reacts with a generic molecule (M) and generate its oxidised form (M_{ox}).

$$O_3 + M \rightarrow M_{ox} \qquad 2.5$$

Radical-type reactions are usually fast and non-selective reactions, strongly effective, but they depend on ozone decomposition rate, which can be affected by pH (it is the faster, the higher is the pH), UV light, ozone concentration and radical scavengers [124]. Ozone decomposition occurs in a chain (Figure 2.2) which can be explained by fundamental reactions described below [125] [126]. Equations 2.6 and 2.7 represent the initial step, where ozone come into the decomposition chain. A decomposition chain is developed from Equations 2.8 to 2.12. Equations 2.13 and 2.14 represent breaks of the chain.

$$O_3 + OH^- \rightarrow HO_2 + O_2^- \quad (2.6)$$

$$HO_2 \leftrightarrow O_2^- + H^+ \quad (2.7)$$

$$O_3 + O_2^- \rightarrow O_3^- + O_2 \quad (2.8)$$

$$O_3^- + H^+ \rightarrow HO_3 \quad (2.9)$$

$$HO_3 \rightarrow HO + O_2 \quad (2.10)$$

$$OH + O_3 \rightarrow HO_2 + O_2 \quad (2.11)$$

$$HO_4 \rightarrow HO_2 + O_2 \quad (2.12)$$

$$HO_4 + HO_4 \rightarrow H_2O_2 + 2O_3 \quad (2.13)$$

$$HO_4 + HO_3 \rightarrow H_2O_2 + O_3 + O_2 \quad (2.14)$$

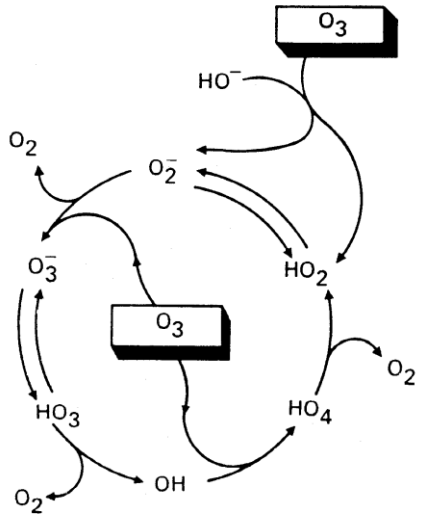

Figure 2.2. Ozone decomposition in water [126]

As far as the operational point of view is concerned, ozonation involves several disadvantages [127, 113]:

- The occurrence of material transferring determines the need of stirring. Stirring can be obtained with dispensers, mixers, contact towers which suggest additional costs
- A high ozone/contaminant proportion is required, thus determining a further increase of costs
- Sometimes, the mineralization of organic matter may be not completed
- Treated water can not contain residual ozone, so a degasifier is fundamental in the last step of the treatment, leading to additional costs

2.2.2. Ozonation with hydrogen peroxide

Ozonation with hydrogen peroxide is a homogeneous AOP [115]. The use of more than one oxidizing agent allows to take advantages of synergic effects which produce additional degradation of organic matter [128]. The use of mixed oxidants makes more difficult to predict final performances, so laboratory assays are essential. Among possible oxidant mixtures, the combination of ozone and hydrogen peroxide is the most employed in different backgrounds [123].
Hydrogen peroxide (Eh=1.78 V, see Table 2.2.) is involved in selective oxidations for the manufacture of many organic compounds, bleaching in the pulp and paper

industry, in fabrication technology, in water and effluent treatment and oxidation of large organic compounds to carbon dioxide [116].

The O_3/H_2O_2 systems was investigated in several studies, which led to the conclusion that the addition of peroxide enhances the efficiency of oxidation of various organic substances [105]. The expected stoichiometry of this reaction is given by Equation 2.15 [111].

$$H_2O_2 + 2O_3 \rightarrow 2HO^{\cdot} + 3O_2 \qquad 2.15$$

According to Equation 2.15, hydrogen peroxide is useful to start ozone decomposition in water (Figure 2.2). It means that the mix H_2O_2/O_3 produces a larger amount of hydroxyl radicals than O_3 only, thus leading to a more effective oxidation (degradation) of compounds in water solution [129]. In conclusion, reaction process of ozonation with hydrogen peroxide is an ozone radical-type reaction (see Section 2.1.1) where hydrogen peroxide enhances the $HO^{\cdot}$ creation rate. So, oxidation proceeds through the combination of two distinct pathways: a slow selective oxidation driven by ozone, and an indirect and fast oxidation driven by hydroxyl radical [126].

2.2.3. Processes involving oxygen, temperature and pressure

The homogeneous treatments listed below use oxygen, temperature and pressure to oxidize several compounds [6]. It is possible to distinguish supercritical water oxidation and subcritical water oxidation (or wet air oxidation), depending on the values of the parameters kept during the process [130]. In line with their names, these two oxidation processes are carried out, respectively, beyond and below the critical point of water, this is, T=374 °C and P=22,06 MPa [131].

2.2.3.1. Supercritical water oxidation (SCWO)

Supercritical water oxidation processes are usually carried under following the conditions [132]:

- P = 24-30 MPa
- T = 450-650 °C

At this supercritical state, water, oxygen and organic waste are mixed and pressurized in a reactor to degrade organic compounds. Then temperature and pressure are reduced to standard conditions, while a phase separator allows to separate water-phase from gas-phase products. A scheme of a reaction system is displayed in Figure 2.3.

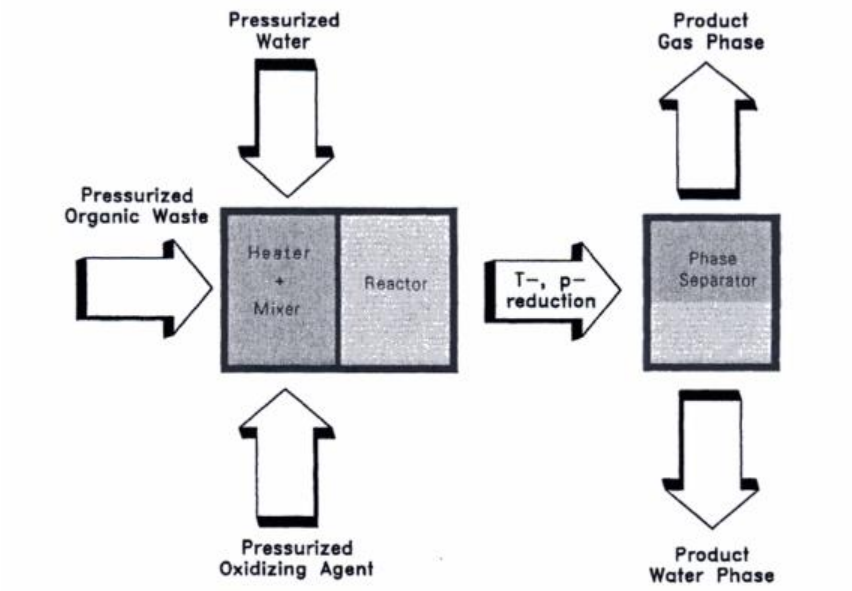

Figure 2.3. Principle for SCWO [132]

Benefits and disadvantages of SCWO treatments are listed below [110] [111] [132].

Advantages

- Widely employed to treat organic residues, sludges, chlorinated and nitrogen-based solvents, pesticides, herbicides, PCBs (polychlorinated biphenyls) residues from chemical and pharmaceutical industries, military products etc…
- Efficiency of oxidation higher than 99,9% with 5-60 s contact time
- Additional treatments on gas phase products are not necessary
- There are no material transfer issues due to high oxygen solubility

Disadvantages

- Possible production of dibenzofurans and dioxins
- The needed technology is expensive due to the necessity to support high operational temperatures and pressures which cause corrosion issues

2.2.3.2. Subcritical water oxidation (wet air oxidation)

Subcritical water oxidations are carried out under the following conditions [132]:

- P = 1–22 MPa
- T = 150-370 °C

Subcritical water oxidation, also called wet air oxidation, is a treatment usually employed to degrade organic compounds in wastewater [133]. Soluble suspended components in water are oxidized through this process, which mainly converts organic contaminants to CO_2, water and biodegradable short chain organic acids, but it oxidizes inorganic compounds too [134]. High temperature and pressure provide a strong driving force for oxidation because the solubility of oxygen in water decrease with increasing temperature and an elevated pressure is useful to keep water in the liquid state [135]. Therefore, the reaction time depends on the temperature and pressure values chosen, while the performance can be enhanced by addition of catalysts as activated carbon [133] or oxidants such as O_2, H_2O_2 or $K_2S_2O_8$ [134]. Figure 2.4 shows a basic scheme for the wet air oxidation process.

Advantage [134]

- Great effectiveness is reached with any kind of residues, the majority of contaminants remain in aqueous phase

Disadvantages [134]

- Mineralisation of organic matter to low molecular weight compounds (carboxylic acids, alcohols, aldehydes and ketones) is incomplete

- Process efficacy is limited due to oxygen solubility which creates mass transfer issues
- A catalyser is fundamental for the degradation of some aromatic compounds and acids (e.g. acetic acid and propionic acid). The catalyser needs a final separation from the effluent

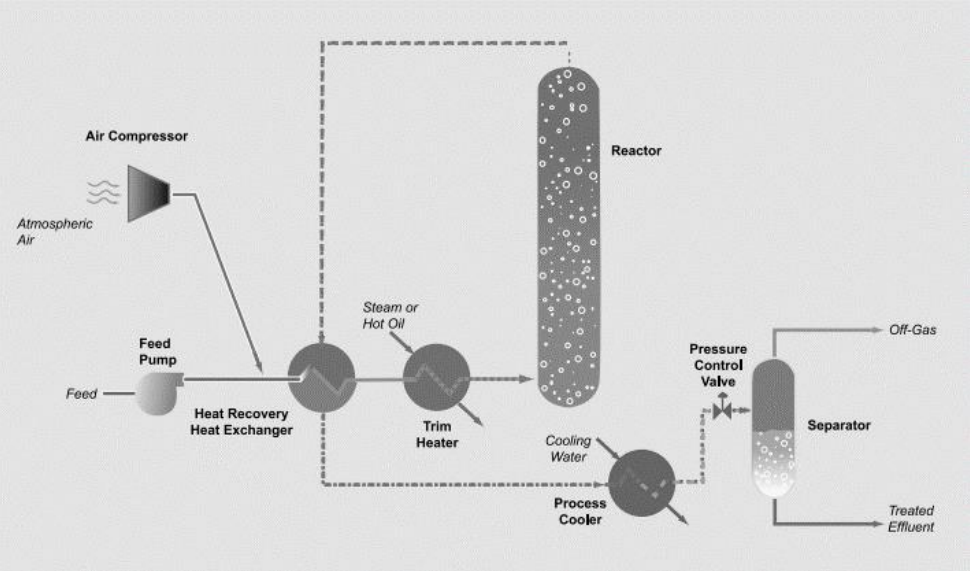

Figure 2.4. Basic flow sheet of wet air oxidation [133]

2.2.4. Application of energy

By applying energy, oxidation processes enhance their performance [104]. The main homogenous oxidation processes which involve energy application are listed below.

2.2.4.1. Electrochemical oxidation

Electric current generation between two electrodes in water produces chemical reactions which create hydroxyl radicals that oxidise organic matter [136]:

1. Anode oxidation

$$H_2O \rightarrow OH\cdot + H^+ + e^- \qquad 2.16$$

2. Cathodic reduction

$$O_2 + 2H^+ + 2e^- \rightarrow H_2O_2 \qquad 2.17$$

Pollutant oxidation is due to reactions described in Equation 2.18-20 [137], where M is a generic organic molecule.

$$M + H_2O \rightarrow M(OH^{\bullet}) + H^+ + e^- \quad 2.18$$

$$2M(OH^{\bullet}) \rightarrow 2MO + H_2O_2 \quad 2.19$$

$$3H_2O \rightarrow O_3 + 6H^+ + 6e^- \quad 2.20$$

The efficacy of this process can be improved by adding a metallic catalyser as iron salt [136].
Electrochemical oxidation produces several advantages [138]:

- There is no chemical oxidant to remove
- The electrochemical equipment it not expensive
- Yields are often adequate or excellent

2.2.4.2. Radiolysis and processes with electron beams

The generation of electrons, radical ions or neutral radicals, which are responsible for oxidation, can be reached by exposing a solution to a beam of high-energy electromagnetic waves (Y-rays, X-rays or Van der-Graaf electron beams) [139]. When electrons penetrate in water, they lose energy by colliding with water molecules and highly reactive species are produced (Equation 2.21).

$$H_2O \rightsquigarrow e^-,\ H^{\bullet},\ OH^{\bullet},\ H_2,\ H_2O_2,\ H^+ \quad 2.21$$

This highly reactive species are responsible of degradation processes.
Main advantages of these treatments are listed below [140]:

- Compounds are mineralised to low-molecular weight products
- Volatile and semi-volatile organic compounds can be treated
- Principal compounds attacked by these treatments are halogenated compound which are barely oxidable

- Residues are not produced, so next further treatments are not necessary

The main disadvantages of these treatment are listed below [140]:

- Aldehydes or organic acids can be produced by using low-intensity radiation
- The treatment needs a high electric consume, so it is expensive for high concentrations of contaminants

2.2.4.3. Non-thermal plasma

"*Plasma is a state of matter that is often thought of as a subset of gases, but the two states behave very differently. Like gases, plasmas have no fixed shape or volume, and are less dense than solids or liquids. But unlike ordinary gases, plasmas are made up of atoms in which some or all of the electrons have been stripped away and positively charged nuclei, called ions, roam freely*" [141]. It is possible to define two categories of plasmas, thermal and non-thermal, on the basis of the condition in which they are created: non thermal plasmas are produced at pressure $<10^5$ Pa and power <50 MW, thermal plasmas are produced at pressure and power relatively higher than previous values [142]. In any case, plasma is a source of both highly reducing and oxidant species, for this reason it can degrade a wide range of contaminants, including SO_x, NO_x, aliphatic hydrocarbons, VOCs in different matrices [143, 144]. The nature and proportions of active species (thus the efficiency of the treatment) depend on the nature of the gas used to create plasma [145].

Non-thermal plasmas used as advanced oxidation processes present several advantages [146]:

- Toxic sub-products as dioxins and furans are not produced
- Operations are carried out at ambient temperature
- Organic compounds and emissions as SO_x/NO_x are simultaneously eliminated
- Catalysts and combustibles are not required

Whereas, important limits related to this kind of treatment are the lack of public information and costs of new technologies control [147, 148].

2.3. Photochemical advanced oxidation processes

In this paragraph, photochemical advanced oxidation processes will be explained. Treatments in this group of AOPs are uniformed by the use of a light source which lead to the dissociation of molecules, enhancing the degradation of contaminants in water [114]. UV-visible radiation is the most common light source used and several advantages are reached by adding it to chemical oxidation [127]:

- Chemical reagents are not indispensable
- UV-visible radiation improves reaction rates
- UV-visible radiation can be associated with several oxidant and operational conditions

Photochemical AOPs are usually employed to eliminate chlorinated, organic and aromatic compounds and phenols, the efficacy of treatments depending on the reactor design (type of lamp, geometry, hydrodynamicist), which reflects on costs and consume of energy [127]. Over the last decades increasing attention has been focused on photochemical reactions for the complete oxidation of organic pollutants in water [149, 150, 151]. This technology is not suitable for solutions with a large amounts of dissolved solids, which reduce its efficacy because they dissipate light [114].
UV-visible radiations on molecules induce photolysis. Photolysis can be resumed in two step:

$$S + h\nu \rightarrow S^* \qquad 2.22$$

$$S^* + O_2 \rightarrow S^{\cdot +} O^{\cdot -}_2 \qquad 2.23$$

Where S is the substrate and S^* is an electronically exited state of the substrate [104]. As mentioned above, the formation of radicals and reactive oxygen species leads to degradation.

2.3.1. UV radiation with hydrogen peroxide

As mentioned in Sections 2.1 and 2.2.2, hydrogen peroxide is a good oxidant (Eh=1.78 V, see Table 2.2). UV radiation enhances this property by allowing the production of hydroxyl radicals (Equation 2.24) [152].

$$H_2O_2 + h\nu \rightarrow 2OH\cdot \qquad 2.24$$

UV lamps used to promote this reaction are usually mercury lamps which emit between 200 nm and 400 nm [153]. This radiation can also convert some compound by direct photolysis, resulting in the formation of by-products whose effects are not fully known. UV radiation combined with hydrogen peroxide has been used since 1990s to degrade organic micropollutants in water [154, 155, 156] and now this treatment is used to degrade mainly organochlorinated molecules, aliphatic and aromatic compounds, phenols and pesticides in wastewater [157, 158, 159].

The main advantages of this treatment are listed below [153]:

- Hydrogen peroxide is not expensive
- Hydrogen peroxide is thermally stable and it can be stored
- Due to hydrogen peroxide high solubility in water, there are no problems about material transfers
- Operational processes are simple
- Oxidation of organic waste in water is effective

On the other side, limitations of this process are listed below [152]:

- At wavelength shorter than 300 nm, the yield of the process is very low, so specific lamps are required
- High oxidant concentrations are necessary
- The process can not degrade fluorinated or chlorinated alkanes
- By working with an excess of hydrogen peroxide, competitive reactions take place, producing the inhibition of degradation due to hydroxyl radical recombination (see Equations 2.25-28 [152])

$$OH^{\cdot} + H_2O_2 \rightarrow OH^{\cdot}_2 + H_2O \quad 2.25$$

$$HO^{\cdot}_2 + H_2O_2 \rightarrow HO^{\cdot} + H_2O + O_2 \quad 2.26$$

$$2HO^{\cdot}_2 \rightarrow H_2O_2 + O_2 \quad 2.27$$

$$HO^{\cdot}_2 + HO^{\cdot} \rightarrow H_2O + O_2 \quad 2.28$$

2.3.2. UV radiation with ozone

UV radiation on ozone in water produces hydrogen peroxide (Equation 2.29 [105]), which in turn produces hydroxyls radicals, according to Equation 2.24.

$$O_3 + h\nu + H_2O \rightarrow H_2O_2 + O_2 \quad 2.29$$

Therefore, UV radiations applied to H_2O_2 (Equation 2.24) or O_3 lead to the production of hydroxyl radicals, which are at the basis of AOPs [105].
This process is effective for potabilization of wastewater, disinfection treatments, decolouration of wastewater coming from paper industry, degradation of aliphatic compounds, chlorinated hydrocarbons and pesticides [160, 161]. Despite the high yield obtained with this kind of process [105], working with ozone always implies some disadvantages [122, 105]:

- Additional equipment and high costs
- Security and health issues
- Limitation in material transfers due to low solubility of ozone in water
- Likely production of VOCs

2.3.3. UV radiation with ozone and hydrogen peroxide

As mentioned in Section 2.2.2, the use of more than one oxidizing agent allows to take advantages of synergic effects which produce additional degradation of organic matter [128]. In this case, light radiation is added to the two oxidants. Processes which involve UV radiation on ozone and hydrogen peroxide are

extremely oxidant because they represent the union of the reactions described in Sections 2.3.1 and 2.3.2. Indeed, UV radiation on both O_3 and H_2O_2 results in the formation of hydroxyl radicals (Equations 2.24 and 2.29) which are responsible for oxidation in AOPs [105], Besides, according to Equation 2.15, hydrogen peroxide is useful to start ozone decomposition in water (Figure 2.2), so the mix H_2O_2/O_3 produces a larger amount of hydroxyl radicals than O_3 only, and a more effective oxidation (degradation) occurs [129].

As well as the UV/H_2O_2 and UV/O_3 processes, the UV/H_2O_2/O_3 treatment is effective for potabilization of wastewater, disinfection treatments, decolouration of wastewater coming from paper industry, degradation of aliphatic and chlorinated hydrocarbons and pesticides [161, 129, 153].

2.3.4. Processes involving TiO_2

TiO_2, titanium dioxide, is a transition metal oxide [162] and a semiconductor, and is involved in photochemical AOPs as the most effective catalyst [104, 163]. TiO_2 is a solid, so the processes in which it is involved are classified as heterogeneous [115]. When TiO_2 is irradiated by UV light (λ=320-380 nm), valence band electrons are exited and promoted to the conduction band, so holes are formed in the valence band [164]. These passages produce charge carriers (h^+ and e^- in Figure 2.5) which carry out a photocatalytic action for oxidation (on the valence band) or reduction (on the conduction band) of the molecules which are adsorbed on the TiO_2 surface [115, 163]. The basic mechanism is shown in Figure 2.5.

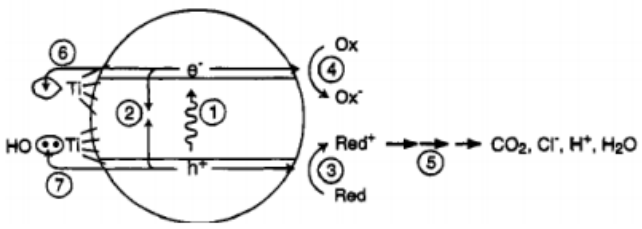

Figure 2.5. Basic mechanism of TiO_2 photocatalytic processes [115]

This treatment presents some limitations mainly due to recovery of TiO_2 microparticles in treated water, so that it should be employed in conjunction with a method which can immobilize the catalyst is necessary [109].

3. FENTON'S REAGENT

Fenton's reagent is a mixture of hydrogen peroxide (H_2O_2) and Fe(II) iron salts which is used to oxidise organic contaminants, thanks to the production of ferric ions and hydroxyl radicals [165].

Henry John Horstman Fenton discovered that many organic molecules are efficiently oxidized in aqueous solution when a water-soluble iron catalyser and hydrogen peroxide are present [166]. When Fenton's processes are carried out without using high temperature or pressure and working with conventional equipment, the best results are obtained at acid pH [167]. In most cases, it was possible to develop detailed kinetic models which demonstrate that oxidation involves various intermediates and elemental steps [155, 168, 107].

A recent investigation [169] has demonstrated that the species responsible for oxidation is the hydroxyl radical OH·. As mentioned in Chapter 2, the ultimate aim of AOPs is the production of hydroxyl radical [105], which is a strong oxidant species [104]. This extremely reactive free-radical is produced by catalytic decomposition of hydrogen peroxide in acid ambient [165] and the presence of a metal is necessary to catalyse this reaction [166]. The involved catalyst is ferrous iron which is generally added in the form of iron sulphate or iron acetate or iron phosphate and it can be associated with other catalytic treatments, for instance UV radiation [168].

Fenton's reaction is a simple redox reaction described in Equation 3.1 [170].

$$Fe_{aq}^{2+} + H_2O_2 \rightarrow Fe_{aq}^{3+} + OH^- + OH\cdot \qquad 3.1$$

According to Equation 3.1, ferrous iron initiates and catalyses the decomposition of H_2O_2, resulting in the generation of a hydroxyl anion and a hydroxyl radical. According to Neyens & Baeyens [171], the generation of OH· radicals gives rise to a complex reaction sequence in aqueous solution, where the Equations 3.1 and 3.2 are also involved.

$$OH\cdot + Fe^{2+} \rightarrow OH^- + Fe^{3+} \qquad 3.2$$

When Fenton's reaction occurs, a cycle of catalyst regeneration can take place in parallel to the degradation process of the organic load [172] and different reactions occur (Equations 3.3-8) [173, 174, 175, 176, 171].

$$Fe^{3+} + H_2O_2 \leftrightarrow FeOOH^{2+} + H^+ \quad 3.3$$

$$FeOOH^{2+} \rightarrow HO_2\cdot + Fe^{2+} \quad 3.4$$

Equations 3.3 and 3.4 (referred to Fenton-like reaction [173, 168]) involve hydrogen peroxide and ferric ions and produce OH· radicals and ferrous ions.

$$Fe^{2+} + HO_2\cdot \rightarrow Fe^{3+} + HO_2^- \quad 3.5$$

$$Fe^{3+} + HO_2\cdot \rightarrow Fe^{2+} + O_2 + H^+ \quad 3.6$$

$$OH\cdot + H_2O_2 \rightarrow H_2O + HO_2\cdot \quad 3.7$$

Equations 3.5 and 3.6 explain how ferrous ion is regenerated. Ferrous ion regeneration is essential for Fenton's reactions because it strongly enhances their performance [170]. Equation 3.7 shows that hydrogen peroxide can also act as an OH· scavenger, not only as an initiator as in Equation 3.1.
OH· is the species which promotes oxidation of organic compounds (RH), leading to the detoxification of water, as described in Equation 3.8 [177, 178, 179].

$$RH + OH\cdot \rightarrow H_2O + R\cdot \rightarrow further\ reactions \quad 3.8$$

In Fenton's reaction, provided the concentration of oxidant and catalyst are not limiting, the organic compounds can be completely degraded by full conversion to CO_2, water and inorganics salts if the treatment is continued [171].
The overall Fenton's reaction (Equation 3.1) was simplified by Walling [119] by accounting for the formation of water (Equation 3.9).

$$2Fe^{2+} + H_2O_2 + 2H^+ \rightarrow 2Fe^{3+} + 2H_2O \quad 3.9$$

This last equation indicates that the decomposition of H_2O_2 can take place in acidic environments. In fact, one of the most important parameters in Fenton's processes is the pH range. For the degradation of organic matter, the best conditions are reached when pH is in a range between 3 and 4, and the mass ratio catalyst/oxidant is 1.5 [167]. Usually, wastewater has a pH higher than that needed for the treatment [180], so that a preliminary acidification and subsequent neutralisation are necessary before the final discharge in the environment, thus increasing operational costs. Anyway, this process allows to reach a satisfactory degradation level of highly refractory compounds, thus decreasing water toxicity to levels which allow a safe discharge of wastewater [181].

Fenton's reaction is employed in several industrial wastewater treatments (from textile, chemical, petrochemical, lather and mechanical industry, dry cleaners, painting works, etc.), in particular on effluents which contain high (or very high) concentrations of organic compounds [182, 183, 184, 185, 160]. Fenton's processes are mainly employed in:

- COD-BOD: oxidation of organic substance (suspended and dissolved) and breakup of complex molecules, thereby increasing biodegradability [175, 185]
- Colour: degradation of chromophore organic molecules [160]
- Surfactants: demolition of aromatic and aliphatic chains [175]
- Phenols: aromatic ring system breakup [181]

However, as highlighted above, one of the most interesting applications is the pre-treatment of industrial wastewater before the biological treatment. Fenton's oxidation increases the wastewater biodegradability degree, so using it before biological depuration is appropriate [185]. By applying this pre-treatment to slightly biodegradable and toxic wastewater, which contains soluble organic matter that can not be removed through physical separation, it is possible to transform organic substances in harmless molecules [175]. It must be underlined, however, that the operational costs are much higher than those of biological treatments [185].

Conventional Fenton's reaction presents two main disadvantages [170]: the first one concerns the ferrous ion regeneration. This step is carried out by thermal

reduction which involves a combination of slow reactions. It may mean that a large amount of catalyst is needed. The second disadvantage is due to possible formation of oxalic acid ($H_2C_2O_4$), which is poisonous and persistent. Its accumulation causes an acidification during the reaction time (to pH=2). In addition, the ferric ion is very efficiently chelated by the oxalate anion, thus reducing the ratio of ferric ion which regenerates ferrous ion. Therefore, all the reactions or processes which can enhance the rate of Fe^{2+} regeneration will accelerate the Fenton reaction.

In the following paragraphs, the main components and issues of Fenton's reaction are explained.

3.1. Hydrogen peroxide: oxidant

In Fenton's regent, H_2O_2 is the oxidant and it acts thanks by the production of hydroxyl radicals, according to Equation 3.1.

An oxidant is a chemical species that removes one or more electrons from another reactant in a chemical reaction. In an oxidation reaction, starting from a substrate, several intermediate species are generally produced in different elementary steps before generation of the final products [186]. The degree of reaction progress depends on the oxidant/substrate ratio, because when oxidant ends the reaction stops. For instance, in a typical application the following series of steps will occur:

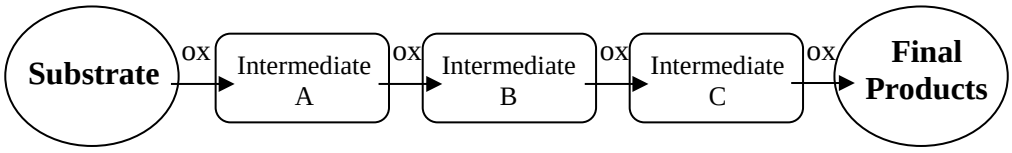

Figure 3.1. Typical oxidation reaction pathway

Each transformation in this series (Figure 3.1.) has its own reaction rate. Oxidation of contaminants in wastewater may lead to the production of unknown intermediates, which may be toxic or harmful. Therefore, if contaminants and oxidation pathways are known, it is important that sufficient H_2O_2 is added to push the reaction to harmless intermediate or known final products [175]. By increasing the hydrogen peroxide dosage, a steady reduction in COD may occur

with little or no change in toxicity until a given threshold, whereupon further addition of H_2O_2 results in a rapid decrease in wastewater toxicity [118].
The main properties, that characterise hydrogen peroxide as a good oxidant, are listed below:

- It is highly water-soluble
- It is not catalogued as a contaminant, so when active oxygen gets free only water is generated as sub-product
- It does not produce toxic or coloured sub-products
- It is very inexpensive compared with other oxidant agents
- It is user-friendly

Hydrogen peroxide oxidation reactions with organic substrates are generally slow and this may help to explain its relatively low toxicity [118].

3.2. Iron: catalyst

Iron is an essential part of the Fenton's mixture, as Fenton discovered in 1894, without iron there is no evidence of hydroxyl radical formation when H_2O_2 is added to organic wastewater. As the iron concentration is increased, organic compound removal is accelerated until a point where further addition of iron becomes inefficient [166]. Reaching an optimal dose range for iron catalyst is fundamental for Fenton's reagents. In particular Bishop, et al. [118], have evaluated that the best ratio catalyst/oxidant is 1.5.
For most applications, it does not matter whether Fe^{2+} or Fe^{3+} salts are used to catalyse the reaction, however if low doses of Fenton's reagent are being used (e.g., <10-25 mg/L H_2O_2), the ferrous iron may be preferred [118]. Neither does it matter whether a chloride or acetate or sulphate or phosphate salt of iron is used, but in some applications (for instance, photo-Fenton), ions resulting from salts may inhibit the oxidation [187, 188]. It is fundamental to choose iron species as a function of pH [170]. The spontaneous chemical oxidation of ferrous to ferric iron by O_2 is a complex process which involves intermediate species which are difficult to characterise or predict. Moreover, it depends on pH, temperature, solution composition and oxidation rate [189].

3.3. Temperature

As Bishop at al. [118] demonstrated (and in accordance with expectation), the rate of the reaction increases by increasing the temperature. The ferric ion produces a rapid oxidation at ambient temperatures, while ferrous ion catalyst system requires elevated temperatures to produce significant oxidation rate. On the other hand, between 40 and 50 °C the efficiency of H_2O_2 utilization is reduced due to its accelerated decomposition into oxygen and water. Therefore, most of the commercial applications of Fenton's reagent are carried out at temperatures between 20-40 °C [118].

3.4. pH

As mentioned above, the pH affects the efficacy of the reaction. Several studies have been carried out about the effect of pH on Fenton's reaction for the degradation of organic compounds in water [190, 191, 118]. As a result, the maximum organic removal (measured by COD), thus the maximum oxidation efficiency, occurred in the 3-5 pH range. At pH<3 the dominant iron species is Fe^{3+}, the regeneration of Fe^{2+} being thus limited. The low efficiency at pH>5 is ascribed to the precipitation of ferric ion as hydroxide, thus making critical the decomposition of H_2O_2 (Equation 3.1) [190]. Moreover, according to Bishop et al. [118], the reason for the inefficient degradation at pH>4 is due to rapid decomposition of H_2O_2 to give essentially O_2 and H_2 molecules, without appreciable amounts of hydroxyl radicals in the solution. Therefore, according to these authors the optimum pH for Fenton's reactions is between 3 and 4.

3.5. Fenton's processes

As mentioned above, every reaction or process which accelerates Fe^{2+} regeneration enhances the performance of Fenton's reaction. A conventional Fenton's reagent can be employed in conjunction with different energy sources or processes which act as further catalysers, enhancing the oxidation performance by promoting ferrous ion regeneration. The main modified processes are: sono-Fenton, electro-Fenton and photo-Fenton, described below.

3.5.1. Electro-Fenton

Electro-Fenton is an AOP in which Fenton's reagent is associated to an electrochemical process. At the base of this process there is the Fenton's reagent regeneration by electrochemical reactions between and anode and a cathode [192].

At the cathode Fe^{3+} is reduced to Fe^{2+}, according to the electrochemical process of Equation 3.10 [193].

$$Fe^{3+} + e^{-} \rightarrow Fe^{2+} \qquad 3.10$$

The generation of Fe^{2+} accelerates the production of hydroxyl radicals, as shown in Equation 3.1.

Moreover, according to Brillas et al. [192], electro-Fenton processes are based on the cathodic electro-generation of hydrogen peroxide. In acid aqueous solution, H_2O_2 can be continuously supplied from the reduction of oxygen gas (Equation 3.11 and 3.12 [194]). Oxygen can be directly injected as pure gas or bubbled air.

$$O_{2(g)} + 2H^{+} + 2e^{-} \rightarrow H_2O_2 \qquad 3.11$$

As the Equations 3.11 shows, the production of hydrogen peroxide is possible in acid medium. In alkaline solution, oxygen gas is reduced to hydroperoxide ion (HO_2^{-}), thus providing he formation of hydrogen peroxide does not occur [192], and production of hydroxyl radicals (Equation 3.1).

At the anode (M) the hydroxyl radical is heterogeneously produced from water oxidation, according to the reaction of Equation 3.12 [195].

$$M + H_2O \rightarrow M(OH^{\cdot}) + H^{+} + e^{-} \qquad 3.12$$

This reaction enhances the degradation of organic compound, thanks to the increase of hydroxyl radicals in the solution.

Electro-Fenton is one of the powerful and environmental-friendly emerging technologies for the remediation of wastewaters containing organic, especially aromatic compounds [196]. Several studies have been carried out to analyse electrochemical processes performances and COD reduction resulted to range

between 41% and 99% for treatments based on different wastewater types, energy consumptions, reaction times, etc. [197, 198, 199, 200]. Kurt, et al. [201] carried out a study in which the efficiency of pollutant removal was evaluated as a function of different variables, such as oxidant doses, energy consumption, reaction time, etc. The main result was that the COD removal did not show any proportionality whith these variables. Anyway, electro-Fenton gave the best results: over 70% of COD removal occurs at pH 3, and over 60% at neutral pH [201].

3.5.2. Sono-Fenton

Sono-Fenton processes associate Fenton's reagent with sonochemistry. Sonochemistry is a term used to describe the effect of ultrasonic sound waves on chemical reactivity [202]. Ultrasounds have a frequency between 20 kHz and 500 MHz, that is in a range that can not be heard by humans (whose normal range of hearing is between 16 Hz and 16 kHz) [202].

Ultrasounds irradiation on wastewater can directly degrade organic pollutants and produces hydroxyl radicals from water, thus promoting further degradation [203]. This process is called sonolysis and it is principally based on transient cavitation. Cavitation is a phenomenon which involves three phases: nucleation (formation), growth and an adiabatic implosive collapse of a gas or vapor bubble [204]. These phases are driven by ultrasound-induced pressure variation in the solution, as shown in Figure 3.2.

Gas pockets trapped in the crevices of solid boundaries of the reaction system constitute the nuclei for cavitation. The growth of the bubble is accompanied by evaporation of a large amount of solvent at the bubble interface (or bubble wall), and diffusion of solvent vapor toward the core of the bubble [205]. During the collapse phase, not all the vapor molecules can diffuse back to the bubble wall and condense [206]. A significant fraction of vapor remains inside the bubble when the bubble motion becomes extremely fast during the final moments of compression. Temperature and pressure inside the bubble in extreme conditions can reach value as high as of 5000 K and 500 atm [207]. The solvent vapor entrapped inside the bubble is subjected to these extreme conditions and undergoes thermal dissociation resulting in a variety of chemical species, also including radicals.

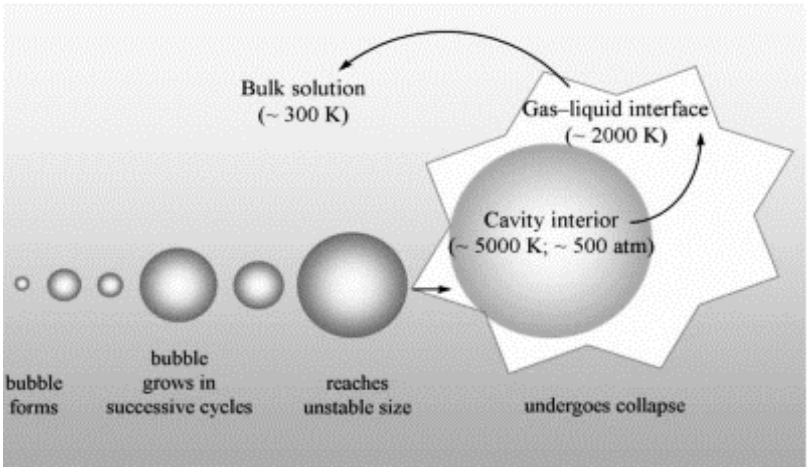

Figure 3.2. Phases of cavitation [204]

When ultrasounds are used as a single treatment, they determine a low mineralization efficiency and a high energy consumption [208]. By combining ultrasounds irradiation with Fenton's reaction (sono-Fenton process) a faster pollutant mineralization is obtained, due to a higher generation of hydroxyl radicals and the regeneration of ferrous ion [209]. The main reactions produced in the system are listed below [203]:

$$Pollutant +))) \rightarrow Degradation\ Products \quad 3.13$$

$$H_2O +))) \rightarrow H^{\cdot} + OH^{\cdot} \quad 3.14$$

$$Pollutant + OH^{\cdot} \rightarrow Degradation\ Products \quad 3.15$$

$$H_2O_2 +))) \rightarrow 2OH^{\cdot} \quad 3.16$$

$$H_2O_2 + OH^{\cdot} \rightarrow H_2O + OOH^{\cdot} \quad 3.17$$

$$Fe^{3+} + H_2O_2 \rightarrow Fe(OOH)^{2+} + H^{+} \quad 3.18$$

$$Fe(OOH)^{2+} +))) \rightarrow Fe^{2+} + OOH^{\cdot} \quad 3.19$$

where))) refers to ultrasound waves. Equations 3.13-15 describe the sonolysis effect on pollutants only due to ultrasound waves. The simultaneous presence of Fenton's reagent leads productions of Fe^{3+}, OH^- and OH· according to Equation 3.1. These products (together with H_2O_2 and Fe^{2+}, see Equations 3.16-19) cause a sizeable increase of the degradation rate of pollutants.

According to Adityosulindro, et al. [203], the mechanism of Equation 3.19 is not yet fully established, although several studies have investigated the sono-Fenton process for the degradation of various organic compounds (phenolic compounds, pesticides and pharmaceuticals) [210, 211, 212, 213].

3.5.3. Photo-Fenton

The photo-Fenton process is an AOP which involves Fenton's reagent and UV-visible radiation. Despite the precise mechanism of photo-Fenton reactions is not yet fully understood, among Fenton's processes, it seems to be the most promising for practical industry application [214, 215]. Classical Fenton's reaction (Equation 3.1) is carried out with UV-visible radiations which accelerate the rate of degradation of a variety of pollutants [214]. This is possible thanks to the photochemical reduction of Fe^{3+} back to Fe^{2+}, according to Equation 3.20.

$$Fe_{aq}^{3+} + H_2O \xrightarrow{h\nu} Fe_{aq}^{2+} + OH\cdot + H^+ \qquad 3.20$$

Besides, UV radiations have a direct effect on H_2O_2, causing dissociation of the O-O bond to give two hydroxyl radicals (Equation 3.21), thus enhancing the oxidation rate [216].

$$H_2O_2 \xrightarrow{h\nu} 2OH\cdot \qquad 3.21$$

As mentioned above, conventional Fenton's reactions reach the best performance in the 3-5 pH range [167]. Machulek et al. [170] studied how the pH affects photo-Fenton's reaction and they concluded that the optimum is reached when pH=3. The explanation can be traced back to the concentration trends of the main Fe^{3+} species as a function of pH (see Figure 3.3 and 3.4). At pH≤2, the dominant species is Fe^{3+} which weakly absorbs above 300 nm, thus reducing the

regeneration ratio of ferrous ion (Equation 3.20). At pH>3 the formation of colloidal iron hydroxide ($Fe(OH)_3$) occurs and that causes the precipitation of hydrated iron oxides. The precipitation of iron species determines a reduction of catalyst doses in the reaction system, thus leading to a worsening in performance. At pH=3 the predominant Fe^{3+} species is $Fe(OH)^{2+}$ which absorbs throughout much of the ultraviolet spectral region [217]. $Fe(OH)^{2+}$ is a very important species for the photo-Fenton performance, because it undergoes photolysis, leading to the reaction in Equation 3.22.

$$Fe(OH)^{2+} \xrightarrow{h\nu} Fe^{2+} + OH\cdot \qquad 3.22$$

Therefore pH=3 is the optimum in photo-Fenton's reactions, because $Fe(OH)^{2+}$ (under UV-visible radiation) leads both to the ferrous ion regeneration and formation of hydroxyl radicals, thus strongly enhancing the reaction.

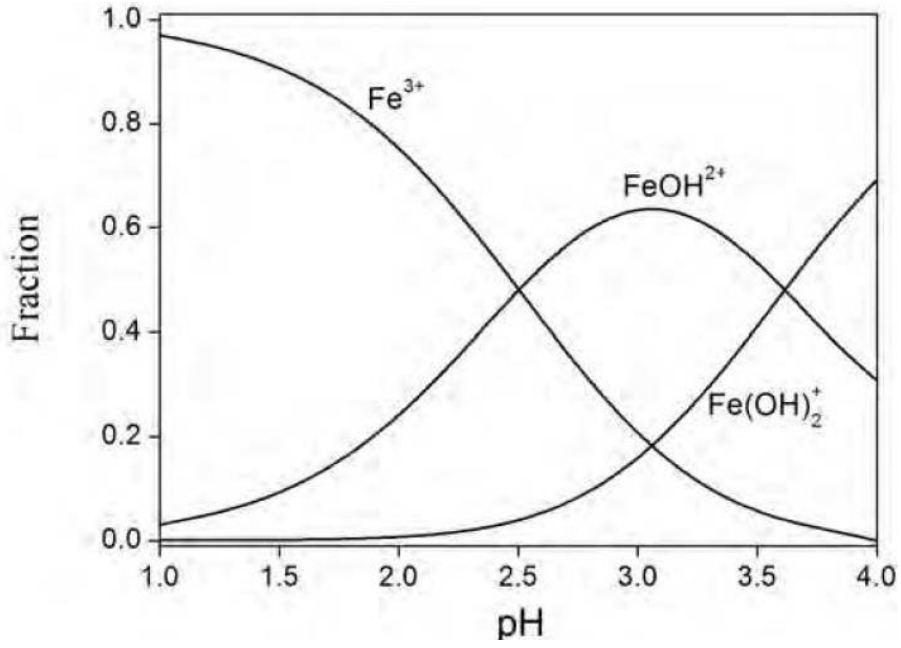

Figure 3.3. Speciation of Fe^{3+} as a function of pH [170]

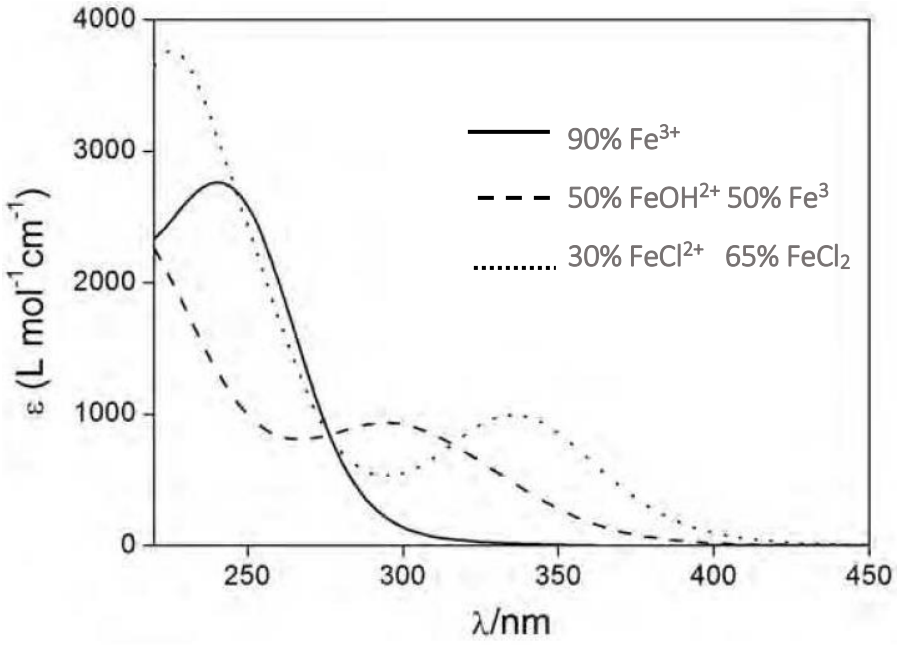

Figure 3.4. Absorption spectra of 0.43 mM Fe^{3+} perchlorate under [170]

The good performances that results by combining UV-visible radiation light to Fenton's reaction are due to several factors:

- It is sufficient a catalyst concentration lower than that used in conventional reactions because UV-visible radiations allow ferrous ion regeneration (Equation 3.20)
- The regeneration of ferrous ion is accompanied by additional formation of hydroxyl radicals (Equations 3.20 and 3.22)
- UV light promotes the production of hydroxyl radicals by direct decomposition of H_2O_2 (Equation 3.21)
- Residual Fe^{3+} can be recovered by increasing the pH, thus causing its precipitation as iron hydroxide. Residual H_2O_2 is spontaneously and environmental-friendly decomposed in water and molecular oxygen [170].

By comparing photo-Fenton to conventional Fenton's reaction, the former presents many advantages [218]:

- The degradation rate is many times higher

- Operational costs are significantly lower due to a lower chemical consumption
- The photo-Fenton process leads to negligible formation of sludge, whilst the classical Fenton entails a wearisome and costly removal of the sludge
- Oxalic acid is not a recalcitrant intermediate, but can act as catalyst [170]

Further attention has to be paid to this last point. As mentioned in Chapter 3, $H_2C_2O_4$ is a possible intermediated of conventional Fenton's reactions and it reduces the ratio of ferric ion in solution, thus worsening the performance. In a study conducted in 1998, the photo-Fenton process has been applied on municipal water and the authors found that the energy efficiency was 30% higher when oxalate was presented in water [219]. This effect has been attributed to ferrioxalate species (the same species which inhibit conventional Fenton's reaction) which catalyse the photo-Fenton process by absorption of both UV and visible light. This high sensitivity would allow the application of sun as a radiation source, thus reducing operational costs. According to a most recent study, the presence of ferrioxalate in wastewater increases the mineralization of organic compounds from the 18-21% to 80.6% [220].

In spite of many advantages, the photo-Fenton process presents some relevant limitation. It is important to pay attention to some operational choices, because some species which inhibit the reaction may be produced. The first species is the chloride ion. In presence of this species the time required is comparable to that of thermal reactions (in presence or absence of chloride ion) [170]. Several studies [221, 222, 223, 224] show that the worsening of the performance is due to the preferential formation of $Cl_2^{\bullet -}$ radical anion instead of $OH^{\bullet}$. This means that, after a certain period of reaction, hydroxyl radicals are not formed, thus leading to the end of the degradation process.

Another inhibition of the photo-Fenton reaction is due to the sulphate anion (SO_4^{2-}) [170]. This anion is often present in photo-Fenton reactions because, as mentioned in Section 3.2, iron can be added in the form of different salts, including the relatively cheap sulphate. According to Benkelberg & Warneck [187] and Lee, et al. [188], the sulphate anion form a complex with the Fe^{3+} ions over a wide pH range, thus preventing their reduction to ferrous ions.

This technology resulted to be adequate to treat industrial water and leaching water from agricultural soils (with nitroaromatic compounds, polychlorinated phenols and pesticides) and several studies were carried out to evaluate its performance for the degradation of many organic compounds [218, 225, 226, 106, 191, 159, 182, 181].
However, the application of the photo-Fenton process to treat and decontaminate wastewaters on a large scale is not actually possible [227]. The main issues are:

- The total mineralization of organic compounds in the effluents needs long irradiation periods
- The electrical power consumption of a lamp-based photochemical reactor determines up to 60% of the total operating cost

Over the last few years, some studies were carried out to evaluate the effectiveness of solar reactors or hybrid lamp/solar reactors [226, 191, 182], or to develop photocatalysts that operate effectively under solar irradiation [228]. These two points are key issues for solving the problem of photo-Fenton applicability on large scale. At least, improvements in the photoreactor design are necessary. Nevertheless, the photo-Fenton process is actually the most promising AOP for practical industry applications.

4. OBJECTIVES

The main purpose of this study is to degrade caffeine in water, which is a contaminant of emerging concern (CEC), to evaluate the possibility of its elimination from wastewater, thus reducing the related environmental impacts. With this aim, we studied the degradation of caffeine in water solution under the attack of an advanced oxidation process (AOP). The AOP used in the experiments was a photo-Fenton reaction, which involves hydrogen peroxide (H_2O_2) as oxidant species, the ferrous ion (Fe^{2+}) as catalyst and UV-visible radiation to enhance the rate and the effectiveness of the process. Two different studies were carried out to analyse different aspects of the degradation.

The first aspect of the present study concerns phenomenological issues about the reaction of degradation, to evaluate water quality after the process. The photo-Fenton process was carried out in a reactor containing a caffeine water solution and Fenton's reagent. During the reaction, conductivity, turbidity, colour and aromaticity were measured to analyse their variation during the oxidation process, in order to understand how the reaction affects the quality of water.

Another important aspect of this work is concerned with the kinetics of degradation. Reactions were carried out in cuvettes containing caffeine, H_2O_2 and Fe^{2+}, and irradiated with UV-visible light. The kinetics of degradation were followed through measurements of a physico-chemical property (absorbance at 272 nm) as a function of time, not by direct measurements of caffeine concentrations. Absorbance is a suitable property, because it is proportional to concentration, provided the latter are sufficiently small that the Lambert-Beer law holds. Absorption spectra of caffeine, hydrogen peroxide and ferrous ion were recorded and analysed with the aim to select a suitable wave length for the measurement of the extinction coefficient as a function of time.

In order to analyse the two aspects listed above, two main experimental series were carried out: the first one by changing the oxidant concentration with a fixed amount of catalyst, and second one by changing the catalyst concentration with a fixed amount of H_2O_2. In both cases a constant concentration of caffeine was used. This experimental scheme was adopted with the aim to evaluate the effects of the oxidant and catalyst doses both on the parameters of water during the reaction and on the caffeine degradation rate, in addition to the order of reaction.

The project aimed at studying the degradation of caffeine was born at the Faculty of Engineering of the University of Basque Country (UPV/EHU), in Vitoria-Gasteiz, during an Erasmus stage (April-September 2017). During this period the phenomenological issues about the way the reaction affects the quality of water were analysed. The kinetic investigation through UV spectroscopy was devised and carried out at the Department of Chemistry G. Ciamician of the University of Bologna (Unibo), Italy.

5. MATERIALS AND METHODS

As mentioned in Chapter 4, the project aimed at studying the degradation of caffeine was born at the Faculty of Engineering of the University of Basque Country (UPV/EHU), then, the kinetic investigation through UV spectroscopy was devised and carried out at the Department of Chemistry G. Ciamician of the University of Bologna (Unibo), Italy. Therefore, different analyses were carried out in the two laboratory to describe the degradation of caffeine oxidised by a photo-Fenton process. In both cases, analyses were carried out using a caffeine aqueous solution and Fenton's reagent (H_2O_2/Fe^{2+}) in different doses. Initial solutions were prepared by dissolving caffeine and iron sulphate heptahydrate in water and diluting hydrogen peroxide. Different dosages of each initial solution were used to develop experimental essays with different concentrations of oxidant and reagents.

5.1. Analyses at the University of Basque Country

At the Faculty of Engineering of the University of Basque Country the photo-Fenton processes on water/caffeine solutions were carried out using the reaction system displayed in Figure 5.1. As shown in the scheme of Figure 5.1, different instruments have been assembled: cryo-thermostat bath (Frigitem-10 Selecta), tube and shell reactor (TQ-150 Heraeus). Two series of experiments were carried out to investigate on the effects produced by the oxidant and the catalyst concentration on water parameters. The first series involves experiments in which the catalyst dosage is constant, and the oxidant dosage is changed. On the contrary, in the second series the oxidant dosage is constant, while the amount of catalyst is changed. Reagents were mixed in a reactor and the total volume of every reaction was 870 mL. Different portions of initial solutions were taken to reach the following concentrations:

1st experimental series:

- Caffeine (Ca_0) 0.592 10^{-3} M
- Catalyst (Fe^{2+}) 0.2 10^{-3} M
- Oxidant (H_2O_2) 0.0 M
  4.0 10^{-3} M
  6.0 10^{-3} M
  8.0 10^{-3} M
  10.0 10^{-3} M
  15.0 10^{-3} M

2nd experimental series:

- Caffeine (Ca_0) 0.592 10^{-3} M
- Oxidant (H_2O_2) 15 10^{-3} M
- Catalyst (Fe^{2+}) 0.0 M
  0.1 10^{-3} M
  0.4 10^{-3} M
  0.4 10^{-3} M
  0.6 10^{-3} M
  0.8 10^{-3} M

Reagents were mixed in a photocatalytic reactor provided with an UV-visible mercury quartz lamp (TQ-150 W Heraeus), shown in Figure 5.2. The caffeine aqueous solution was homogenized by a magnetic stirrer (Agimatic P-Selecta), then catalyst and oxidant were added in different dosages depending on each experimental assay. Each experiment started by turning on the UV-visible light. The experiments were carried out at constant temperature (25 °C) fixed with a cryo-thermostat bath, and a pH=3. This operating pH was continually monitored, 0,2-M NaOH and 0,1-M HCl being manually added to keep is constant.

Throughout the reaction, the solution was sampled to measure different parameters. First of all, the extent of caffeine degradation was evaluated by measuring its concentration with High Performance Liquid Chromatography (HPLC). Moreover, four parameters (conductivity, turbidity, colour and aromaticity) were measured to evaluate their changes during the reaction. Each parameter was measured before the start of the reaction (t=0), then the solution was sampled at intervals of about 1 minute at the beginning of the reaction, then of 10 minutes, for two hours.

The features of the UV-visible lamp are listed below:

- Hg medium pressure
- 95% of transmission between 300 nm and 570 nm
- Voltage = 230 V/50 Hz
- Intensity = 2.5 A
- Power = 150 W

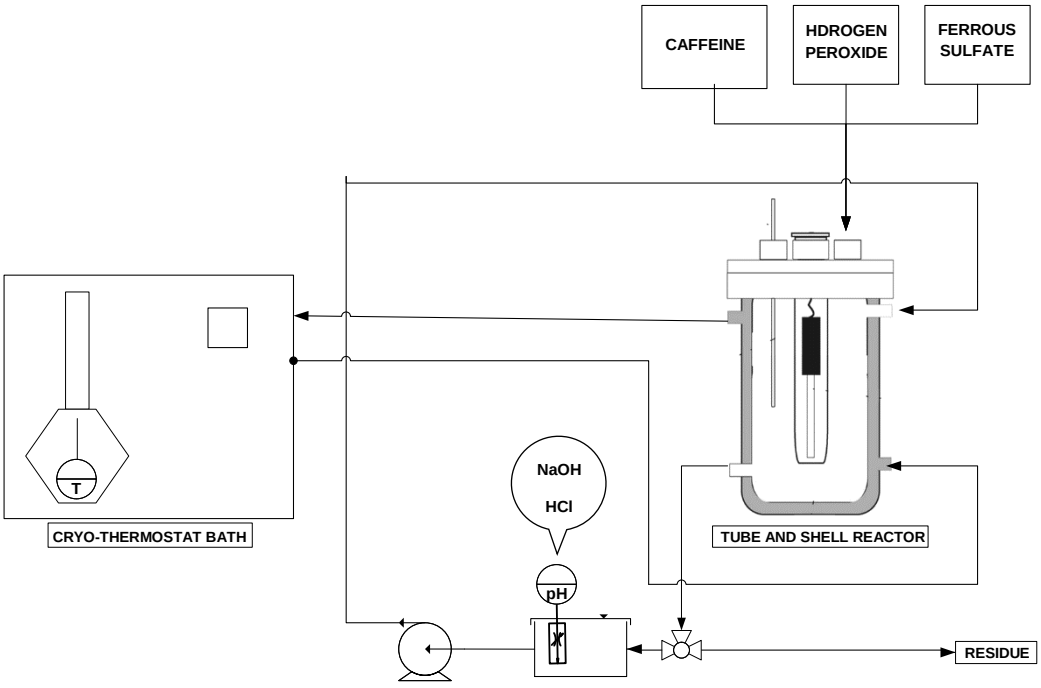

Figure 5.1. Experimental equipment used for caffeine oxidation essays

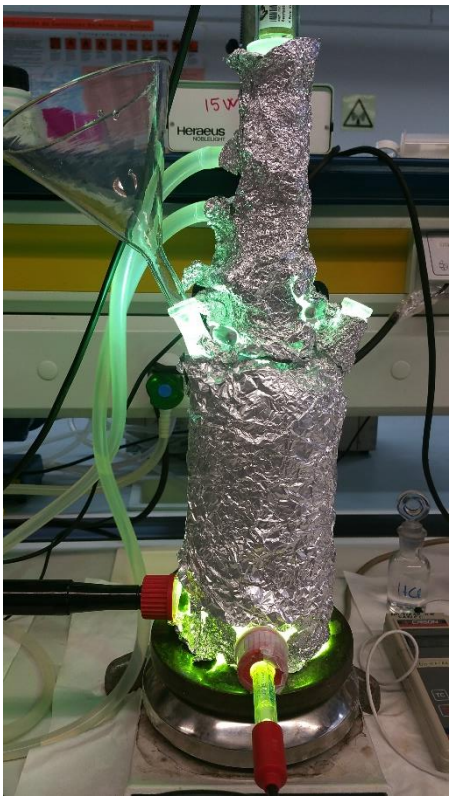

Figure 5.2. Photocatalytic reactor with a UV-visible 150-W lamp

5.1.1. High performance liquid chromatography

The caffeine concentrations were determined with High Performance Liquid Chromatography (HPLC) using an Agilent Technologies apparatus (1200 Series). HPLC is generally used for qualitative and quantitative analysis, thus playing a key role in analytical methods. It is based on differential migrations of sample components which are distributed between a stationary and mobile phase depending on their affinities for the two phases [229]. In HPLC, both phases are liquid, and the stationary phase is detained in the instrument before a column, whereas the mobile phase moves along that column in only one direction. Solutes have different migration velocities depending on their partition between the two phases. On the basis of the properties of the analyte, in this case caffeine, it is necessary to choose appropriate phases for the success of the analysis. Considering a one-solute system, this solute (A) is distributed between the stationary (s) and mobile (m) phases, according to the partition coefficient (K_D):

$$K_D = \frac{[A]_s}{[A]_m} \qquad 5.1$$

High K_D values imply that the solute is preferentially distributed in the stationary phase, so that it moves slowly along the column. On the contrary, low K_D values imply that the solute has little affinity for the stationary phase and moves quickly. The time necessary to move along the column is the retention time and it is specific for every analyte. As represented in Figure 5.3, an HPLC instrument includes some fundamental tools, such as an injection unit, a column, an in-line detector and a device for displaying the detector signals.

Moreover, it is worth to point out an important technical consideration. Between the points where the sample is introduced and detected, the "dead volume" (that is, the empty space between these two points) should be as small as possible because it can lead to losses in efficiency. For this reason, it is important that an HPLC equipment includes a degasser. Other sources of dead volume can in principle be the injection unit, the tubing and the detector cell. However, these parts are generally designed with internal volumes as small as possible, so that the presence of dead volumes is minimized [230].

Figure 5.3 shows a generic HPLC apparatus. In this case, the instrument is equipped with a manual injection system for introducing samples into the column, and the detector is linked with a computer that, through a dedicated software, shows and saves the measured signals. The HPLC instrumentation used in this research is shown in Figure 5.4.

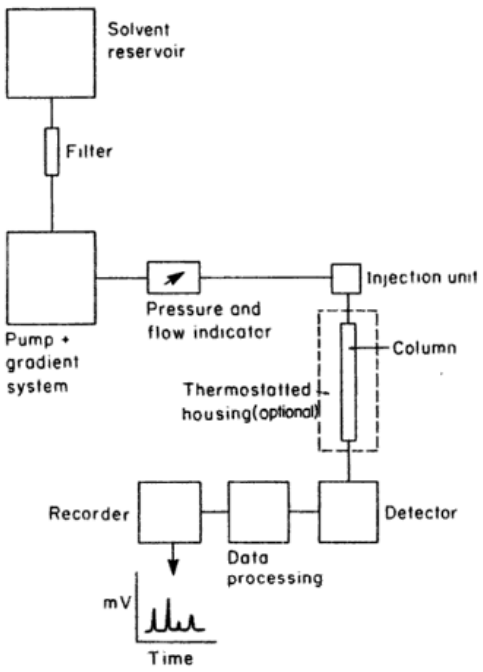

Figure 5.3. High Performance Liquid Chromatography equipment [230]

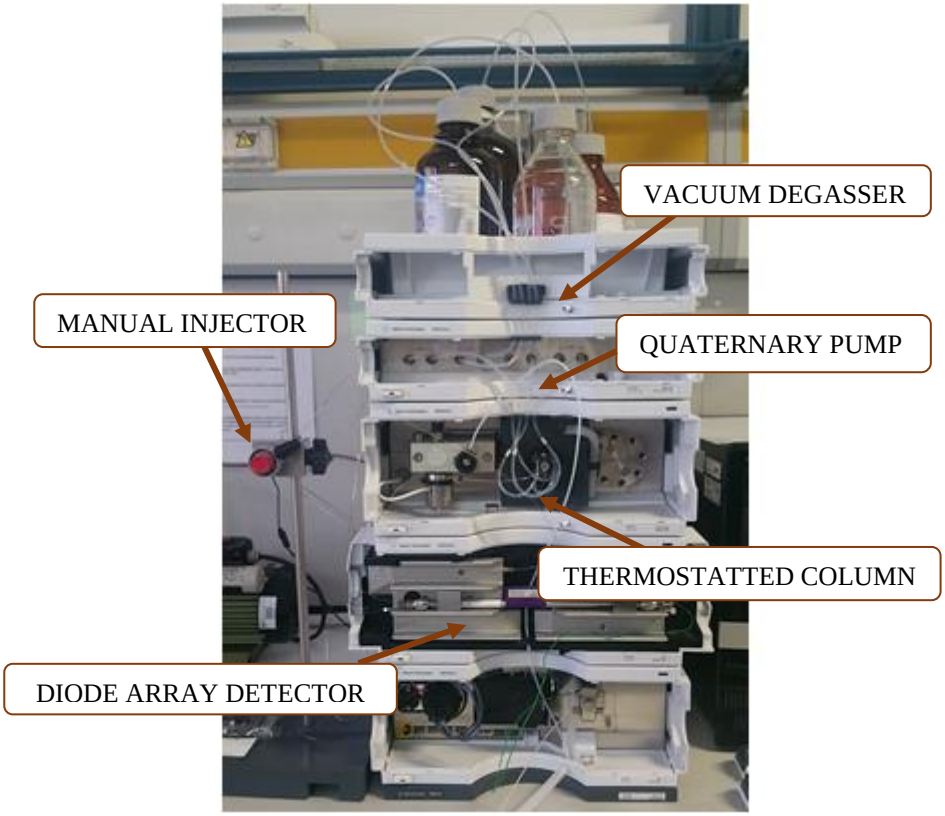

Figure 5.4. High Performance Liquid Chromatograph (Agilent Technologies 1200 Series)

Specific HPLC tools are listed below:

- Manual injector: this tool allows to introduce the sample into the instrument to start the analysis. To avoid injection of air, the injector is always closed by a cap, and it is opened only when a known volume of sample is injected with a syringe.
- Vacuum degasser: a pump system sucks up the solvent from its reservoir, then the solvent passes through specific plastic membranes of the vacuum container. While the solvent moves along vacuum tubing, dissolved gases pass through these membranes and they run into a vacuum container, so the solvent is degassed.
- Quaternary pump: this pump is composed of solvents reservoirs, a vacuum degasser and a pump with a gradient system. Quaternary pump includes a high-speed partition valve and a pump station, and its function consists in creating solvent flows used for the analysis.

- Thermostatted column compartment: it allows to control the temperature of the column. Its purpose is to ensure the reproducibility of the retention time, heating and cooling the column.
- Diode array detector: the detector design allows to get the best optical performance. Its radiation source is composed of a deuterium arc discharge lamp, which emits light in the ultraviolet wavelength range, and a tungsten lamp which emits in the visible and near infrared range. In a spectrophotometer, polychromatic light passes through a cell where a grating separates the different wavelengths of the beam. The intensities are measured by an array or photodiodes.

In this study, quantitative analysis of caffeine was performed using HPLC coupled with an UV-Visible light spectrophotometer. Chromatographic components and analysis conditions are listed below:

- Quaternary pump propulsion system Agilent Serie 1200
- 5.0 µm diameter Phenyl C_{18} column WATERS
- Dual wavelength Diode Array Detector (DAD) and Multiple Wavelength Detector (MDW) Agilent 1200

Operating conditions:

- Eluent composition MeOH/H_2O
- Proportion 40/60
- Flow 1.0 mL/min
- Pressure 3000-3300 psi
- Manual injection volume 25 µL
- Temperature 25.0 °C
- Wavelength 280 nm

The analyte quantitative analysis has been made with the calibration curve shown in Graph 5.1:

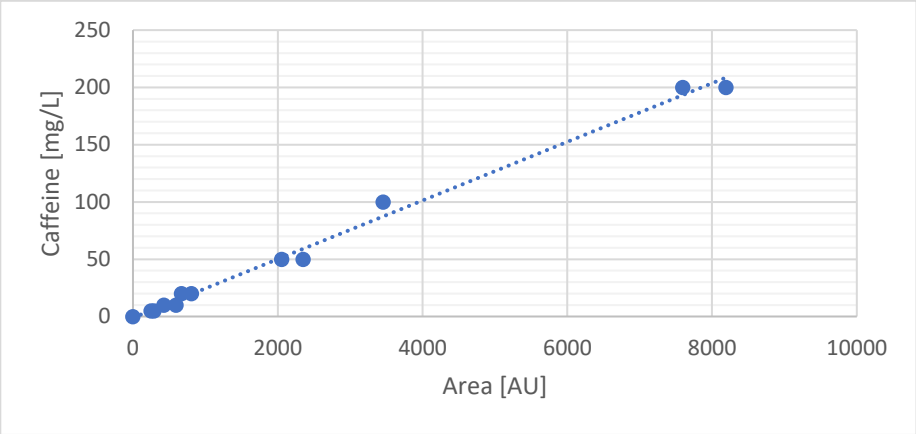

Graph 5.1. Caffeine calibration with HPLC

Points in Graph 5.1 lead to the following straight-line equation:

$$Caffeine\ \left[\frac{mg}{L}\right] = 0{,}0256\,A - 1{,}1032 \qquad 5.2$$
$$R^2 = 0{,}9932$$

where A is the area of the peak [Arbitrary Units].

5.1.2. pH monitoring

As mentioned in Section 3.5.3, the photo-Fenton process presents the best performance in a pH range between 3 and 5, in particular at pH=3. In order to reach and keep this value the pH was constantly monitored with a pH-meter. A pH-meter is a voltmeter sensitive to the concentration of H^+ ions. The measured pH (defined as –log [H^+]) of a solution normally falls in the 0-14 range [231]. pH monitoring into the photolytic reactor was obtained with the pH-meter (Basic 20 Crison) shown in Figure 5.5. The desired pH conditions were reached and kept adding diluted NaOH or HCl to the solution (respectively, to rise and reduce pH) with a Pasteur pipette.

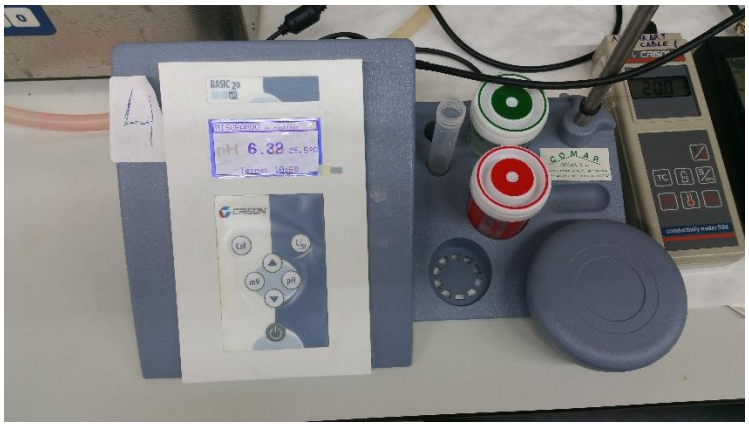

Figure 5.5. pH-meter Basic 20 Crison

5.1.3. Temperature monitoring

As mentioned in Section 3.3, most of the commercial applications of Fenton's reagent are carried out at temperatures between 20 and 40 °C. In this study, the temperature was monitored and kept constant at 25 °C by using a refrigerated recirculation bath (Frigiterm-TFT-30-Selecta). A peristaltic pump permits water recirculation, keeping a constant reaction temperature (Figure 5.6). The thermostat bath is also equipped with an agitation/recirculation pump which allows water recirculation in an external circuit. The current water temperature is indicated on the screen as PV (Point Value) and the target water temperature is indicated as SV (Set Value).

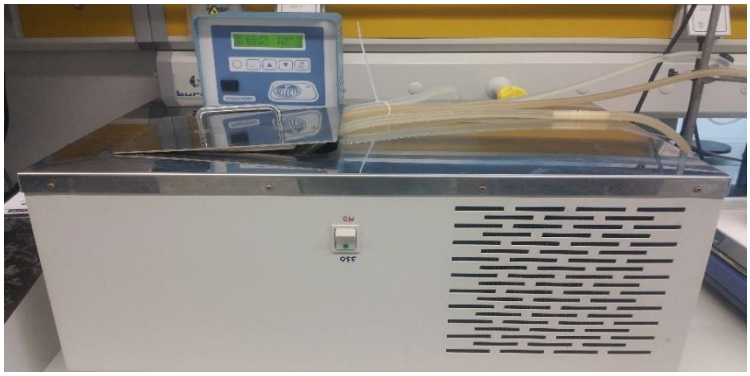

Figure 5.6. Refrigerated recirculation bath Frigiterm-TFT-30-Selecta

5.1.4. Conductivity

According to Ohm's law:

$$i = \frac{\Delta\phi}{R} \qquad 5.3$$

where i is a current intensity [Coulomb $s^{-1} \equiv$ Ampere], $\Delta\phi$ is a potential difference [Joule/Coulomb ≡Volt] and R is a resistance [Ohm], which is proportional to the length (r) and inversely proportional to the cross-section area (A) of a conductor. The specific resistance is the resistance normalizer per unit length and surface.

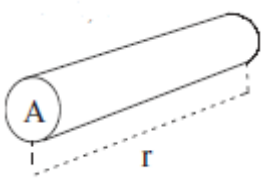

$$R \cdot \frac{A}{r}\ [Ohm\ cm] \qquad 5.4$$

Conductivity [$Ohm^{-1}\ cm^{-1} \equiv$ Siemens cm^{-1}] is the inverse of the specific resistance

$$Conductivity = \frac{1}{R}\frac{r}{A} \qquad 5.5$$

that is, the conductance of electrolytes in solution normalized per unit surface and distance between electrodes of a cell, where the conductance [$Ohm^{-1} \equiv$Siemens] is simply the inverse of resistance

$$\frac{1}{R} = \frac{i}{\triangle\phi} \qquad 5.6$$

The conductivity of a solution is proportional to the ion concentration and the ionic equivalent conductivity [$Ohm^{-1}\ cm^{-1}$ /equivalent $cm^{-3} \equiv Ohm^{-1}\ cm^2\ equiv^{-1}$] is the conductivity normalized for the concentration of charges [equivalent cm^{-3}]. The equivalent conductivity is different for different ionic species, because of their different frictional coefficients which determine different transport velocities. Solutions of most inorganic compound are relatively good

conductors, conversely, molecules of organic compounds that do not dissociate in aqueous solution conduct a current very poorly, if any [232].

Conductivity is a parameter useful to evaluate many aspect of water quality, in particular: define the mineralization level of water, evaluate variations in concentration of a mineral dissolved in water, establish the total dissolved solids concentration in water and the concentrations of either cations or anions in a water sample [232].

In this study conductivity measurements were carried out with a Crison Conductivity Meter 524 (Figure 5.7). This is a portable instrument whose electronic system is based on SMD technology (Surface Mounting Device). It includes a device able to set the desired analysis conditions, a display, and a graphite probe provided with an automatic temperature compensation, so all values read on the display are automatically compensated for temperature variation.

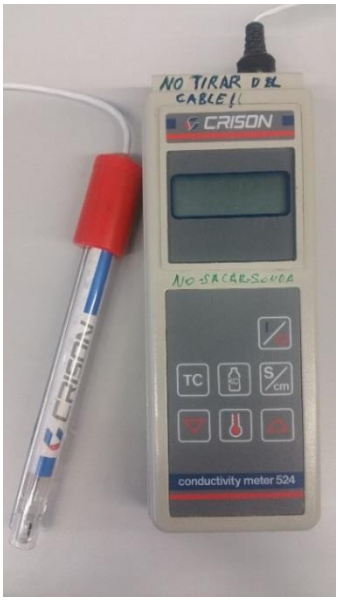

Figure 5.7. Conductivity Meter 524 Crison

5.1.5. Turbidity

Turbidity depends on suspended particles in water and its measure reflects the cloudiness degree of a water sample. It is not to be confused with suspended solids, because these are expressed in terms of weight of suspend material in a liquid sample. Instead, turbidity is an optical property measured in terms of light scattered from this material. In simple terms, suspended particles scatter or absorb

light rays, so the water appears cloudy. Low-turbidity is typical of a clear water, where very little light is scattered, while high-turbidity (cloudy water) is associated with a lot of suspended particles that scatter light. Turbidity is expressed in Nephelometric Turbidity Units (NTU) and its analysis is significant mainly in connection with public health hazard [231].

In the current study, turbidity analysis has been carried out with a nephelometric turbidimeter (2100Q-Hach) provided with a 10-ml glass sample cell (Figure 5.8). Turbidity is measured by the ratio between the light reflected at 90 °, due to suspended particles, and the incident light.

Figure 5.8. Turbidimeter 2100 Q-Hach

5.1.6. Colour

Water colour results from the presence of different species. It is related to turbidity, because suspended particulate scatters the light transmitted through the liquid, thus altering its colour. Therefore, it is possible to define the difference between true colour and apparent colour. The first is the water colour measured in a sample after pre-treatment with the aim to remove colloidal or suspended sources of turbidity. On the other hand, the apparent colour is that measured in the original water sample in its turbidity unalerted state. Anyway, to determine water colour with the currently accepted methods, turbidity must be removed before analysis. There are several ways to remove turbidity from water, such as filtration, centrifugation, dilution etc. Every method has its own advantages and

disadvantages, so the method choice depends on the aim [233]. Another strong colour influence is due to pH, so in every measure it is really important to specify the pH at which the colour is determined.

The water colour can be analysed in two different ways: visual comparison method and spectrophotometric method. The visual comparison method is applicable to nearly all samples of potable water, but water wastes (primarily industrial waste) may produce unusual colours that can not be matched [233].

In the visual comparison method, water samples are compared with a standard sample whose concentration of coloured solution is known, or with a special calibrated glass colour disk. Another way is the platinum-cobalt method (EPA Method 110.2 and Standard Method 2120B), where standards are composed by 1 mg platinum/L in the form of chloroplatinate ion and cobalt (Alpha-Hazen scale). That proportion is usually satisfactory to match colours in natural water samples, but the platinum ratio can be varied to match the colour in every specific case. In any case, the standard method is not applicable to most highly coloured industrial waters [234].

The most accurate method for colour analysis is the spectrophotometric one. It is widely used for every water type, ranging from domestic water to water analysis with complex and varied colour components [235].

Spectrophotometry measures how much a chemical substance absorbs or transmits light, providing a quantitative result in terms of absorbance. This is possible because every compound absorbs, transmits or reflects light over a certain range of wavelengths. A light beam flows through a solution sample and the instrument measures the amount of photons by the sample. With this technique, it is possible to determine the concentration of a known chemical substance measuring the intensity of light detected [236].

On the basis of the wavelength range of the light source, spectrophotometers are classified as follows:

• UV/Visible spectrophotometer	UV range:	185-400 nm
	Visible range:	400-700 nm
• IR spectrophotometer	Infrared range:	700-15000 nm

According to Bricaud et al. [235], organic compounds are important components of water which govern light propagation, altering its colour. In particular, organic compounds mainly determine a yellow-orange coloration, and they absorb light in a range between 375 nm and 500 nm [235]. In the current study, colour analysis has been carried out whit a UV-visible spectrophotometer (Kontron Uvikon 930), shown in Figure 5.9, setting the incident wavelength to λ=455 nm.
Observations on colour of water are usually reported in Apha-Hazen units [mg_{Pt} L^{-1}] according to the platinum cobalt scale [237]. The relation which links this evaluation with absorbance is reported in Equation 5.7 [238].

$$mg/L \approx 500 \times Absorbance \qquad 5.7$$

The spectrophotometer Kontron Uvikon 930 is composed of:

- Deuterium lamp
- Halogen lamp without holder
- Damper for sample chamber cover

Figure 5.9. Spectrophotometer Kontron Uvikon 930

5.1.7. Aromaticity

Aromatic molecules are chemical compounds which contain conjugated planar ring systems with delocalized electron clouds instead of discrete alternating single and double bonds [239]. According to Badger [240], the classical definition of aromaticity was based on the cyclic nature, stability and chemical reactivity of a compound. Any definition of aromaticity is therefore open to serious objections,

because chemical reactivity is not a property of the molecule in its ground state, but it depends on the difference in free energy between the ground states of two or more molecular systems [240]. Although aromaticity is not a function of the stability and chemical reactivity, it is a function of the electronic structure [240] which determines the characteristics of a compound. The aromatic character can not be rigidly defined, but the main properties of aromatic compounds may be summarized as follow [239]:

- Hydrocarbon ring is a strong molecular structure, which confers stability
- Although saturated hydrocarbons are not usually attacked, aromatic compounds tend to react by substitution with greater or lesser facility
- Parent aromatic substances are, in general, remarkably stable to oxidizing agents

The analysis of aromaticity during a degradation process is important to understand how strong the degradation is. In this study, aromaticity was measured by using a UV-visible spectrophotometer (Kontron Uvikon 941), shown in Figure 5.5. Its features are listed in Section 5.1.6.
To measure the aromaticity of the solution, the incident wavelength was set at λ=254 nm. According to Korshing et al. [241], the absorbance at this wave length is suitable to quantify the aromaticity of compounds, because it is determined by aromatic group with carrying degrees of activation [241].

5.2. Spectrophotometric measurement at the University of Bologna

All the analyses carried out at the University Bologna were aimed at studying the kinetics of degradation of caffeine by using a photo-Fenton process. The experimental assays were carried out using a reaction system different from that used in Basque Country. In particular Fenton's reagent and caffeine were put in a cuvette which was irradiated with a UV- visible lamp (Helios Italquartz Polymer 125). The reactions started by turning on the mercury lamp and were temporarily stopped by turning irradiation off at pre-established intervals of time, in order to allow measurements of the absorbance. The absorption spectra were recorded in

the 220-500 nm range. The absorbance values and their changes as a function of time were read at 272 nm, that is, on a maximum due to electron excitation from the highest occupied molecular orbital (HOMO) to the lowest unoccupied molecular orbital (LUMO) of caffeine [242]. The absorbance measurements ended up when the absorbance value at this wavelength did not decrease anymore. Two series of experiments were carried out to investigate the effects produced by the oxidant (H_2O_2) and the catalyst (Fe^{2+}) on the kinetics of degradation of caffeine. The first series involves experiments in which the catalyst dosage is kept constant, while the oxidant dosage is changed. In the second series the oxidant dosage kept constant, while the amount of catalyst is changed.
The main features of the UV-visible lamp (Helios Italquartz Polymer 125) are listed below:

- Hg medium pressure
- Power = 125 W

Caffeine and Fenton's reagent were mixed in different dosages in a total volume of 87 mL. Then, an aliquot of the solution was taken using a Pasteur pipette and put in a cuvette for the irradiation. The concentrations of each experiment are listed below.

1st experimental series:

- Caffeine (Ca_0) $0.0592\ 10^{-3}$ M
- Catalyst (Fe^{2+}) $0.02\ 10^{-3}$ M
- Oxidant (H_2O_2) $1.0\ 10^{-3}$ M
  $2.0\ 10^{-3}$ M
  $4.0\ 10^{-3}$ M
  $6.0\ 10^{-3}$ M
  $8.0\ 10^{-3}$ M

2nd experimental series:

- Caffeine (Ca_0) $0.0592\ 10^{-3}$ M
- Oxidant (H_2O_2) $2.0\ 10^{-3}$ M
- Catalyst (Fe^{2+}) $0.02\ 10^{-3}$ M
  $0.04\ 10^{-3}$ M
  $0.08\ 10^{-3}$ M
  $0.12\ 10^{-3}$ M
  $0.16\ 10^{-3}$ M

Figure 5.10 shows the reaction system: the cuvette irradiated by the UV-visible lamp with a probe for pH measurement.

Figure 5.10. Reaction system

During these analyses pH and temperature were not adjusted to keep them constant. However, they were measured to evaluate if they fell into the suggested range (see Chapter 3).

In Section5.1.6, the functioning of a general spectrophotometer is illustrated. The main features of the spectrophotometer employed (Varian Cary 50 bio, Agilent Technology) for the present measurements are listed below and the instrument is shown in Figure 5.11.

- Dual beam
- Monochromator: Czerny-Turner
- Wave length range: 190 to 1100 nm
- Xe pulse lamp
- Dual Si diode detector
- Quartz overcoated optic
- Maximum scan rate: 24000 nm/min
- 80 data points/s

Figure 5.11. Varian Cary 50 Scan UV-visible spectrophotometer [252]

In order to describe the kinetic of the degradation of caffeine by using a photo-Fenton process, measurements of a physico-chemical property (absorbance) as a function of time were used. The quantity most directly involved in a kinetic study is concentration, but concentration measurements as a function of time may result difficult or very time consuming. For this reason, it is quite convenient to replace concentration measurement with measurements of a physical property (λ) of the whole system as a function of time [243]. To this purpose, three requirements have to be fulfilled. First of all, variation of the λ must be much greater than the sensitivity of the instrument. Moreover, it must be taken in account the additivity of λ; the total value of λ must be given by the sum of the partial values of the single components. Finally, a specific mathematical relation between the concentration and λ must exist, the elaboration of the data being much easy when

this relationship is a simple proportionality [243]. It is not requested that the proportionality constant be the same for various components which contribute to λ. In this study the chosen property λ was the absorbance (at a wavelength of 272 nm). Absorbance is a suitable property, because it is proportional to concentration, provided the latter are sufficiently small that the Lambert-Beer law holds. To employ this property, it was necessary to record the absorption spectra of reagents (caffeine, hydrogen peroxide and ferrous ion), in order to select the appropriate wave length for the measurement of the extinction coefficient as a function of time. The Lambert-Beer's laws describes the relationship between the concentration of an absorbing substance and the extent to which radiant energy is absorbed. The Lambert-Beer law is described by Equation 5.8 [244].

$$-ln\frac{I}{I_0} = ln\frac{I_0}{I} = A = \varepsilon_\lambda \cdot l \cdot M \qquad 5.8$$

where, I/I_0 is the transmittance, A is the measure of absorbance, ε_λ is the molar extinction coefficient (constant for each substance) [L mol^{-1} cm^{-1}], l is the path length of the sample [cm] and M is the molar concentration [mol L^{-1}]. Transmittance is the fraction of light that passes through the sample, in fact I_0 is the original intensity of the beam of light and I is the light intensity after the beam of light passes through the cuvette [236].

The simplest case is represented by the transformation of a single reagent (A) which reacts completely to produce a single product (B), in a solvent

$$A \rightarrow B \qquad 5.9$$

It can be easily demonstrated that the results can be extended to more complex reactions. With reference to reaction 5.9, at any time (t) Equations 5.10-15 are valid [243].

$$\lambda = k_A[A] + k_B([A_0] - [A]) + k_B[B_0] + \lambda_{SOL} \qquad 5.10$$

At t=0

$$\lambda_0 = k_A[A_0] + k_B[B_0] + \lambda_{SOL} \qquad 5.11$$

At t=∞

$$\lambda_\infty = k_B[A_0] + k_B[B_0] + \lambda_{SOL} \quad 5.12$$

$$\lambda - \lambda_\infty = k_A[A] + k_B([A_0] - [A]) - k_B[A_0] = (k_A - k_B)[A] \quad 5.13$$

$$\lambda_0 - \lambda_\infty = k_A[A_0] - k_B[A_0] = (k_A - k_B)[A_0] \quad 5.14$$

$$(\lambda - \lambda_\infty)/\ (\lambda_0 - \lambda_\infty) = [A]/[A_0] \quad 5.15$$

For a first order reaction, where

$$ln\left(\frac{[A]}{[A_0]}\right) = -kt \quad 5.16$$

Equation 5.17 is valid.

$$\ln\left(\frac{[A]}{[A_0]}\right) = ln\ \left[\frac{\lambda-\lambda_\infty}{\lambda_0-\lambda_\infty}\right] = -kt \quad 5.17$$

For a second order reaction, it can be demonstrated that the integrated kinetic equation is

$$\left(\frac{1}{[A]}\right) - \left(\frac{1}{[A_0]}\right) = kt \quad 5.18$$

Equation 5.19 is valid.

$$\left(\frac{1}{[A_0]}\right)(\lambda_0 - \lambda_\infty)/(\lambda - \lambda_\infty)\left(\frac{1}{[A_0]}\right) = kt \quad 5.19$$

i.e. there must be a linear relationship between $1/(\lambda - \lambda\infty)$ and t, with slope $k\ A_0/(\lambda_0 - \lambda\infty)$.

Density functional theory (DFT) calculations were performed with the Gaussian 09 set of programs [245]. Evaluations of the reaction energies (total electronic energies) for the reactions reported in Table 6.8 were performed using the B3LYP hybrid functional [246] with the minimal 6-31G(d) basis set. The excitation energies of caffeine in the gas phase and in water solvent were calculated with the TD-B3LYP method [247]. In this case, because of the involvement of normally empty molecular orbitals (characterised by a larger spatial diffusion) the 6-31+G(d) basis set was used, which includes addition of diffuse functions (namely *s* and *p* type diffuse functions at the non-hydrogen atoms). The effects of a solvated (water) environment were evaluated with the Polarizable Continuum Model [248].

6. RESULTS AND DISCUSSION

In this work caffeine oxidation using an AOP is investigated, including some aspects related to the quality of water and the kinetic of the degradation. The results obtained at the University of Basque Country and at the University of Bologna are presented in two different Sections. The first part concerns phenomenological issues about the quality of water after the degradation of caffeine by photo-Fenton process. The second one concerns the kinetics of the reaction. For both investigations, two series of experiments were devised: one in which the concentration of the oxidant changes keeping the catalyst dosage constants, and another series in which the oxidant concentration is constant while the catalyst concentration changes.

6.1. Quality of the water after caffeine degradation

These results focus on the quality of the water solution once caffeine has been degraded employing a photo-Fenton process. Conductivity, turbidity, colour and aromaticity of water were examined while the process takes place and when completion of the reaction is reached. The concentration of caffeine and the properties listed above are correlated with the oxidant and catalyst amounts. Tables 6.1 and 6.2 show the experimental conditions followed to degrade caffeine with various initial concentration of oxidant and catalyst. Each experiment was carried out throughout a period of 2 hours.

Table 6.1. Experimental conditions in the series of reactions with different oxidant concentrations

1st experimental series	
Temperature	25.0 °C
pH	3.0
Caffeine	0.592 10^{-3} M
Catalyst: Fe^{2+}	0.2 10^{-3} M
Oxidant: H_2O_2	0.0 M 4.0 10^{-3} M 6.0 10^{-3} M 8.0 10^{-3} M 10.0 10^{-3} M 15.0 10^{-3} M

Table 6.2. Experimental conditions in the series of reactions with different catalyst concentrations

2nd experimental series	
Temperature	25.0 °C
pH	3.0
Caffeine	0.592 10^{-3} M
Oxidant: H_2O_2	15.0 10^{-3} M
Catalyst: Fe^{2+}	0.0 M 0.1 10^{-3} M 0.2 10^{-3} M 0.4 10^{-3} M 0.6 10^{-3} M 0.8 10^{-3} M

6.1.1. Caffeine concentration

First of all, it is to be noted that the first HPLC measurement was made at t=0, then the second one after about 20 minutes, that is, when caffeine resulted to be almost completely consumed. Therefore, these results do not allow a kinetic study, where some data of caffeine concentration vs. time would be required. Before starting the reaction, i.e., before turning on the UV lamp, a sample of solution was injected in the HPLC apparatus to measure the initial caffeine concentration (t=0). Then the reactor was irradiated, thus starting the degradation. The retention time of the caffeine in HPLC was 20-25 minutes, so that, during the two hours of reaction, only 5 samples were analysed, including t=0. Anyway, according to Graph 6.1, after 20 minutes most of the caffeine in the reactor was degraded, even with the lowest oxidant concentration employed (H_2O_2 4.0 10^{-3} M; Fe^{+2} 0.2 10^{-3} M; T = 25 °C; pH 3, see Table 6.1). Graph 6.1 indicates that in these conditions caffeine is completely degraded after 25-30 minutes. The fact that this reaction goes to completion (i.e., is not an equilibrium reaction) is an important information for elaborating the absorption data as a function of time in the kinetic study described in the next Section.

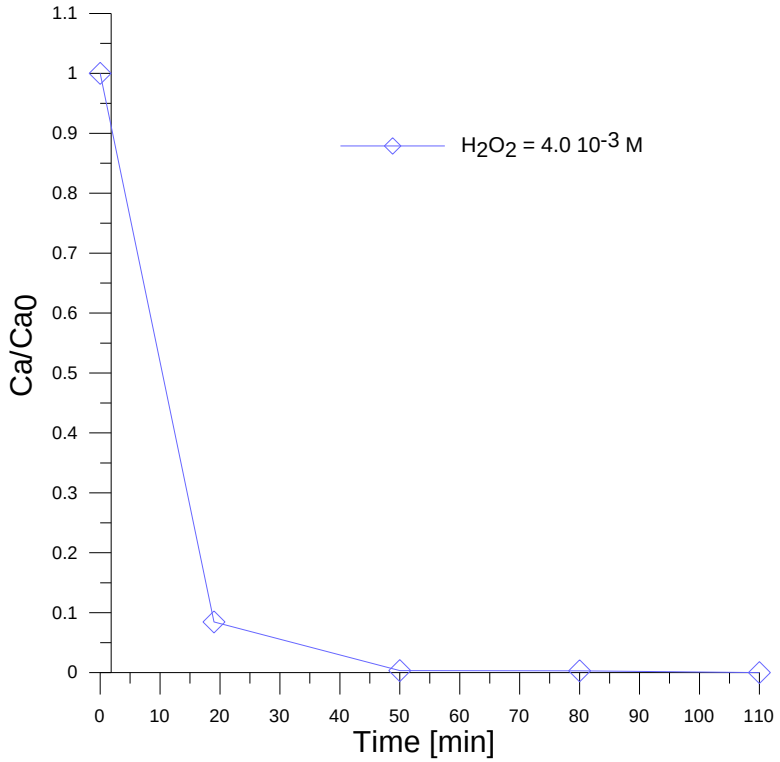

Graph 6.1. Caffeine degradation as a function of time.
Experimental conditions: Ca_0=0.592 10^{-3} M; Fe^{2+}=0.2 10^{-3} M; H_2O_2=4.0 10^{-3} M; pH=3.0; UV lamp=150 W; T=25.0 °C

6.1.2. Conductivity

Graph 6.2 shows the conductivity values measured during the reactions carried out with various oxidant concentrations (see Table 6.1). According to Graph 6.2, the presence of oxidant causes an increase of conductivity in the first 5-10 minutes, although all the trends and absolute values of conductivity seem to be independent of oxidant concentrations. When the oxidant is not present, the conductivity remains approximately constant during the entire experiment.
Graph 6.3 shows the analogous conductivity trends observed in the series of reactions with different catalyst concentrations (see Table 6.2). Throughout each experiment, conductivity undergoes only small variations. The sharp peaks displayed in Graph 6.3 are due to pH adjustments. As expected, conductivity is sizeably affected by catalyst concentration, in agreement with dissociation of iron sulphate into positive and negative ions. Graph 6.4 displays average conductivity values as a function of catalyst concentration and shows the existence of a linear relationship. The linear fit of the points of Graph 6.4 is described by equation 6.1:

$$Conductivity = 1382951.022\, Fe^{2+} + 363.735 \qquad 6.1$$
$$R^2 = 0.9702$$

with:

Conductivity= Average conductivity [µS cm^{-1}]
Fe^{2+}= Ferrous ion [M]

According to the European Directive 98/83/EC, the conductivity of drinking water must be smaller than 2500 µS cm^{-1} (at 20 °C). This means that application of the photo-Fenton process to water for human consumption, under experimental conditions similar to those used here, does not need further processes to reduce conductivity. Also in surface water conductivity should be smaller: 1000 µS cm^{-1} (at 20 °C) (75/440/EEC, Surface Water Regulations of 1989).

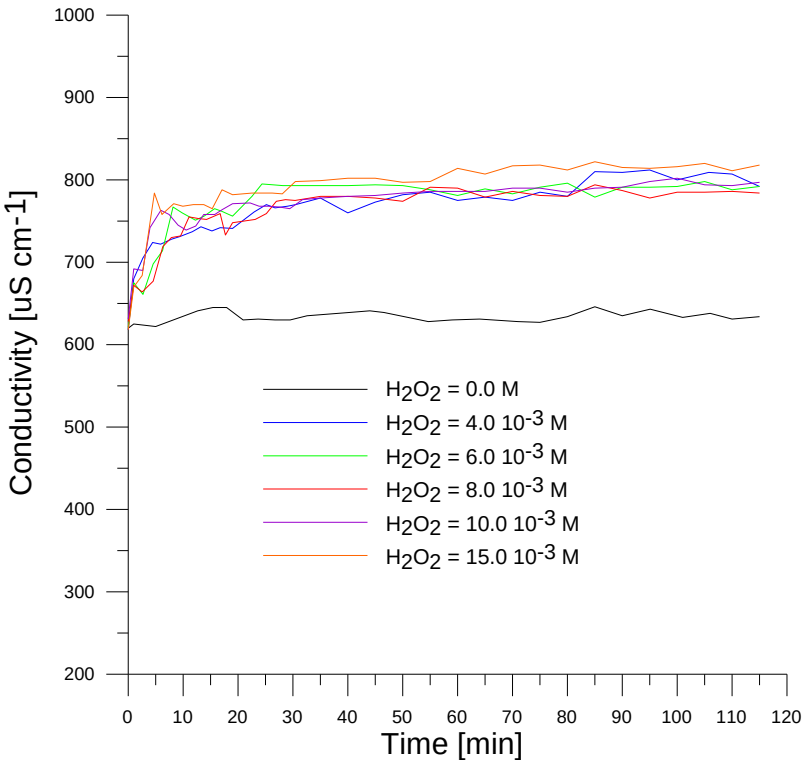

Graph 6.2. Conductivity as a function of time for different oxidant concentrations. Experimental conditions: Ca_0=0.592 10^{-3} M; Fe^{2+}=0.2 10^{-3} M; pH=3.0; UV lamp=150 W; T=25.0 °C

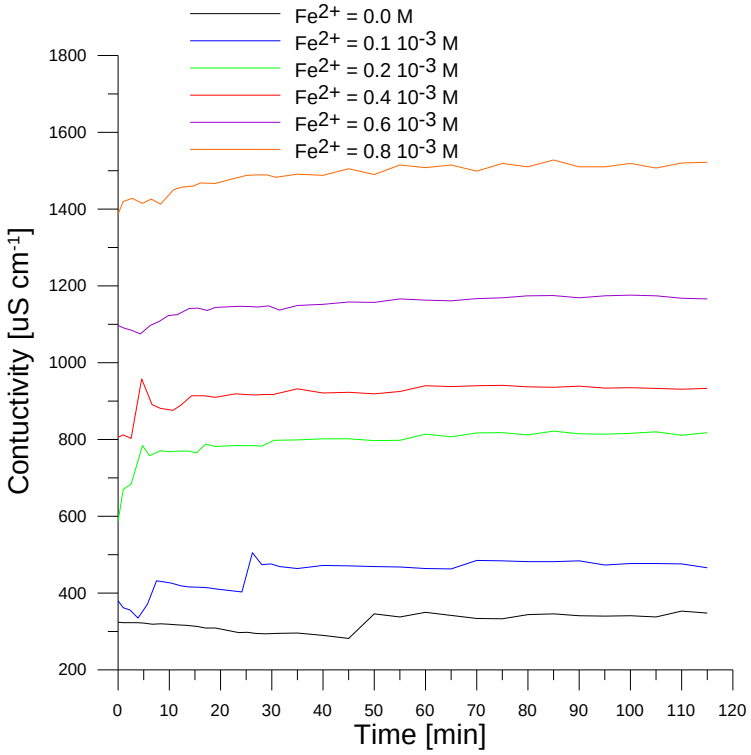

Graph 6.3. Conductivity as a function of time for different catalyst concentrations. Experimental conditions: Ca_0=0.592 10^{-3} M; H_2O_2=15.0 10^{-3} M; pH=3.0; UV lamp=150 W; T=25.0 °C

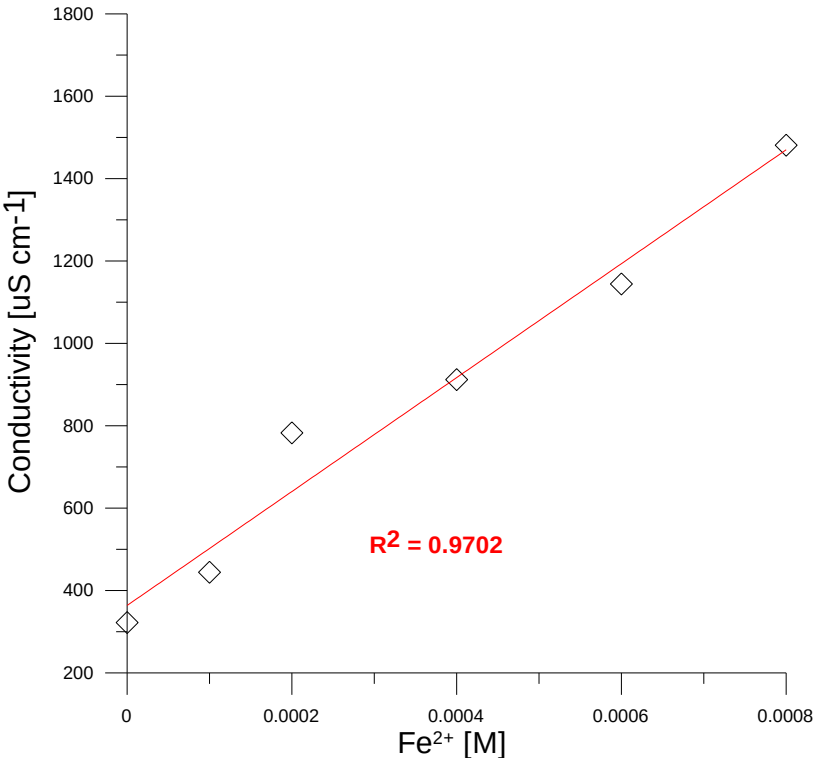

Graph 6.4. Average conductivity as a function of catalyst concentration. Experimental conditions: Ca_0=0.592 10^{-3} M; H_2O_2=15.0 10^{-3} M; pH=3.0; UV lamp=150 W; T=25.0 °C

6.1.3. Turbidity

Graph 6.5 shows the turbidity as a function of time, measured for each oxidant concentration in the first experimental series (see Table 6.1). According to our experimental procedure, the initial turbidity value should not be affected by the oxidant concentration, as actually found within experimental limits. However, the presence of oxidant causes a notable turbidity increases during the reaction period, while turbidity remains approximately constant in the experiment without H_2O_2. In the presence of oxidant, regardless of its concentration, a nearly linear turbidity increase is observed during the first 45-50 minutes, then turbidity reaches a plateau. Evidence for a dependence of this turbidity increase on oxidant concentration is not observed. This might suggest that the photo-Fenton process produces intermediates or products with a molecular structure larger than that of the reagents. The final turbidity values are not far from each other, their differences likely falling within the experimental uncertainty.

Graph 6.6 shows turbidity trends during caffeine degradation reactions with various catalyst concentrations (see Table 6.2). The initial turbidity values (t=0)

seem to be proportional to the catalyst concentration When the catalyst is present, every curve of turbidity grows up to a maximum whose value is roughly proportional to the catalyst concentration. Then turbidity remains nearly constant until the end of the experiment. The time necessary to reach the maximum value depends on the catalyst concentration in an inverse fashion. In the absence of catalyst, turbidity remains constant and close to zero, in line with a very small (if any) reaction rate.

The turbidity trends displayed in Graph 6.7 might suggest that caffeine degradation produces large molecules which interfere with light transmission in turbidity measurements. As mentioned in Section 5.1.5, turbidity is due to the amount of light scattered by particles, so the bigger are the molecules the higher are the turbidity values. As far as the initial turbidity is concerned, it is to be noticed that catalyst concentration affects this property even before the beginning of the reaction. As mentioned in Section 3.2, adding Fe^{2+} in a water/caffeine solution, ferrous ion reacts with the dissolved oxygen causing oxidation to ferric ion. This oxidation involves intermediate species which are difficult to characterise or predict, because they also depend on pH. In water, ferric ion can precipitate as $Fe(OH)_3$. This precipitation increases the yellow-orange colour and the turbidity of the solution, because of the production of sediments consisting of crystalline jarosites, amorphous ferric hydroxysulfates, or both [249]. The initial values of turbidity are plotted in Graph 6.7 as a function of Fe^{2+} concentration, leading to the linear Equation 6.2:

$$Turbidity_0 = 8771.579\ Fe^{2+} + 0.578 \qquad 6.2$$
$$R^2 = 0.9721$$

with:

$Turbidity_0$= Turbidity at initial state [NTU]
Fe^{2+}= Ferrous ion [M]

The extrapolated linear relationship (R^2=0.9721) indicates that the initial turbidity of the solution is proportional to the ferrous ion concentration.

Analogous findings are associated with the final state turbidity values (see Graph 6.7). All values are higher, but even in this case a linear relationship is observed, described by the Equation 6.3:

$$Turbidity_F = 33393.684\, Fe^{2+} - 1.348 \qquad 6.3$$
$$R^2 = 0.9834$$

with:

$Turbidity_F$ = Turbidity at final state [NTU]
Fe^{2+}= Ferrous ion [M]

Even in this case, the square correlation coefficient (R^2) of the linear regression indicates the proportionality between turbidity and ferrous ion concentration. In summary, it can be concluded that the turbidity increase caused by the present photo-Fenton process is independent from the amount of oxidant and proportional to the concentration of iron sulphate. Given that the initial caffeine concentration was held constant in all experiments, these findings also suggest that the turbidity is likely not associated with the products of caffeine degradation.
Drinking Water Directive (98/83/EC) does not fix a limit value for the turbidity of water for human consumption. However, the Directive states that turbidity must be "Acceptable to consumers and with no abnormal change". Besides, the Directive states that "In case of surface water treatment, Member States should strive for a parametric value not exceeding 1.0 NTU in the water ex treatment works".
The latter statement would imply that in case of application of this AOP to surface or drinking water, further operations would be required to eliminate or reduce turbidity.

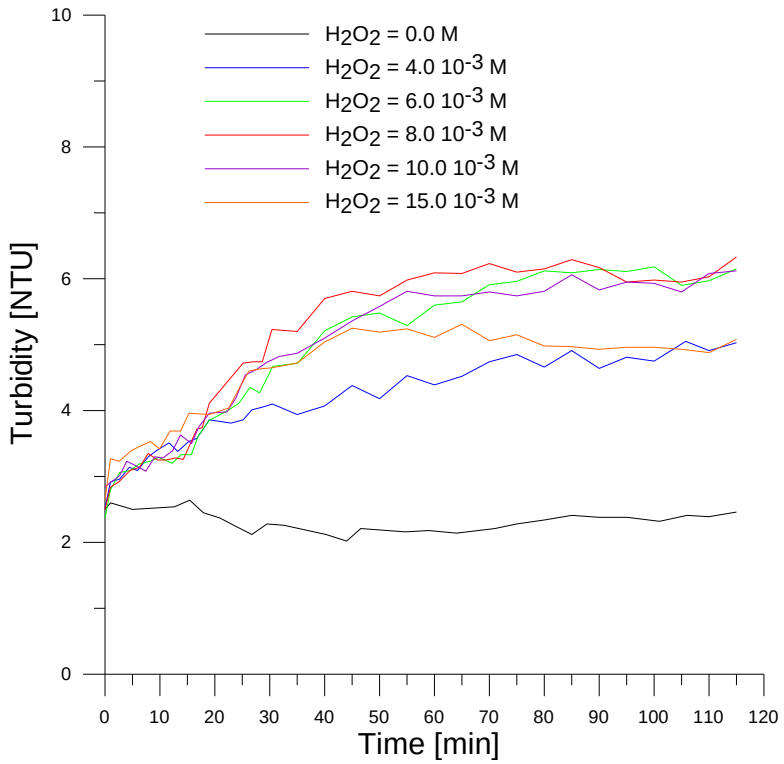

Graph 6.5. Turbidity as a function of time for different oxidant concentrations. Experimental conditions: Ca_0=0.592 10^{-3} M; Fe=0.2 10^{-3} M; pH=3.0; UV lamp=150 W; T=25.0 °C

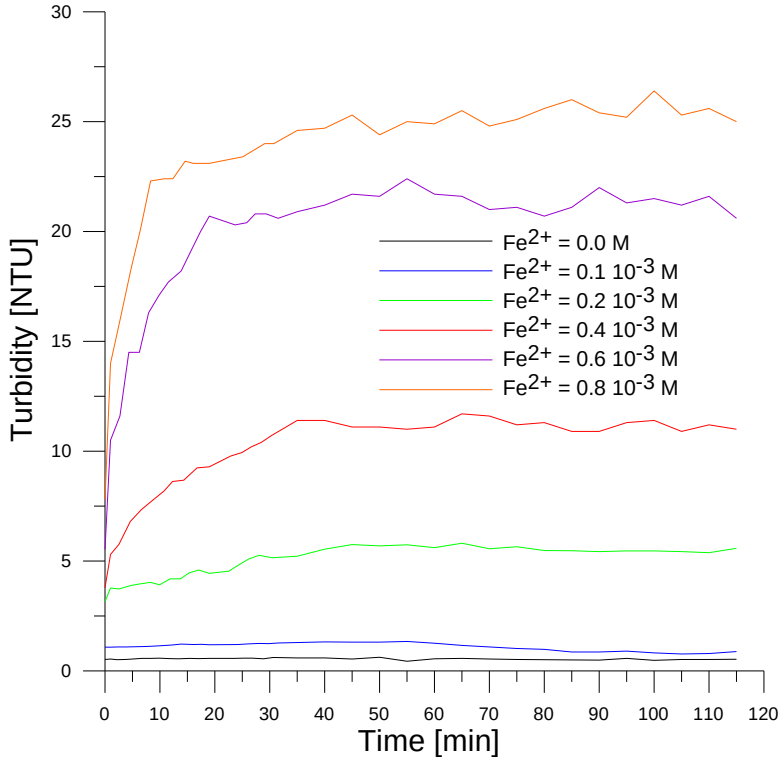

Graph 6.6. Turbidity as a function of time for different catalyst concentrations. Experimental conditions: Ca_0=0.592 10^{-3} M; H_2O_2=15.0 10^{-3} M; pH=3.0; UV lamp=150 W; T=25.0 °C

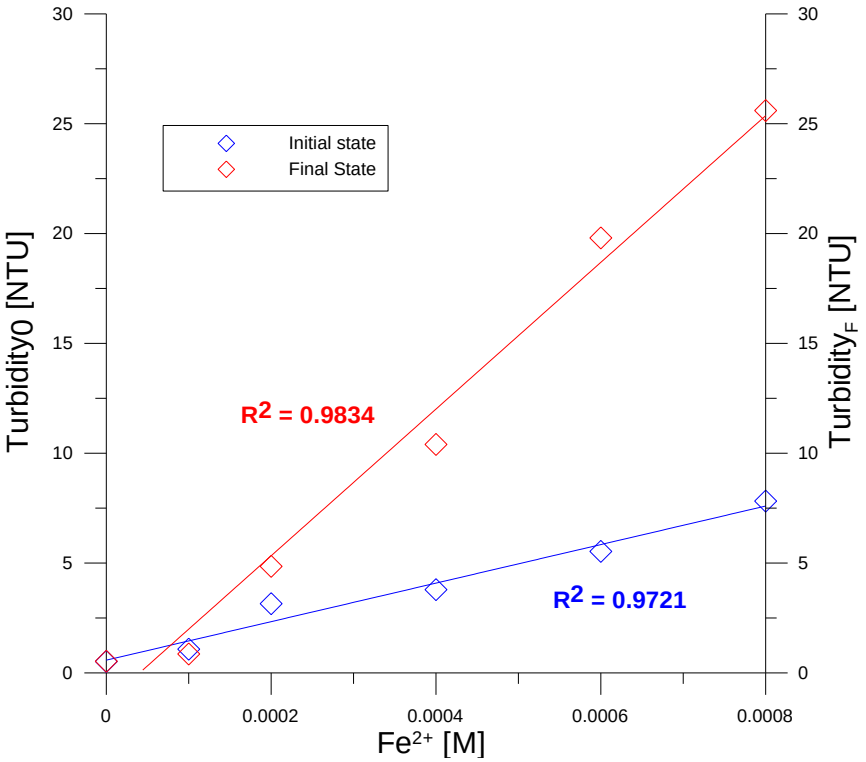

Graph 6.7. Initial and final state of turbidity as a function of catalyst concentrations. Experimental conditions: Ca_0=0.592 10^{-3} M; H_2O_2=15.0 10^{-3} M; pH=3.0; UV lamp=150 W; T=25.0 °C

6.1.4. Colour

As mentioned in Section 5.1.6, colour has been measured by using a UV/visible spectrophotometer, setting the incident wavelength to λ=455 nm (which correspond to a yellow-orange observed colour).

Graph 6.8 shows the absorbance as a function of time for the various oxidant concentrations of the first experimental series (see Table 6.1). The initial colour is expected to be not affected by the oxidant concentration, in line with the present findings. As shown in Graph 6.8, when the oxidant is absent no significant colour changes are measured, whereas when the oxidant is present notable colour variations occur during the reaction period. In analogy with the turbidity trends, the curves displayed in Graph 6.8 indicate that colour changes are essentially independent of the oxidant concentrations. When the oxidant is present all curves present the same shape. After an initial increase in the first 45-50 minutes a plateau is reached. Therefore, when the oxidant is present the reaction generates products with chromophore properties, but these might be iron compounds. Graph 6.9 shows the colour trends observed in the second experimental series, where the catalyst concentration changes (see Table 6.2). The effect of catalyst

concentration is evident. Even at t=0, before the reaction starts, the absorbance increases with increasing ferrous ion concentration. The colour values then undergo an initial increase up to a maximum which is proportional to the catalyst concentration. After reaching this maximum, each curve remains nearly constant until the end of the experiment. The time necessary to reach the maximum value depends on the catalyst concentration in an inverse fashion.

When the catalyst is absent, absorbance value remains constant and close to 0.10. The colour trends displayed in Graph 6.9 suggest that the reaction produces chromophore molecules. However, these are plausibly to be ascribed to iron species, rather than to degraded caffeine derivatives.

Graph 6.10 shows the colour values measured at t=0 and t=120 min for each of the iron concentrations used. Catalyst concentration affects the colour of the solution even before the beginning of the reaction. As well as for turbidity, iron species can increase yellow-orange colour through ferric ion precipitates [249]. For the initial colour values, the best fit is linear

$$Absorbance_0 = 108.947\ Fe^{2+} + 0.077 \qquad 6.4$$
$$R^2 = 0.9474$$

with:

$Absorbance_0$= Absorbance at 455 nm at initial state

Fe^{2+}= Ferrous ion [M]

As far as the final state colour values are concerned, the best fit of the data turns out to be exponential, although the curve is close to a straight line (see Graph 6.10):

$$Absorbance_F = 0.125e^{1256.983Fe^{2+}} \qquad 6.5$$
$$R^2 = 0{,}954$$

with:

$Absorbance_F$ = Absorbance at 455 nm at final state

Fe^{2+}= Ferrous ion [M]

The increase of colour during the reaction is not dependent on the oxidant doses, but it is dependent on the catalyst doses in a nearly proportional way. Because of the strict dependence on the iron concentration, the increase of colour is plausibly not associated with degradation products of caffeine. More likely it could be ascribed to formation of Fe^{3+} derivatives.

Drinking Water Directive (98/83/EC) does not fix a limit for water colour, but it states that it must be "Acceptable to consumers and with no abnormal change" after a simple filtration. Surface Water Regulation (1989) fix the limit of colour in natural water in a range between 20 mg_{Pt} L^{-1} and 150 mg_{Pt} L^{-1}. According to what mentioned in Section 5.1.6, this one approximately corresponds to the absorbance range 0.04-0.3.

Therefore, the application of photo-Fenton reactions on surface or drinking water needs further treatments to reduce the colour of water.

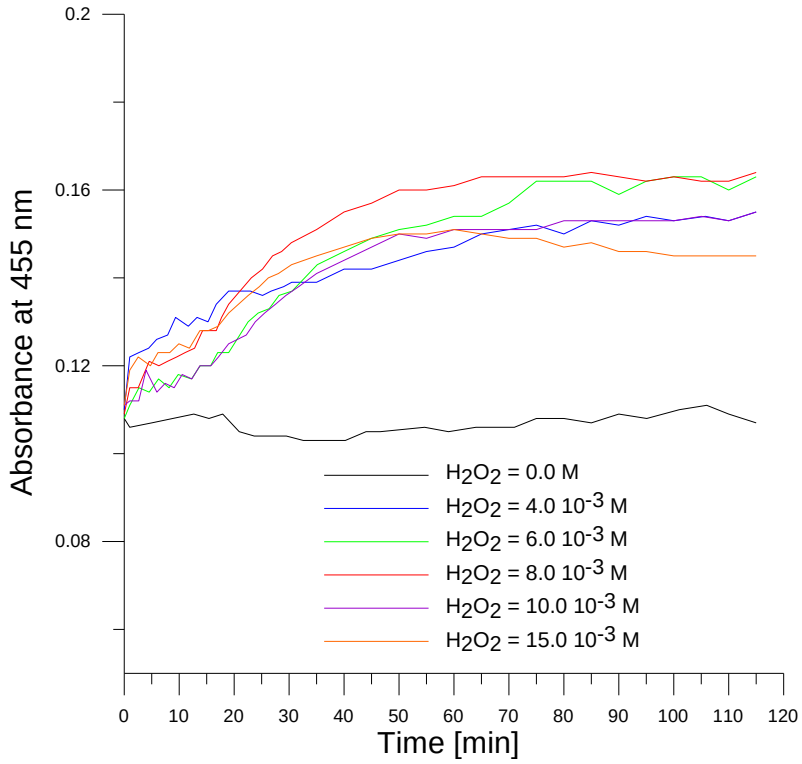

Graph 6.8. Colour as a function of time for different oxidant concentrations. Experimental conditions: Ca_0=0.592 10^{-3} M; Fe=0.2 10^{-3} M; pH=3.0; UV lamp=150 W; T=25.0 °C

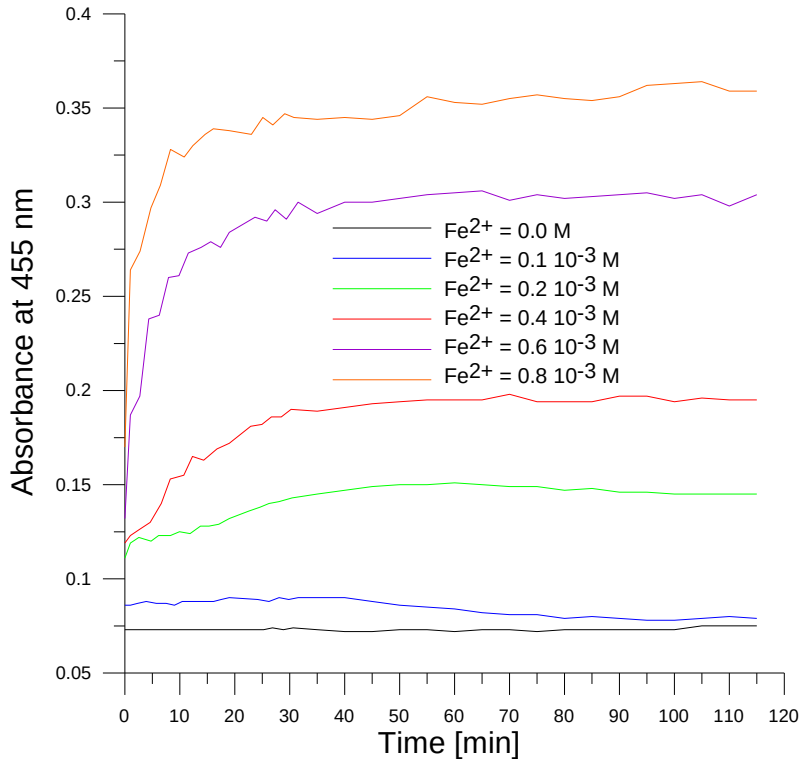

Graph 6.9. Colour as a function of time for different catalyst concentrations. Experimental conditions: Ca_0=0.592 10^{-3} M; H_2O_2=15.0 10^{-3} M; pH=3.0; UV lamp=150 W; T=25.0 °C

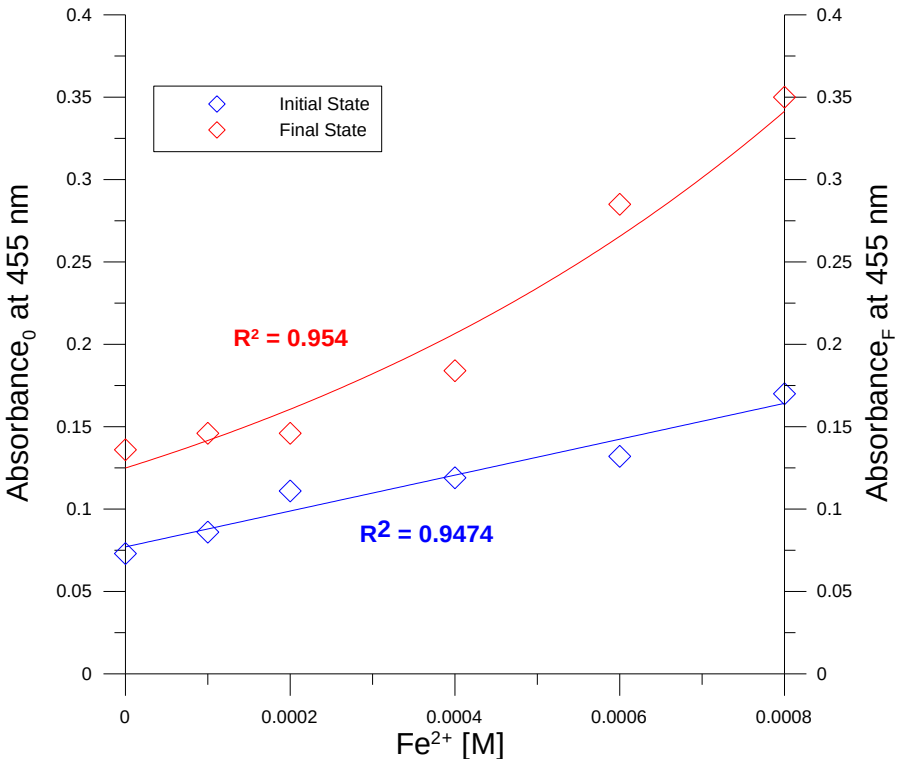

Graph 6.10. Initial and final state of colour as a function of catalyst concentration. Experimental conditions: Ca_0=0.592 10^{-3} M; H_2O_2=15.0 10^{-3} M; pH=3.0; UV lamp=150 W; T=25.0 °C

6.1.5. Aromaticity

As mentioned in Section 5.1.7, aromaticity has been measured by using a UV/visible spectrophotometer, setting the incident wavelength at λ=254 nm. Graph 6.11 shows the aromaticity trends observed for the various oxidant concentrations of the first experimental series (see Table 6.1). It was not possible to measure the aromaticity data for the run without oxidant because of an instrumental failure. As displayed in Graph 6.11, aromaticity slightly increases in the first 5-10 minutes. Then it reaches a plateau and remains nearly constant until the end of the experiment. The observed aromaticities are similar to each other, independently of the oxidant concentrations.

Graph 6.12 shows the analogous aromaticity trends observed in the experiments of the second series, where the catalyst concentration changes (see Table 6.2). At t=0, the aromaticity increases with increasing concentration of the ferrous ion. The aromaticity trends show an initial increase up to a maximum which is proportional to the catalyst concentration. Then each curve remains nearly constant until the end of the experimental period. The time necessary to reach the maximum value depends on the catalyst concentration in an inverse fashion, as observed above for turbidity and colour. When the catalyst is absent, aromaticity remains approximately constant during the entire experiment.

Graph 6.13 shows the aromaticity values measured at t=0 and t=120 minutes. Given that at t=0 the reaction has not yet started, differences in aromaticity values can not be due to caffeine intermediates or degradation products. According to the graph, aromaticity and ferrous ion concentration at t=0 are linearly correlated, although R^2 is only 0.778, mainly due to a single value (the one measured with Fe^{2+} 0.4 10^{-3} M). The absorption spectrum of iron sulphate (displayed below in Graph 6.14, Section 6.2) explains the proportionality between the absorbance at 254 nm and iron concentration. Actually, iron sulphate has a fairly large extinction coefficient at this wavelength, so that its presence prevents aromaticity measurements based on absorption at 254 nm.

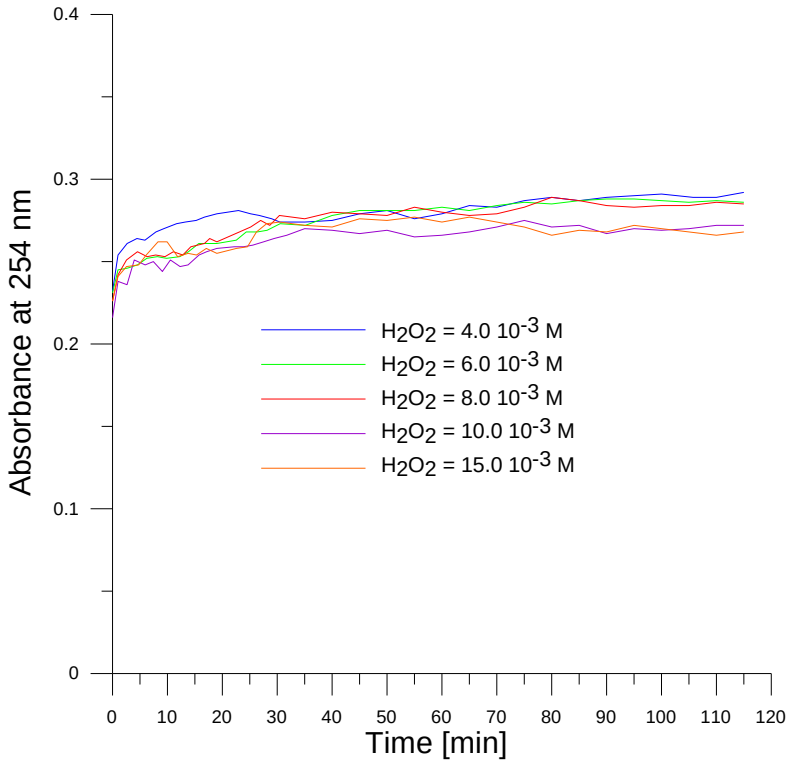

Graph 6.11. Aromaticity as a function of the time for different oxidant concentrations. Experimental conditions: Ca_0=0.592 10^{-3} M; Fe=0.2 10^{-3} M; pH=3.0; UV lamp=150 W; T=25.0 °C

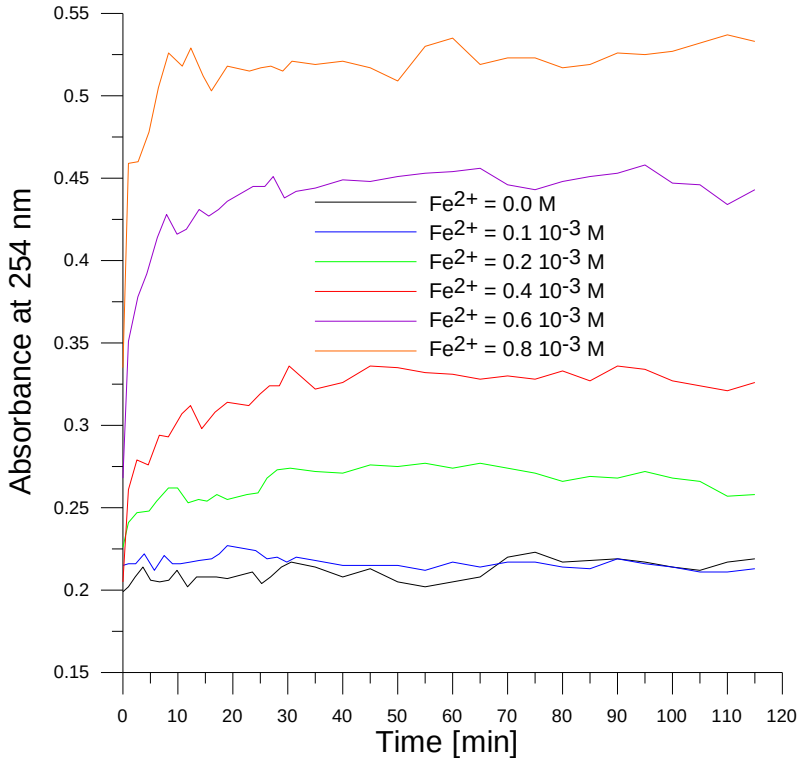

Graph 6.12. Aromaticity as a function of the time for different catalyst concentrations. Experimental conditions: Ca_0=0.592 10^{-3} M; H_2O_2=15.0 10^{-3} M; pH=3.0; UV lamp=150 W; T=25.0 °C

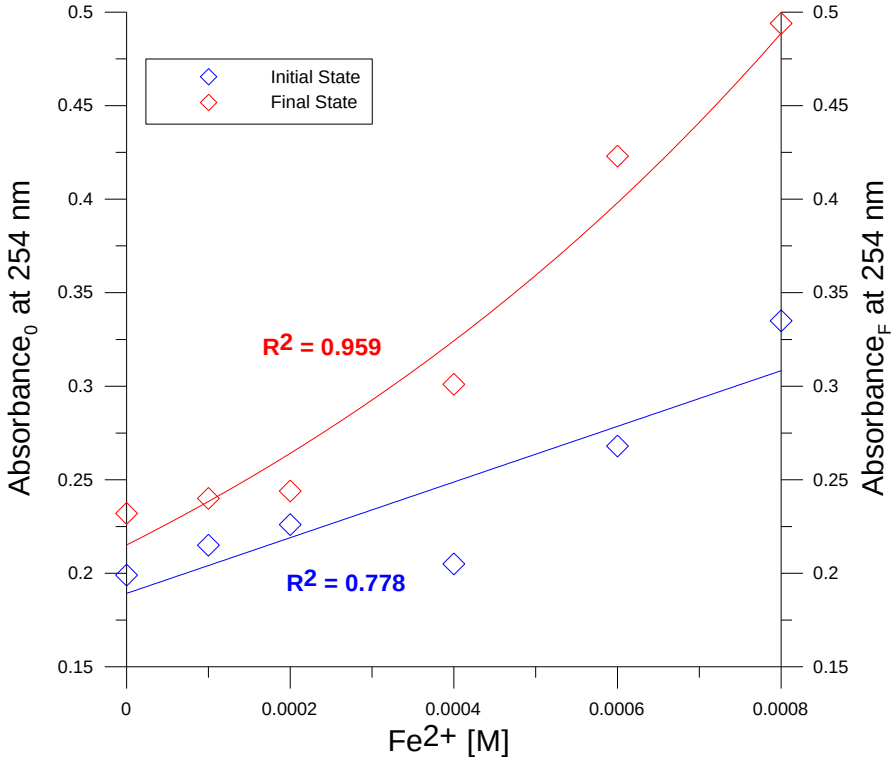

Graph 6.13. Initial and final state of aromaticity ad a function of catalyst concentration. Experimental conditions: Ca_0=0.592 10^{-3} M; H_2O_2=15.0 10^{-3} M; pH=3.0; UV lamp=150 W; T=25.0 °C

6.2. Kinetics of degradation

As mentioned above, the analyses carried out at UPV/EHU did not provide useful information about caffeine degradation, except that caffeine is completely degraded (see Graph 6.1). Therefore, the kinetics of the degradation of caffeine has been investigated in further studies at University of Bologna.

The results reported below are grouped in three parts. The first one concerns preliminary analyses to evaluate caffeine degradation by means of the UV-visible spectroscopy. The second one studies the kinetics of caffeine degradation and the effects of the catalyst and oxidant concentration. The last one concerns calculations carried out to obtain two main kinds of information. The first one gives insight into the energetics of possible degradation reactions of caffeine, the second one is related to the electronic excitation energies of caffeine and the localization properties of the molecular orbitals involved in the first excited states.

6.2.1. Evaluation of the rate and the extent of degradation of caffeine

These preliminary results focused on the possibility to use measurements of a physical property of the reaction system instead of determinations of caffeine concentration as a function of time, in order to carry out a kinetic study (rate law, order of reaction).

The chosen physical property was absorbance at 272 nm, corresponding to a maximum in the absorbance spectrum of caffeine [242]. This wavelength is suitable, because it undergoes a sizeable variation as a function of time, and the contributions of the various species are proportional to their concentrations, provided the latter are sufficiently small that the Lambert-Beer equation holds. Graph 6.14 shows the absorbance spectra of caffeine, H_2O_2 and iron sulphate in water in the 220-500 nm range. As displayed in Graph 6.14, the extinction coefficient of H_2O_2 at 272 nm is very small, while the contribution of the ferrous ion is somewhat larger.

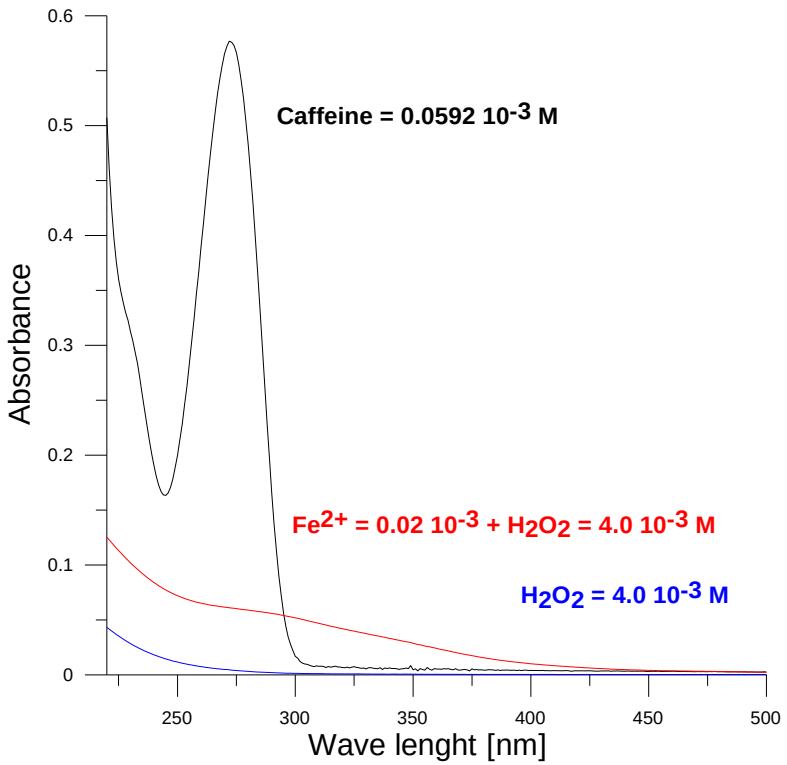

Graph 6.14. Recorded spectra for caffeine, iron sulphate solution and hydrogen peroxide

A preliminary experiment was carried out to evaluate if the method was actually able to fulfil the expectations described at the end of Chapter 5 (see Equations

5.17 and 5.19), namely, to unveil the reaction order (first or second order) and supply the values of the kinetic constants.

Graph 6.15 shows the absorption spectra of the reaction solution during the photo-Fenton process. The various absorption spectra have been recorded at different times of reaction, the spectrum at t=0 (before the reaction start) being the highest curve. As time goes by, the 272 nm maximum decreases in line with the reduction of caffeine concentration.

The values of absorbance at 272 nm at each corresponding time have been put into Equation 5.17 and 5.19 to evaluate the order of reaction. Graph 6.16 displays a plot the logarithm of the difference between the absorbance (A) at any time (t) and the (constant) absorbance at the end of the reaction (A_{inf}) versus t. According to Equation 5.17 this plot should give a linear relationship in the case of a reaction of order 1, as actually found, the kinetic constant being supplied by the slope (=–K). Interpolation of the points provides a good straight line (R^2=0.9654), indicating a rate law of order 1 in these experimental conditions.

For the sake of further evidence, Graph 6.17 reports the reciprocal of the difference ($A-A_{inf}$) versus time. In the case of second order kinetics, this plot is expected to be linear. As Graph 6.17 shows, this plot is clearly not linear, thus ruling out a second order reaction.

The results of this preliminary experiment showed that caffeine is degraded by means of this photo-Fenton reaction, and that its degradation follows a first order (or pseudo first order) rate law.

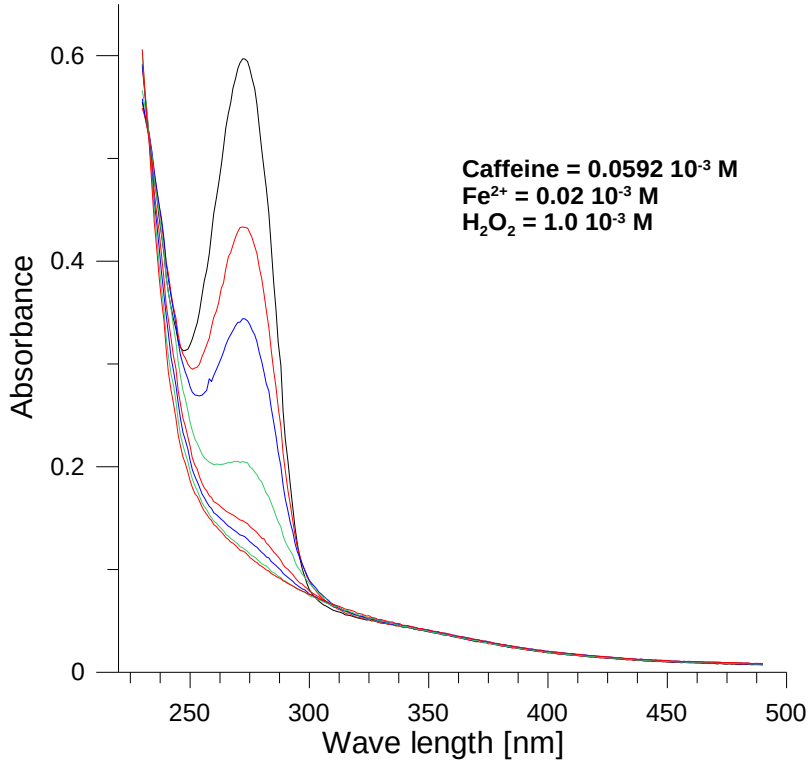

Graph 6.15. Absorption spectra of caffeine during the photo-Fenton reaction. Experimental conditions: Ca_0=0.0592 10^{-3} M; Fe^{2+}=0.02 10^{-3} M; H_2O_2=1.0; 10^{-3} M; UV lamp=125 W

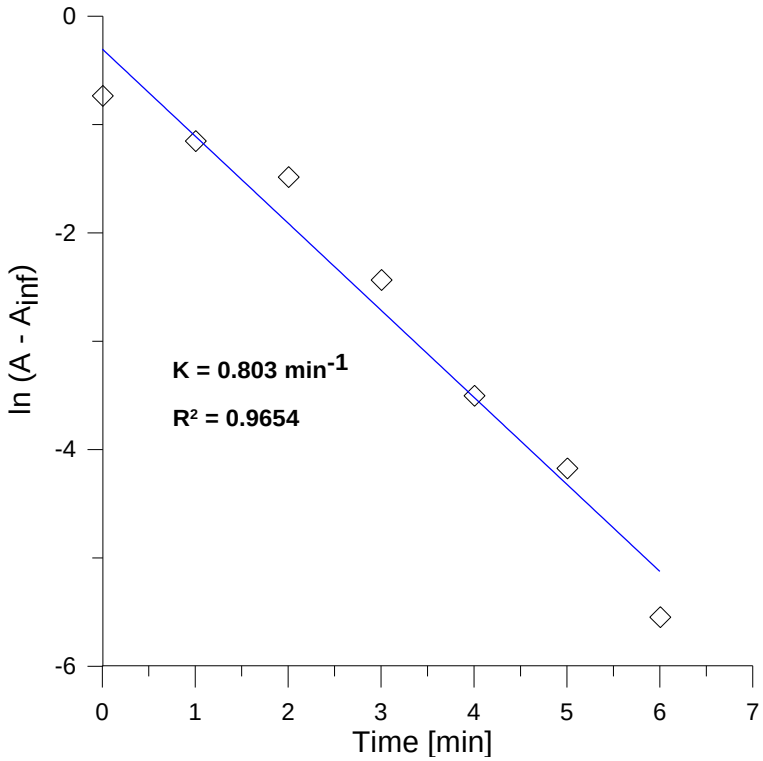

Graph 6.16. Linear correlation expected for a first order reaction

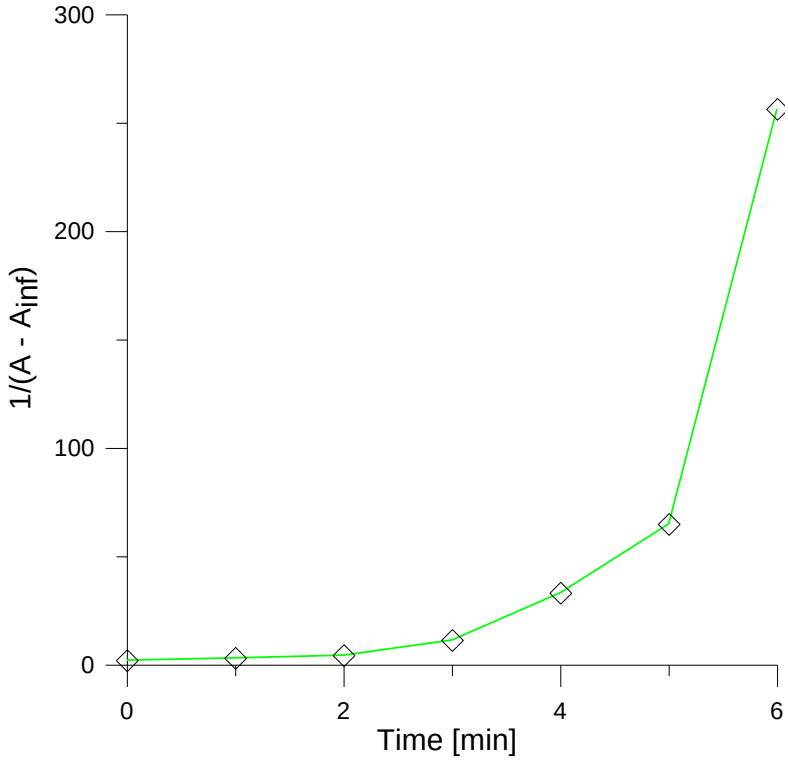

Graph 6.17. A second order reaction should give a linear plot

As mentioned in Section 5.2, pH and temperature were not kept constant during the essays, in order to simplify the experimental conditions. However, to assess the pH and temperature trends during the reaction, these two quantities were measured for 40 minutes. It turned out that pH remained approximately constant (≈4.80) during all the reaction time, while the temperature increased from 16.0 °C to 21.6 °C in our experimental conditions. Given that the best pH for photo-Fenton reaction is 3 [170], the performance of our reactions could be probably improved by pH adjustments, but only in terms of rate of reaction. In fact at the end of the reactions the absorbance peak at 272 nm due to caffeine is completely disappeared, indicating its complete degradation. The increase of temperature is due to irradiation, so that the rate of temperature increase depends on the power of the lamp and amount of solution processed.

6.2.2. Effects of the regents dosage on the kinetics of reaction

The degradation reactions were carried out with different concentrations of oxidant and catalyst (H_2O_2 and Fe^{2+}, respectively) to investigate their effects on

the rates of degradation. Tables 6.3 and 6.4 show the experimental conditions followed in each kinetic run.

Graphs 6.18-22 describe the first series of kinetic runs (see Table 6.3), where the catalyst concentration ($0.2\ 10^{-4}$ M) is kept constant while the concentration of oxidant changes. Each graph shows the absorption spectra of caffeine recorded at time intervals in the range 0.5-5 minutes, according to the reaction rates. In the slower reactions, the absorbance peak of caffeine disappears completely after less than 45 minutes. At first glance, the various kinetic runs (Graphs 6.18-22) suggest that the dependence of the reaction rate on the oxidant concentration is relatively small. In this regard, it can be noted (see Table 6.3) that the smallest concentration of H_2O_2 employed is about 16 times larger than that of caffeine. This point will be considered more quantitatively below.

Graphs 6.23-26, including the Graph 6.19, describe the second experimental series (see Table 6.4), where the oxidant dosage is kept constant while the concentration of catalyst changes. Each graph displays the absorption spectra evolution as a function of time. The caffeine peak broadens with increasing concentration of catalyst, due to absorption of the latter in this wavelength range (see Graph 6.14). Regardless of this factor, in this case the effect of catalyst concentration on the reaction rate is evident even at a qualitative level. The higher is the catalyst concentration the smaller is the time required to reach the end of the reaction.

Interestingly, it can be noted the presence of an isosbestic point in each set of spectra, at about 300 nm, where the various spectra recorded at different reaction times cross each other (at least up to more than 50% completion of the reaction). The presence of an isosbestic point (the absorbance of the products is the same as that of the reagents at a specific wavelength) indicates that essentially a single reaction is taking place. When other reactions (for instance, degradation of the products of reaction of caffeine) become important, the isosbestic point is lost.

Table 6.3. Experimental conditions to analyse the effects of different oxidant concentrations

1st experimental series	
Caffeine	0.0592 10^{-3} M
Catalyst: Fe^{2+}	0.02 10^{-3} M
Oxidant: H_2O_2	1.0 10^{-3} M 2.0 10^{-3} M 4.0 10^{-3} M 6.0 10^{-3} M 8.0 10^{-3} M

Table 6.4. Experimental conditions to analyse the effects of different oxidant concentrations

2nd experimental series	
Caffeine	0.0592 10^{-3} M
Oxidant: H_2O_2	2 10^{-3} M
Catalyst: Fe^{2+}	0.02 10^{-3} M 0.04 10^{-3} M 0.08 10^{-3} M 0.12 10^{-3} M 0.16 10^{-3} M

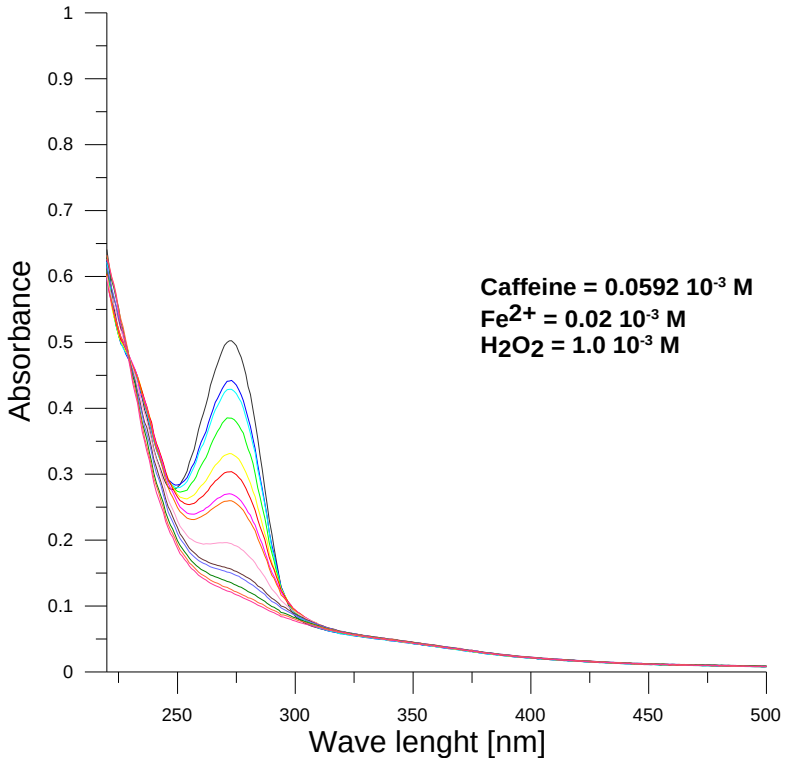

Graph 6.18. Absorption spectra of caffeine during the photo-Fenton reaction. Experimental conditions: Ca_0=0.0592 10^{-3} M; Fe^{2+}=0.02 10^{-3} M; H_2O_2=1.0; 10^{-3} M; UV lamp=125 W

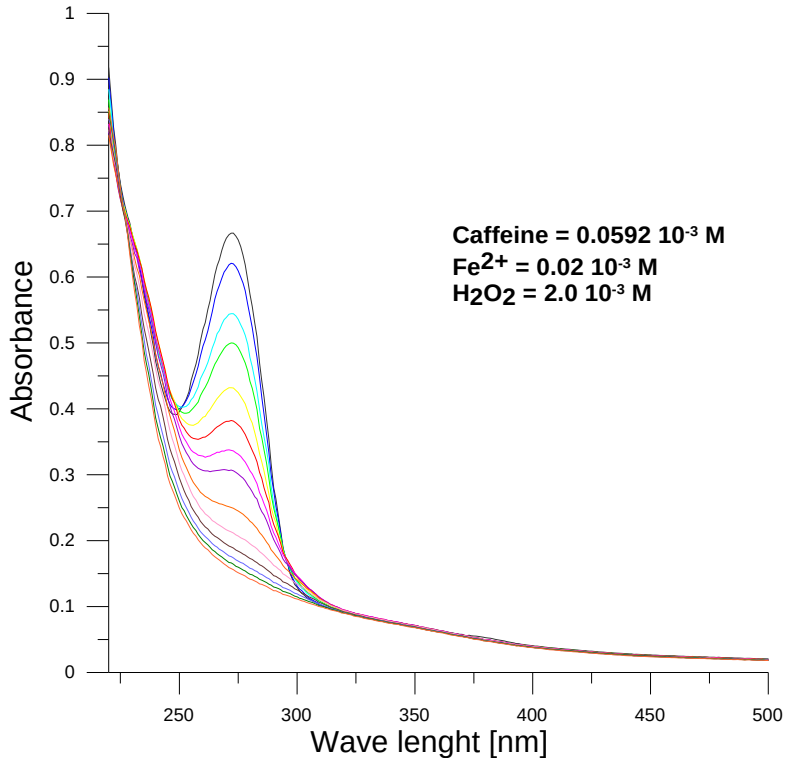

Graph 6.19. Absorption spectra of caffeine during the photo-Fenton reaction. Experimental conditions: Ca_0=0.0592 10^{-3} M; Fe^{2+}=0.02 10^{-3} M; H_2O_2=2.0; 10^{-3} M; UV lamp=125 W

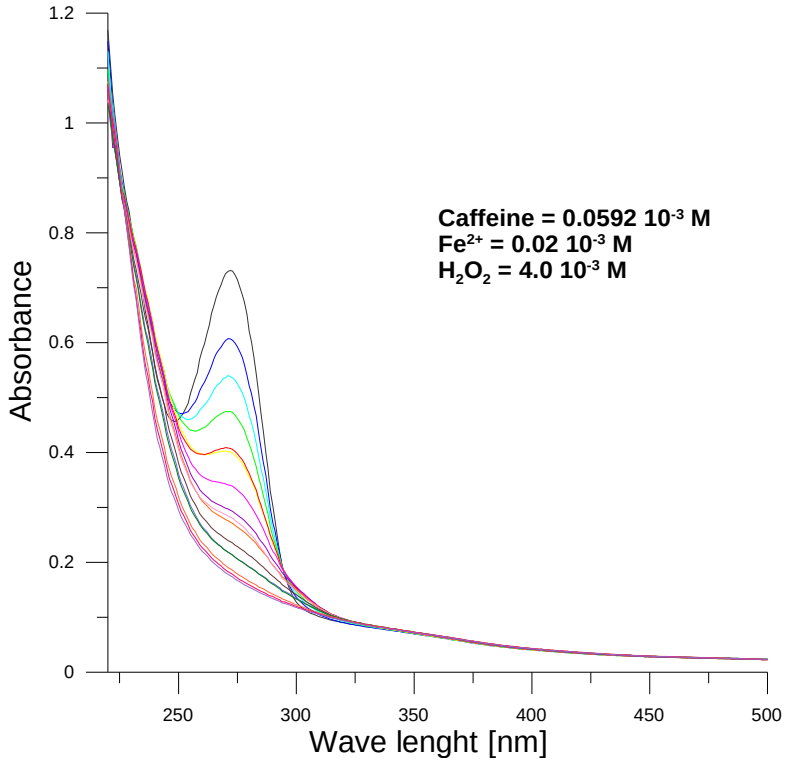

Graph 6.20.Absorption spectra of caffeine during the photo-Fenton reaction. Experimental conditions: Ca_0=0.0592 10^{-3} M; Fe^{2+}=0.02 10^{-3} M; H_2O_2=4.0; 10^{-3} M; UV lamp=125 W

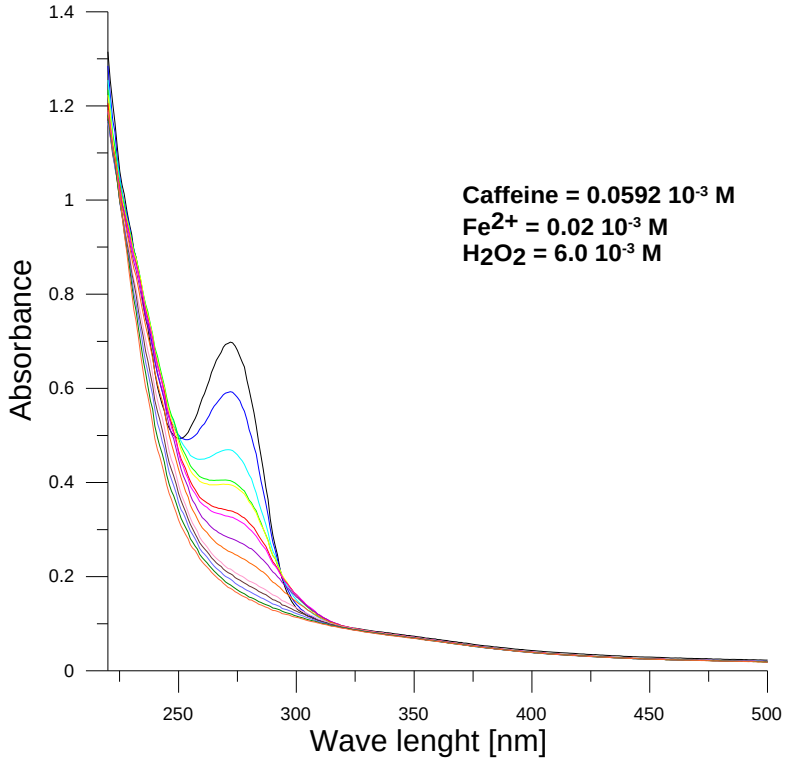

Graph 6.21. Absorption spectra of caffeine during the photo-Fenton reaction. Experimental conditions Ca_0=0.0592 10^{-3} M; Fe^{2+}=0.02 10^{-3} M; H_2O_2=6.0; 10^{-3} M; UV lamp=125 W

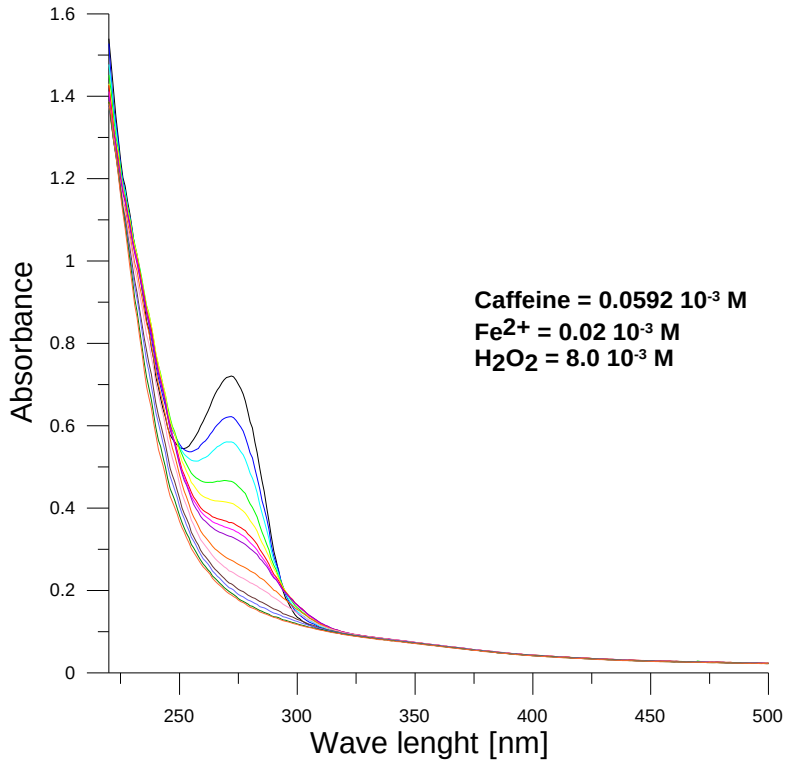

Graph 6.22. Absorption spectra of caffeine during the photo-Fenton reaction. Experimental conditions: Ca_0=0.0592 10^{-3} M; Fe^{2+}=0.02 10^{-3} M; H_2O_2=8.0; 10^{-3} M; UV lamp=125 W

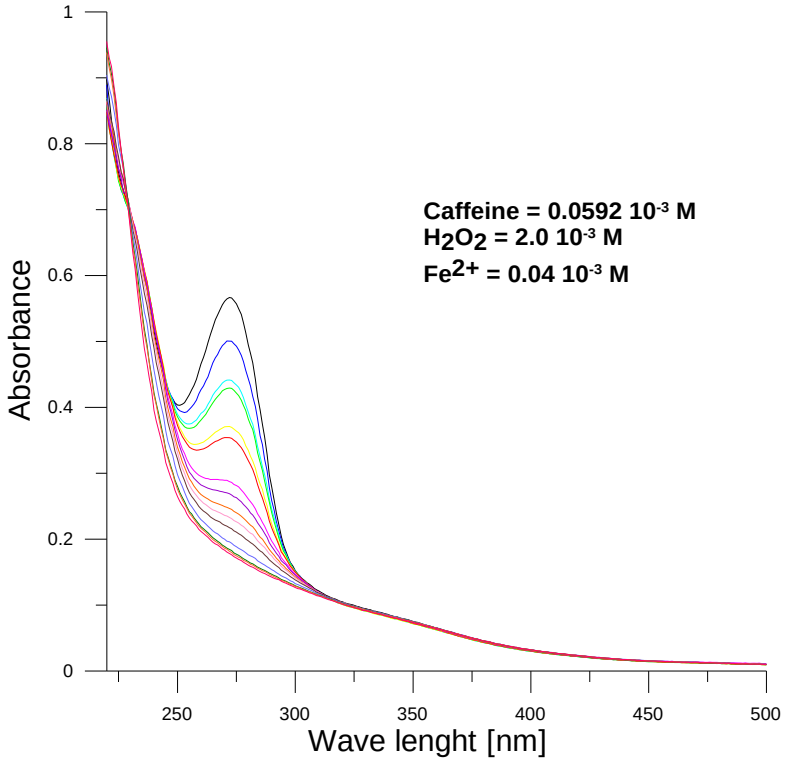

Graph 6.23. Absorption spectra of caffeine during the photo-Fenton reaction. Experimental conditions: Ca_0=0.0592 10^{-3} M; H_2O_2=2.0 10^{-3} M; Fe^{2+}=0.04 10^{-3} M; UV lamp=125 W

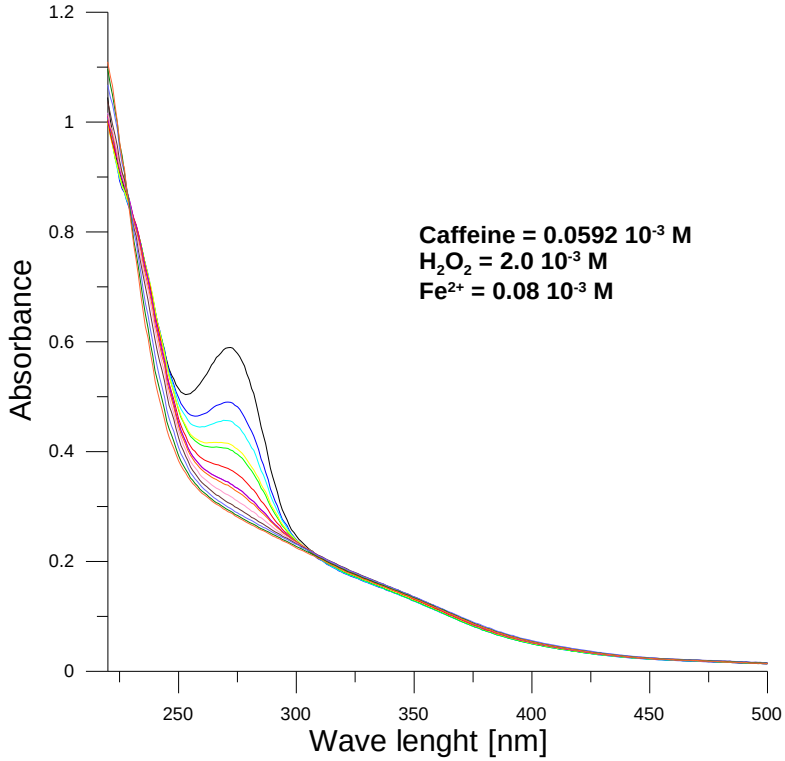

Graph 6.24. Absorption spectra of caffeine during the photo-Fenton reaction. Experimental conditions: Ca_0=0.0592 10^{-3} M; H_2O_2=2.0 10^{-3} M; Fe^{2+}=0.08 10^{-3} M; UV lamp=125 W

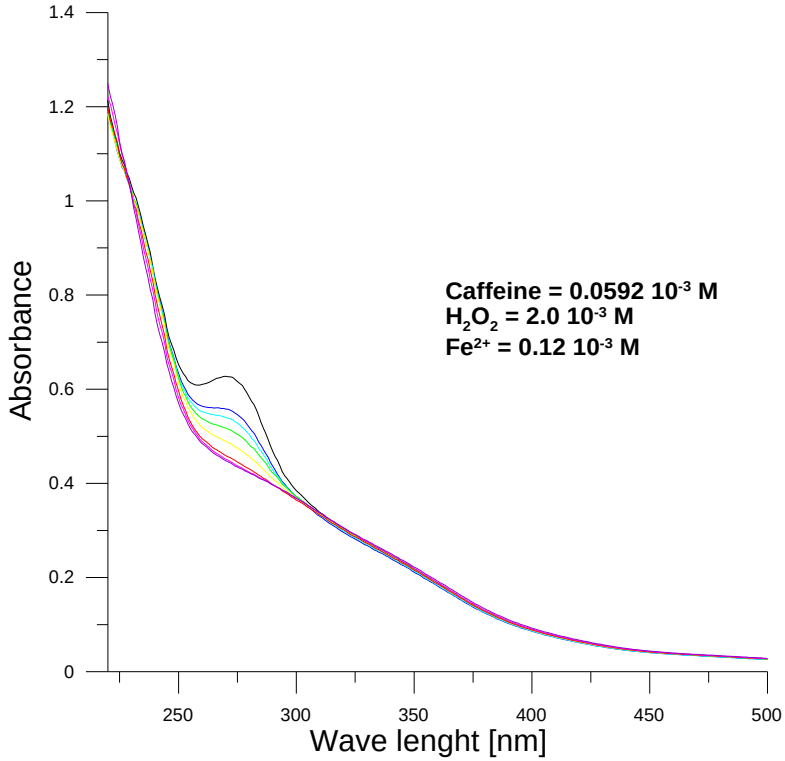

Graph 6.25. Absorption spectra of caffeine during the photo-Fenton reaction. Experimental conditions: Ca_0=0.0592 10^{-3} M; H_2O_2=2.0 10^{-3} M; Fe^{2+}=0.12 10^{-3} M; UV lamp=125 W

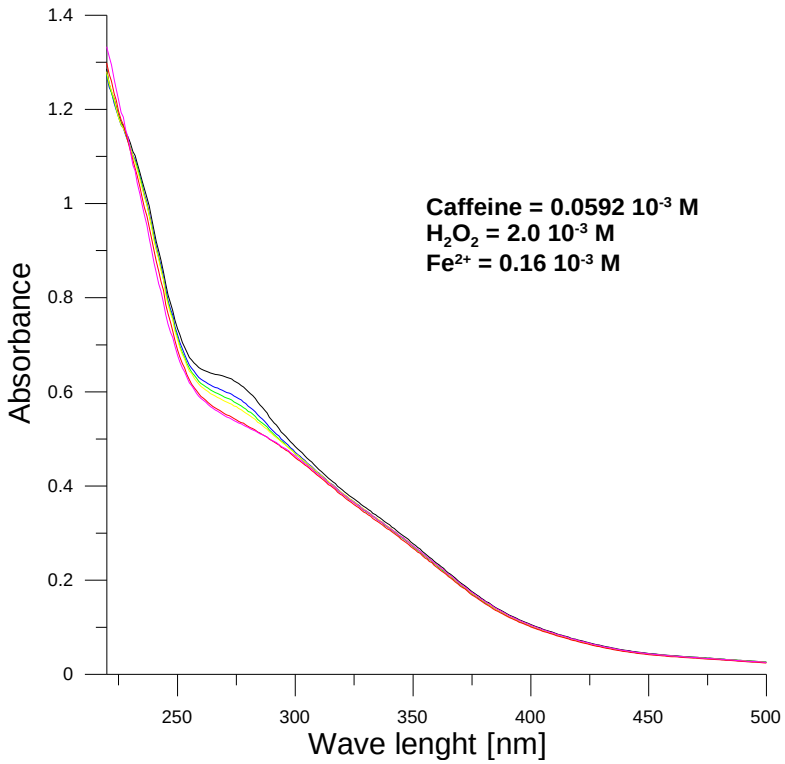

Graph 6.26. Absorption spectra of caffeine during the photo-Fenton reaction. Experimental conditions: Ca_0=0.0592 10^{-3} M; H_2O_2=2.0 10^{-3} M; Fe^{2+}=0.16 10^{-3} M; UV lamp=125 W

Once the absorption spectrum does not change any more (end of the reaction) the measurements can be interrupted. Each set of spectra recorded as a function of time provides a kinetic constant associated with the specific experimental conditions. The slope of the linear correlation found by plotting $\ln(A - A_{inf})$ vs. time is the negative of the kinetic constant, where A_{inf} is the final absorbance value at 272 nm.

Graphs 6.27-31 show these plots for the first series of kinetic runs (see Table 6.3). Good linear correlations are obtained up to a large degree of completion of the reactions. The corresponding kinetic constants are listed in Table 6.5.

Table 6.5 also includes the values of the kinetic constants and oxidant each normalized to its lowest value (defined as 1). Graph 6.32 plots the normalized kinetic constants (K_{Rel}) versus the corresponding relative oxidant concentrations. The slope of the extrapolated line is only slightly positive, thus indicating that the oxidant concentration affects only slightly the reaction rate. However, as mentioned above, the smallest H_2O_2 concentration is about 16 times and 50 times, respectively, larger than that of caffeine and Fe^{2+}, so that the latter could be

saturated. Future work would be necessary to investigate the effect of oxidant at lower concentrations.

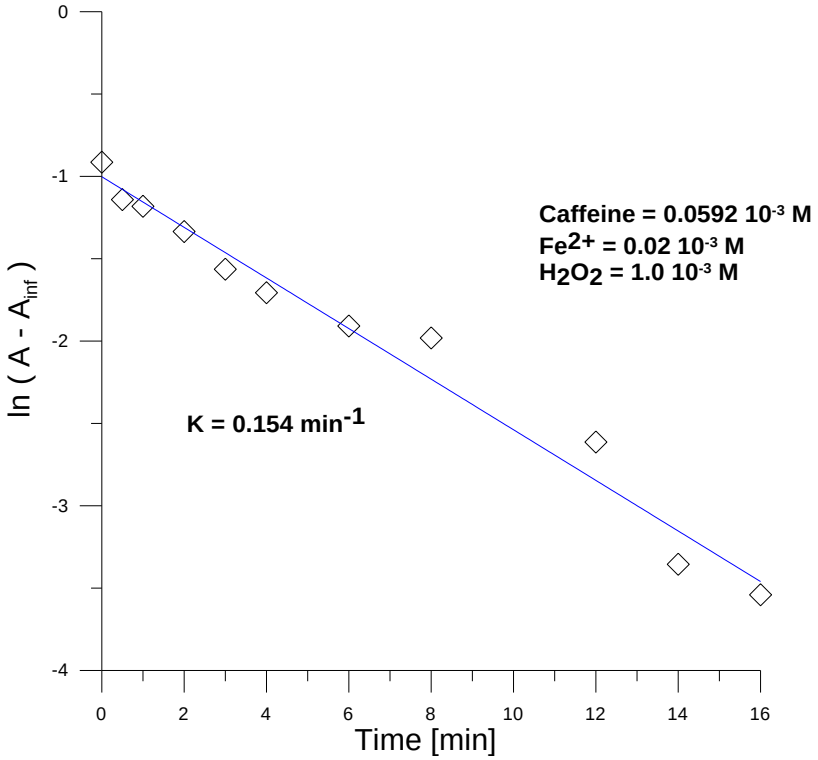

Graph 6.27. Linear correlation of a first order reaction
Experimental conditions: Ca_0=0.0592 10^{-3} M; Fe^{2+}=0.02 10^{-3} M; H_2O_2=1.0 10^{-3} M; UV lamp=125 W

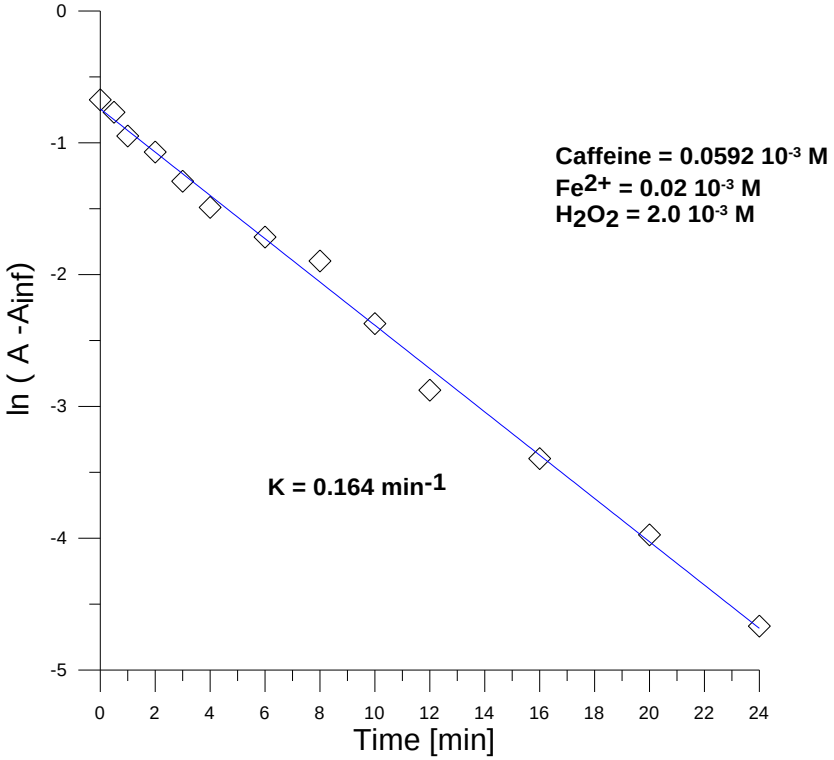

Graph 6.28. Linear correlation of a first order reaction
Experimental conditions: Ca_0=0.0592 10^{-3} M; Fe^{2+}=0.02 10^{-3} M; H_2O_2=2.0 10^{-3} M; UV lamp=125 W

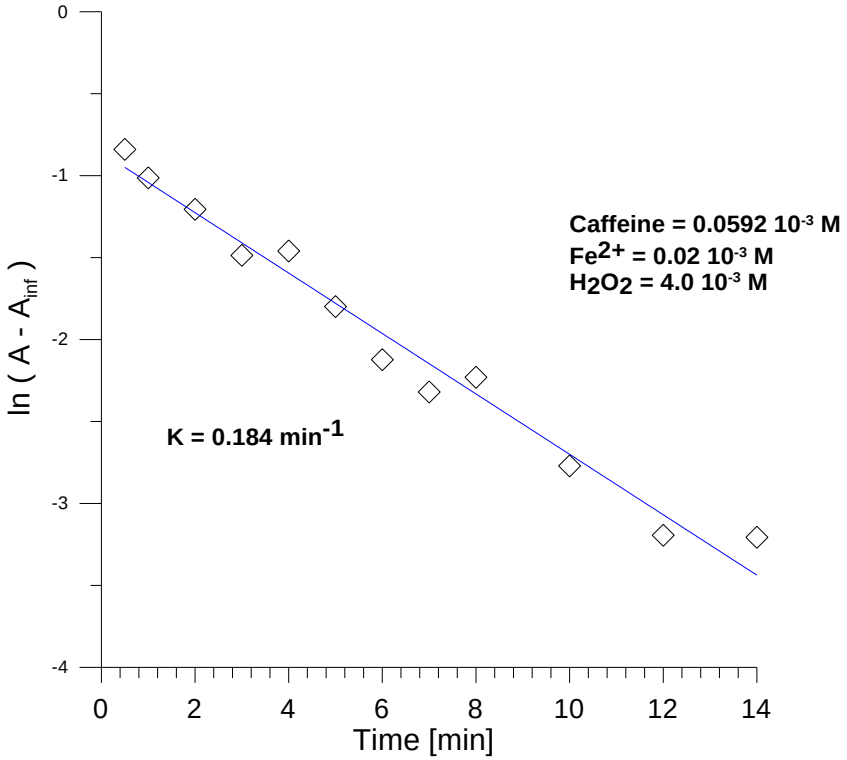

Graph 6.29. Linear correlation of a first order reaction
Experimental conditions: Ca_0=0.0592 10^{-3} M; Fe^{2+}=0.02 10^{-3} M; H_2O_2=4.0 10^{-3} M; UV lamp=125 W

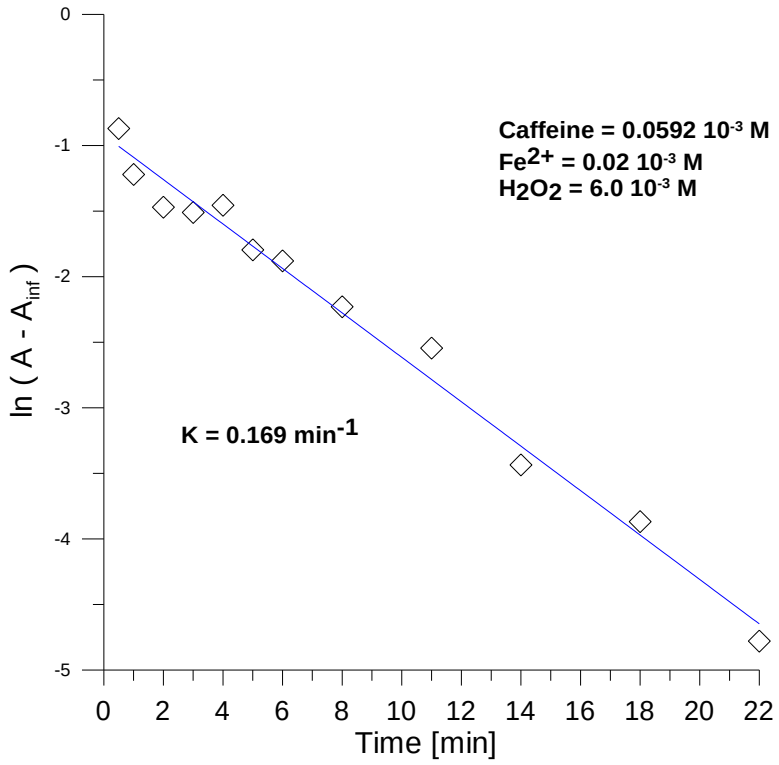

Graph 6.30. Linear correlation of a first order reaction
Experimental conditions: Ca_0=0.0592 10^{-3} M; Fe^{2+}=0.02 10^{-3} M; H_2O_2=6.0 10^{-3} M; UV lamp=125 W

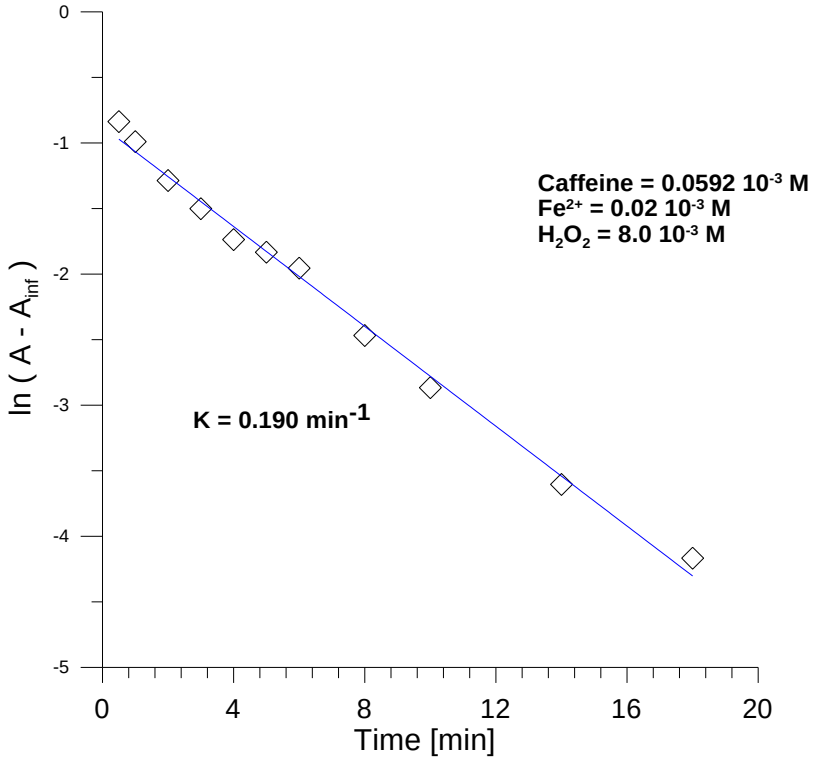

Graph 6.31. Linear correlation of a first order reaction
Experimental conditions: Ca_0=0.0592 10^{-3} M; Fe^{2+}=0.02 10^{-3} M; H_2O_2=8.0 10^{-3} M; UV lamp=125 W

Table 6.5. Kinetic constants for the first experimental series

H_2O_2 [M]	K [min^{-1}]	K/K_{MIN}	$[H_2O_2]/[H_2O_2]_{MIN}$
1.0 10^{-3}	0.154	1.000	1
2.0 10^{-3}	0.164	1.065	2
4.0 10^{-3}	0.184	1.195	4
6.0 10^{-3}	0.169	1.097	6
8.0 10^{-3}	0.190	1.234	8

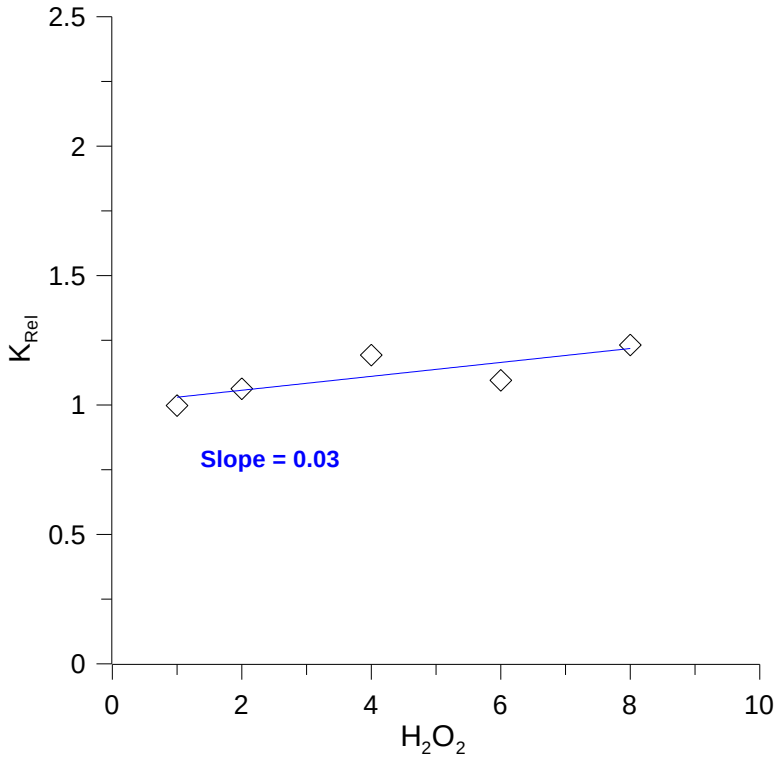

Graph 6.32. Relative kinetic constants as a function of the oxidant relative concentration

Graphs 6.33-36 (including Graph 6.28) show the logarithm of the absorbance values (at 272 nm) as a function of time for the kinetic runs of the second series, where the oxidant concentration is kept constant (2.0 10^{-3} M) and that of the catalyst is changed (see Table 6.4). The kinetic constants evaluated from the linear plots are listed in Table 6.6. The same Table reports the relative values of the kinetic constants and the Fe^{2+} concentrations, each normalized to its lowest value (defined as 1). Graph 6.37 shows the normalized kinetic constants (K_{Rel}) as a function of the catalyst relative concentrations. In this case, there is a clear linear dependence of the kinetic constants on the ferrous ion concentration, with a slope 0.70. A slope equal to 1 would indicate a direct proportionality between the reaction rate and the catalyst concentration. This finding will be discussed with more detail below.

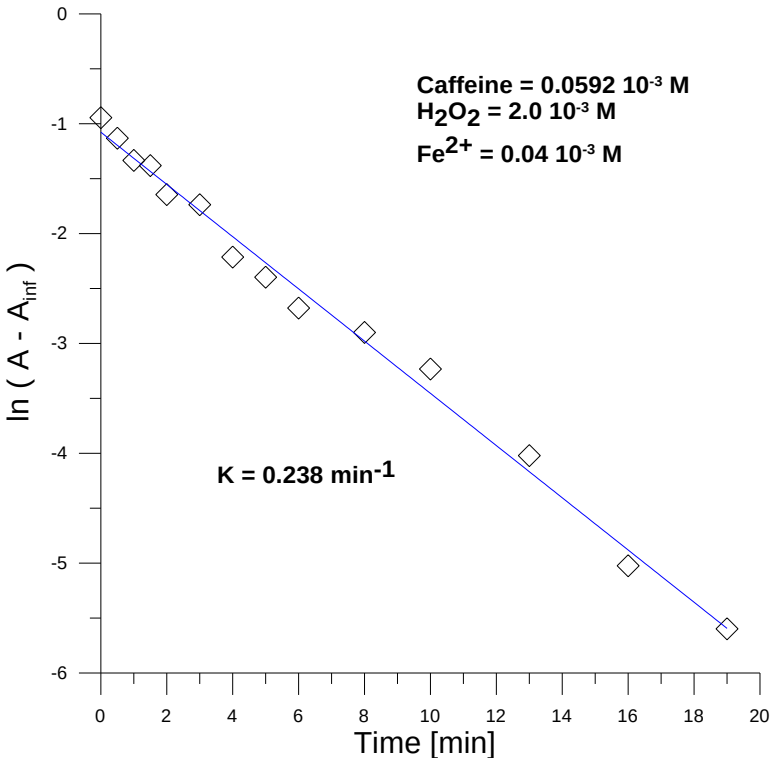

Graph 6.33. Linear correlation of a first order reaction
Experimental conditions: Ca_0=0.0592 10^{-3} M; H_2O_2=2.0 10^{-3} M; Fe^{2+}=0.04 10^{-3} M; UV lamp=125 W

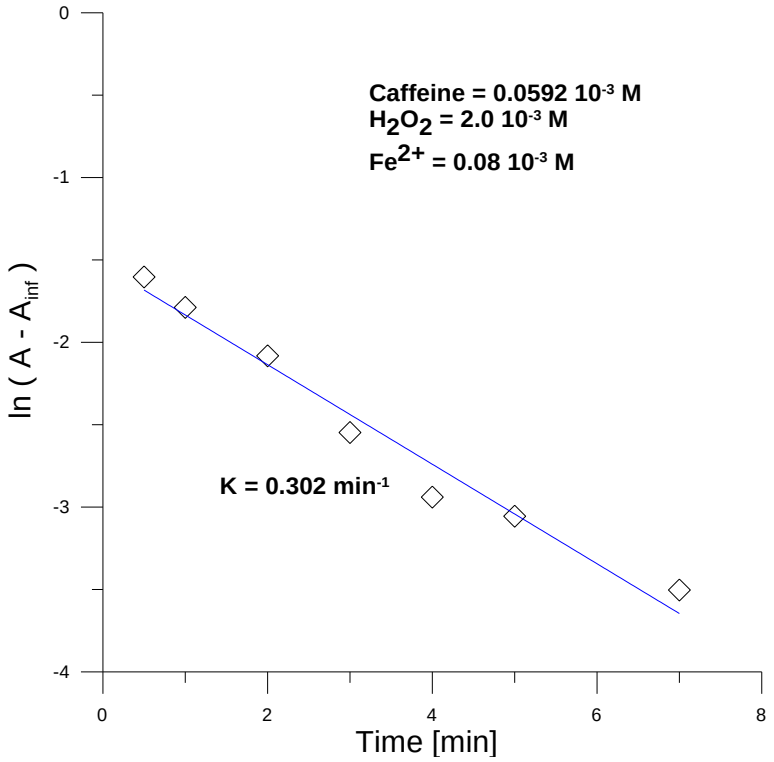

Graph 6.34. Linear correlation of a first order reaction
Experimental conditions: Ca_0=0.0592 10^{-3} M; H_2O_2=2.0 10^{-3} M; Fe^{2+}=0.08 10^{-3} M; UV lamp=125 W

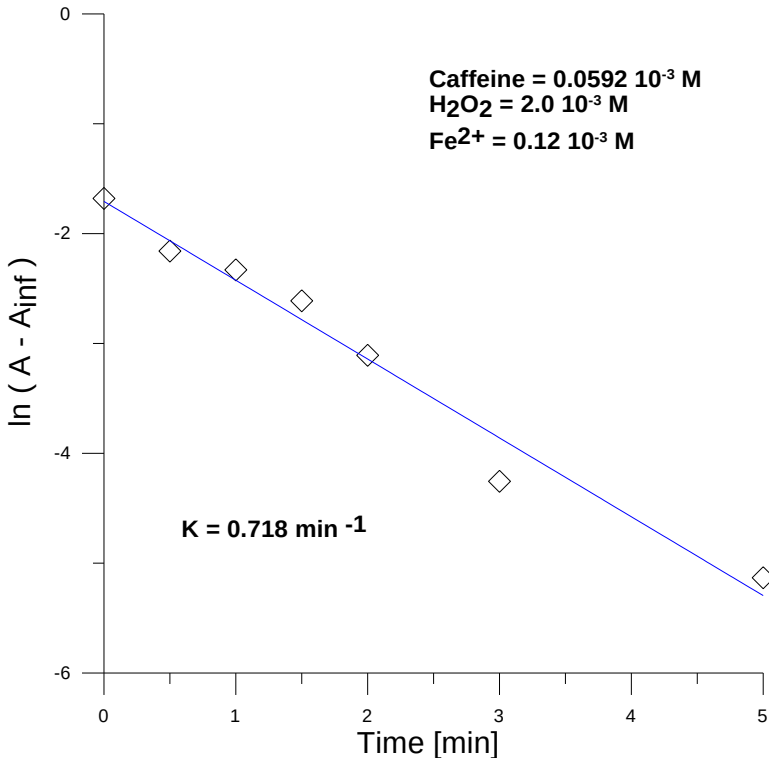

Graph 6.35. Linear correlation of a first order reaction
Experimental conditions: Ca_0=0.0592 10^{-3} M; H_2O_2=2.0 10^{-3} M; Fe^{2+}=0.12 10^{-3} M; UV lamp=125 W

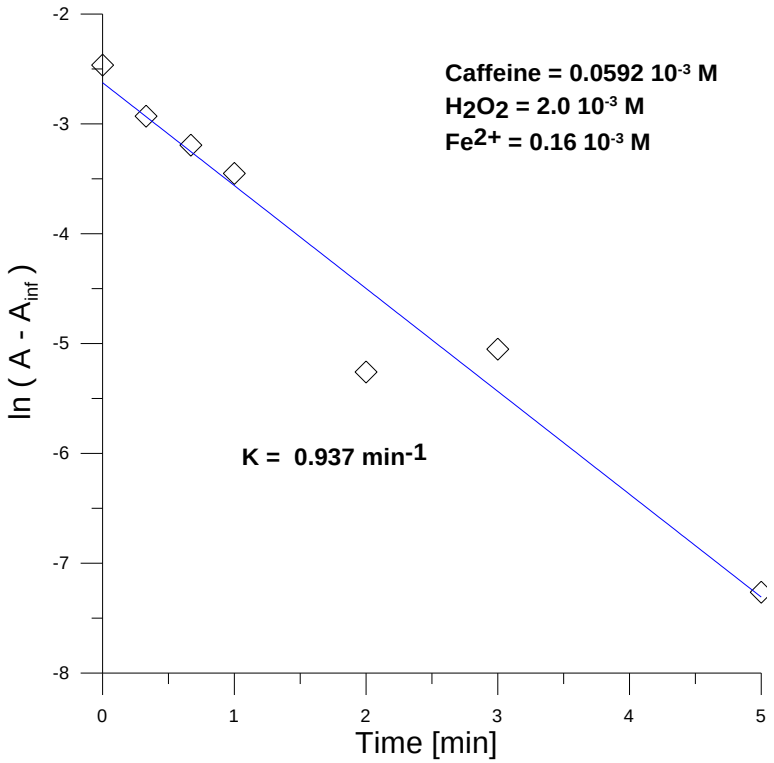

Graph 6.36. Linear correlation of a first order reaction
Experimental conditions: Ca_0=0.0592 10^{-3} M; H_2O_2=2.0 10^{-3} M; Fe^{2+}=0.16 10^{-3} M; UV lamp=125 W

Table 6.6. Kinetic constants for the second experimental series

Fe^{2+} [M]	K [min^{-1}]	K/K_{MIN}	$[Fe^{2+}]/[Fe^{2+}]_{MIN}$
$0.02\ 10^{-3}$	0.164	1.000	1
$0.04\ 10^{-3}$	0.238	1.451	2
$0.08\ 10^{-3}$	0.302	1.842	4
$0.12\ 10^{-3}$	0.718	4.378	6
$0.16\ 10^{-3}$	0.937	5.713	8

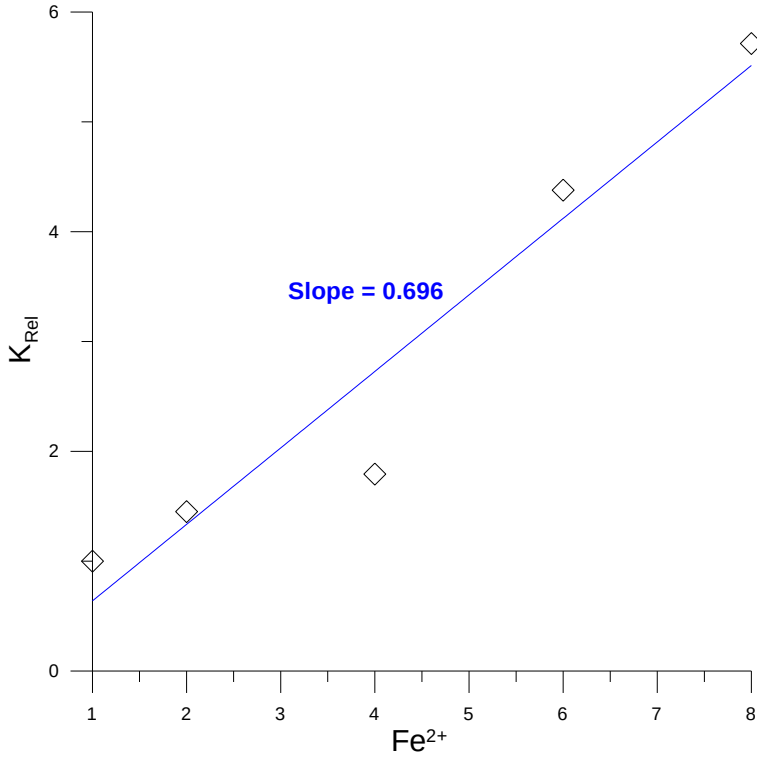

Graph 6.37. Relative kinetic constants as a function of the relative concentrations of catalyst

Further analyses were carried out in addition to the two experimental series described above, aimed at investigating the degradation rate of caffeine in the presence of irradiation, but without one or both the two Fenton's reagents (H_2O_2 or Fe^{2+}). Three kinetic runs were carried out with the experimental conditions listed in Table 6.7.

Graph 6.38 shows the absorbance spectra recorded during the irradiation of caffeine without both the Fenton's reagents (blank, see Table 6.7). During a 45 minutes reaction time only the 6% of caffeine was degraded. Therefore, UV-visible irradiation can degrade caffeine, but a complete reaction would need a very long time.

Graph 6.39 shows the absorbance spectra recorded during the photo-Fenton reaction carried out with 0.2 10^{-4} M catalyst, but without H_2O_2 (see Table 6.7). During a 45 minutes reaction time the 11% of caffeine was degraded. Therefore, the ferrous ion gives some contribution to the degradation of caffeine even in the absence of H_2O_2, but the observed reaction rate was not much higher than that of the blank reaction.

Finally, Graph 6.40 shows the absorbance spectra recorded as a function of time with H_2O_2 10^{-3} M, without catalyst (see Table 6.7). The rate of caffeine degradation is not much smaller than that observed in the corresponding experiment of the first series where also Fe^{2+} 0.2 10^{-4} M was present (Graphs 6.18-22), thus suggesting that H_2O_2 is the reagent mainly responsible for the degradation of caffeine during the photo-Fenton process. The kinetic constant of this last reaction as derived from Graph 6.41, was K=0.109 min^{-1}, approximately 2/3 of the value (K=0.154, see Table 6.6) found in the experiment with Fe^{2+} 0.2 10^{-4} M. Also in this case, the reaction mechanism involves OH· radicals, but their production completely relies on the dissociative effect of the radiation on H_2O_2, with no role played by the (absent) catalyst.

Graph 6.42 is similar to Graph 6.37, but in addition to the previous fit (which involves all the data) it also shows the linear fit obtained with the exclusion of the first two points, associated with the two smallest catalyst concentrations. This last fit has a slope very close to 1 (0.97), indicating that the degradation rate is directly proportional to the catalyst concentration. The first two data are associated with kinetic constants somewhat larger than those predicted by this last fit. A possible explanation could be traced back to the mechanism of reaction which does not rely on the presence of catalyst, its contribution becoming relatively more important with decreasing catalyst concentration.

Table 6.7. Experimental condition of kinetic runs where at least one reagent is missing

	Caffeine	H_2O_2	Fe^{2+}
Blank	0.0529 10^{-3} M		
Catalyst	0.0529 10^{-3} M		0.02 10^{-3} M
Oxidant	0.0529 10^{-3} M	0.1 10^{-3} M	

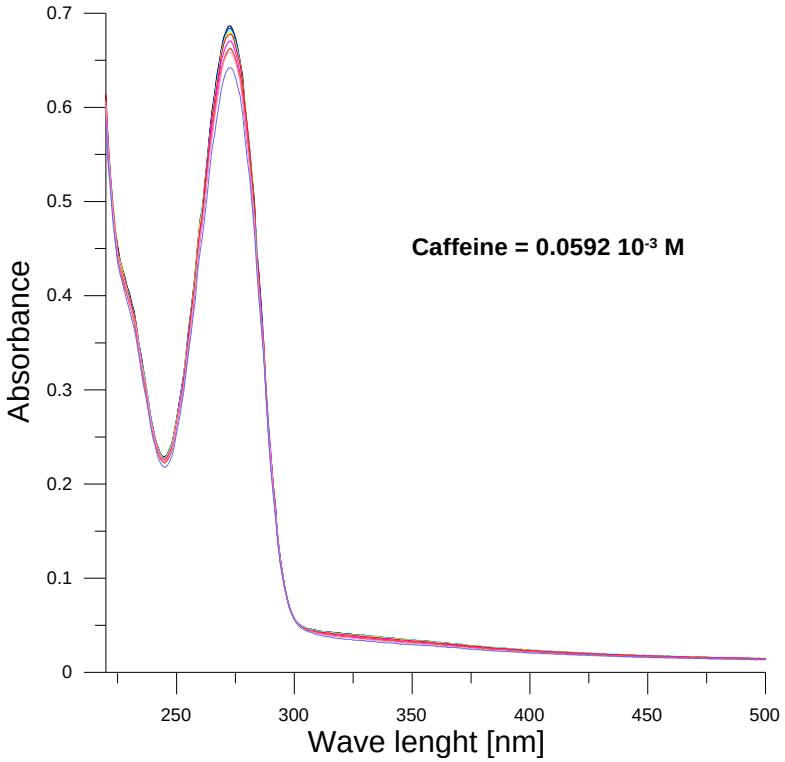

Graph 6.38. Absorption spectra as a function of time in the absence of both Fenton's reagents. Experimental conditions: Ca_0=0.0592 10^{-3} M; UV lamp=125 W

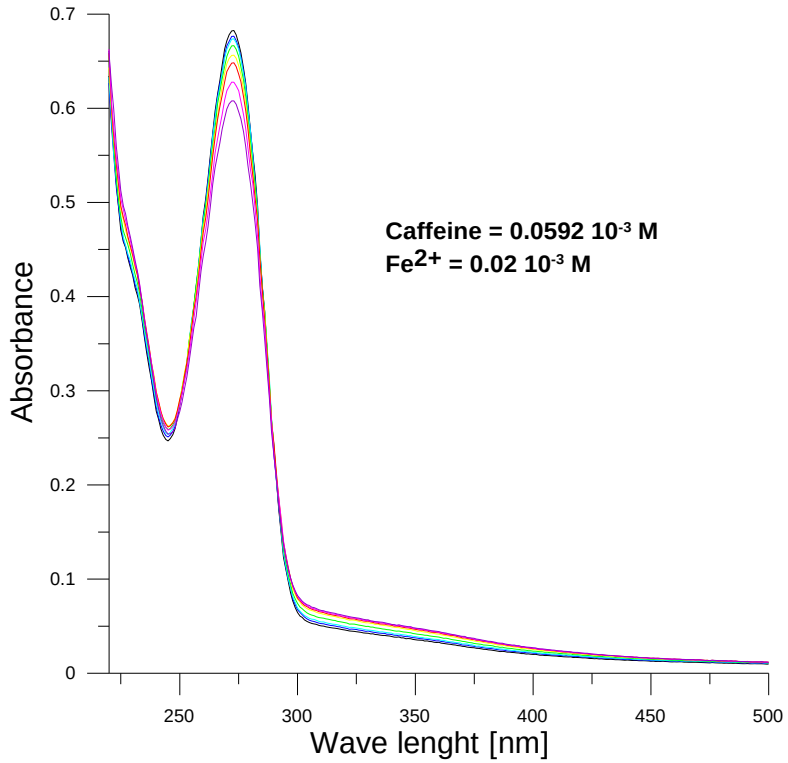

Graph 6.39. Absorption spectra as a function of time in absence of H_2O_2. Experimental conditions: Ca_0=0.0592 10^{-3} M; Fe^{2+}=0.02 10^{-3} M; UV lamp=125 W

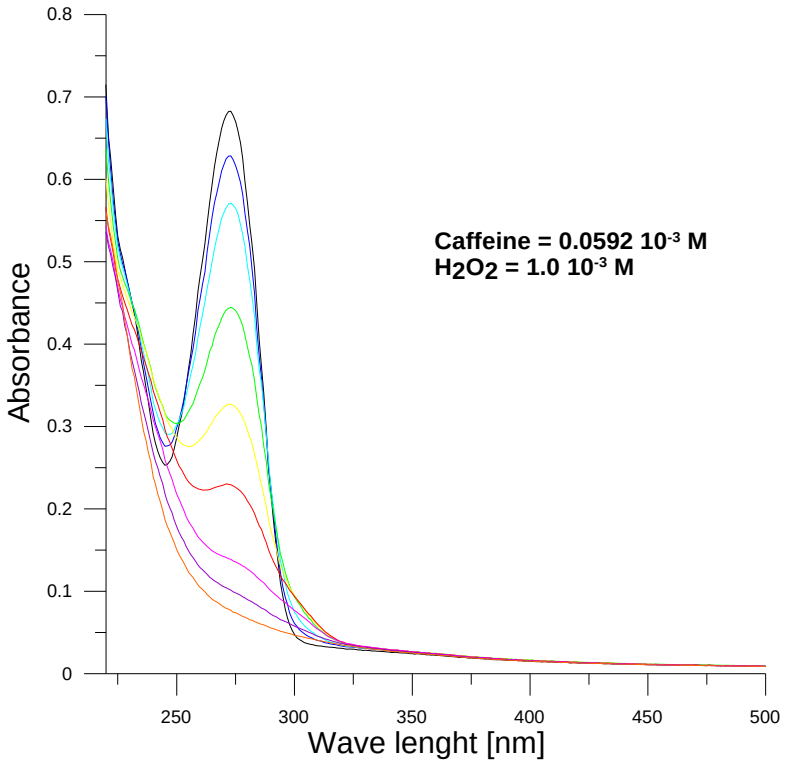

Graph 6.40. Absorption spectra as a function of time in the absence of Fe^{2+}. Experimental conditions: Ca_0=0.0592 10^{-3} M; H_2O_2=1.0 10^{-3} M; UV lamp=125 W

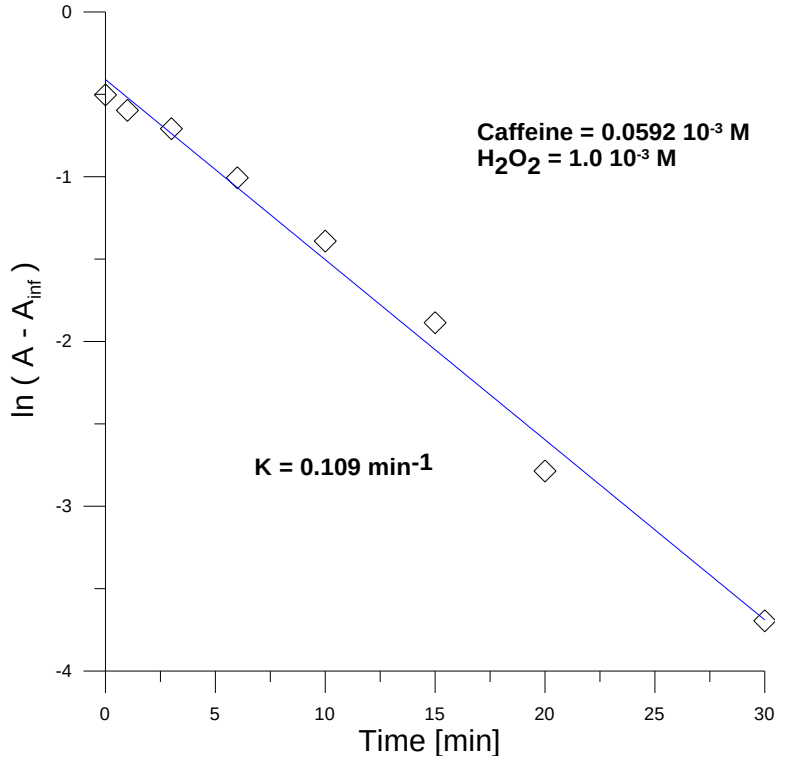

Graph 6.41. Linear correlation of a first order reaction Experimental conditions: Ca_0=0.0592 10^{-3} M; H_2O_2=1.0 10^{-3} M; UV lamp=125 W

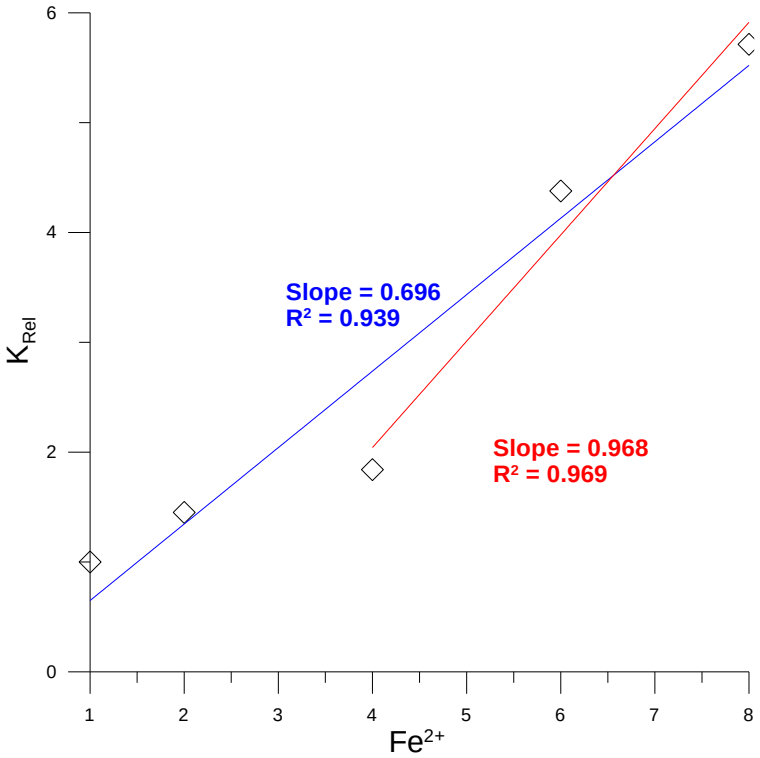

Graph 6.42. Relative kinetic constants as a function of the relative concentrations of catalyst

6.2.3. Theoretical calculations

This section contains the results obtained from calculation performed with the Gaussian 09 set of programs [245]. The reaction energies were evaluated for the reactions reported in Table 6.8. These reactions were selected on the basis of the scheme of Figure 1.10, in which possible pathways of the enzymatic degradation of caffeine are displayed. It is important to underline that actually the reactions which occur in a photo-Fenton process may be quite different. In Table 6.8 reactions which involve caffeine and possible reaction products are listed with the corresponding energy differences (ΔE) between products and reactants, supplied by density functional theory (DFT) calculations employing the hybrid B3LYP functional and the minimal 6-31G(d) basis set [246]. Figure 6.1 shows the geometries of the molecules involved, optimised with the same computational method. The numeric labels correspond to those also reported in Table 6.8.

According to the calculations (see Table 6.8) most of the reactions are strongly favoured on an energetic basis: negative ΔE values imply that the products are more stable than the reagents. Among the four possible products of the first step of caffeine degradation reported in Figure 1.10, formation of 1,3,7-trimethyl uric

acid (from caffeine and hydrogen peroxide) is the most favoured. Caffeine and hydrogen peroxide can also react to give theobromine, or theophylline or paraxanthine. All these reactions are energetically favoured, as well as the following oxidations which lead to the formation of methylxanthines and then xanthines. Paraxanthine can also react with hydrogen peroxide forming 1,7-dimethyluric acid. Finally, the formation of theophylline from a reaction between caffeine and water and direct formation of xanthine from caffeine are not favoured.

Starting from these result, the products or the intermediates eventually formed during the photo-Fenton reaction can not be defined, but a preliminary evaluation about the most favoured reactions catalysed by enzymes can be made. Further experimental work would be required to analyse and identify the products of the photo-Fenton reaction.

Table 6.8. Reactions which involve caffeine in water and respective ΔE

Reaction	ΔE [eV]	ΔE [kJ mol^{-1}]
$C_8H_{10}N_4O_2$ (**1**) + $HOOH \rightarrow C_8H_{10}N_4O_3$(**3**) + H_20 *caffeine* *1,3,7-trimethyl uric acid*	-3.017	-291.1
$C_8H_{10}N_4O_3$ (**3**) + $HOOH \rightarrow C_7H_{12}N_4O_3$(**4**) + CO_2 *1,3,7-trimethyl uric acid* *3,6,8-thrimethylallantoin*	-3.883	-374.6
$C_7H_{12}N_4O_3$ (**3**) + $2H_2O \rightarrow C_3H_8N_2O$(**15**) + $C_2H_6N_2O$(**16**) + $HOC(O)CHO$ *1,3,7-trimethyl uric acid* *dimethylurea* *methylurea*	0.177	17.1
$C_8H_{10}N_4O_2$ (**1**) + $HOOH \rightarrow C_7H_8N_4O_2$(**5**) + $CH_2(OH)_2$ *caffeine* *theophylline* *dihydroxymethane*	-2.444	-235.8
$C_7H_8N_4O_2$ (**5**) + $HOOH \rightarrow C_6H_6N_4O_2$(**6**) + $CH_2(OH)_2$ *theophylline* *3-methylxanthine* *dihydroxymethane*	-2.561	-247.1
$C_6H_6N_4O_2 + HOOH \rightarrow C_5H_4N_4O_2$ (**2**) + $CH_2(OH)_2$ *3-methylxantine* *xanthine* *dihydroxymethane*	-2.496	-240.8
$C_8H_{10}N_4O_2$ (**1**) + $HOOH \rightarrow C_7H_8N_4O_2$(**7**) + $CH_2(OH)_2$ *caffeine* *theobromine* *dihydroxymethane*	-2.567	-247.6
$C_7H_8N_4O_2$ (**7**) + $HOOH \rightarrow C_6H_6N_4O_2$(**8**) + $CH_2(OH)_2$ *theobromine* *7-methylxanthine* *dihydroxymethane*	-2.496	-240.9
$C_6H_6N_4O_2$ (**7**) + $HOOH \rightarrow C_5H_4N_4O_2$ (**2**) + $CH_2(OH)_2$ *theobromine* *xanthine* *dihydroxymethane*	-2.437	-235.2
$C_8H_{10}N_4O_2$ (**1**) + $HOOH \rightarrow C_7H_8N_4O_2$(**9**) + $CH_2(OH)_2$ *caffeine* *paraxanthine* *dihydroxymethane*	-2.513	-242.5
$C_7H_8N_4O_2$ (**9**) + $HOOH \rightarrow C_6H_6N_4O_2$(**10**) + $CH_2(OH)_2$ *paraxanthine* *1-methylxanthine* *dihydroxymethane*	-2.443	-235.7
$C_6H_6N_4O_2 + HOOH \rightarrow C_5H_4N_4O_2$ (**2**) + $CH_2(OH)_2$ *1-methylxanthine* *xanthine* *dihydroxymethane*	-2.544	-245.4
$C_7H_8N_4O_2$ (**9**) + $HOOH \rightarrow C_7H_8N_4O_3$(**11**) + H_2O *paraxanthine* *1,7-dimethyluric acid*	-2.993	-288.8
$C_8H_{10}N_4O_2$ (**1**) + $H_2O \rightarrow C_7H_8N_4O_2$(**5**) + CH_3OH *caffeine* *theophylline*	0.247	23.8
$C_8H_{10}N_4O_2$ (**1**) $\rightarrow C_5H_4N_4O_2$(**2**) + C_3H_6 *caffeine* *xanthine* *cyclopropane*	1.149	110.9

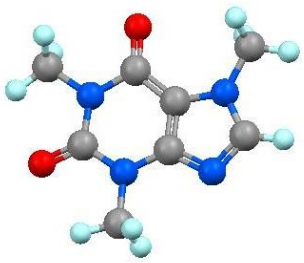

caffeine **(1)**

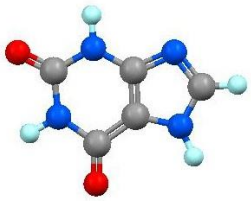

xanthine **(2)**

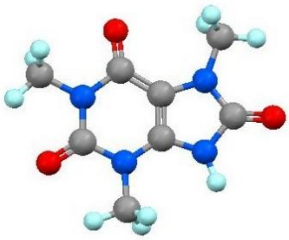

1,3,7-trimethyiluric acid **(3)**

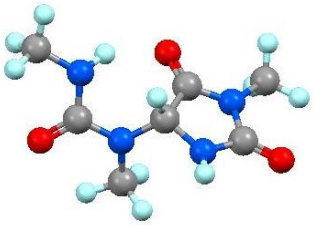

3,6,8-trimethylallantoin **(4)**

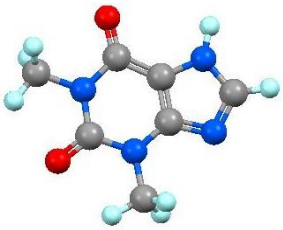

theohylline **(5)**

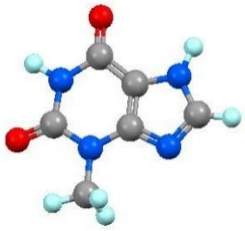

3-methylxanthine **(6)**

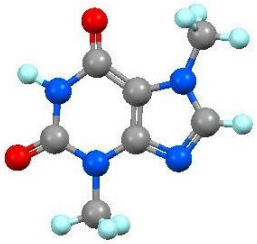

theobromine **(7)**

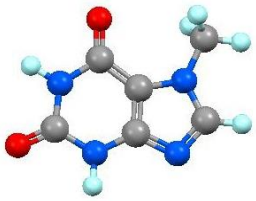

7-methylxanthine **(8)**

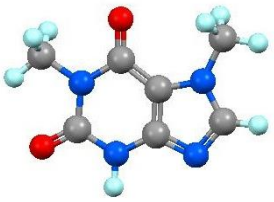

paraxanthine **(9)**

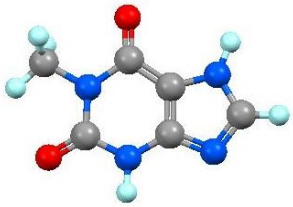

1-methylxanthine **(10)**

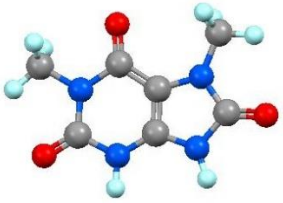

1,7-dimethyluric acid **(11)**

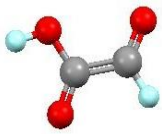

glyxolate **(12)**

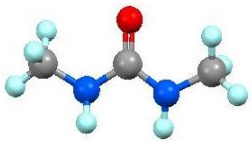

dimethylurea **(15)**

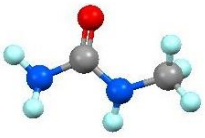

methylurea **(14)**

Figure 6.1. Optimized molecular geometry obtained with calculations B3LYP/6-31G (d)

The excitation energies of caffeine in the gas phase and in water solvent were also calculated, using the TD-B3LYP method [247]. Figure 6.2 shows the representation of the localisation properties of the three outermost filled orbitals (MOs) and the first three empty MOs of caffeine in the gas phase, as supplied by B3LYP/6-31G(d) calculations. The caffeine molecule is drawn with different colours which represent the different atoms: carbon is green, oxygen red, hydrogen white, and nitrogen light blue. The frontier orbitals of a molecule are the outermost occupied MOs and the lowest unoccupied MOs [250].The highest occupied MO (HOMO) is the easiest to be ionised, whereas the lowest unoccupied MO (LUMO) is the one associated with the electron affinity of the molecule. The HOMO-LUMO energy gap is represented by the difference in energy between these two MOs [250]. Therefore, the HOMO-LUMO gap is usually associated with the first electronic transition, that is, the one which occurs at the lowest energy. When caffeine absorbs UV radiations around 272 nm the neutral ground state is excited to the first excited state, where an electron is transferred from the HOMO to the LUMO, two MOs with p symmetry which possess the localisation properties displayed in Figure 6.2. The frontiers MOs involved in chemical reactivity are not always the HOMO and/or the LUMO, depending on their symmetry of the molecule [251]. When the symmetries of the HOMO and LUMO are not suitable for a transition to occur, the HOMO+1 or the LUMO+1 can be involved in the lowest transition.

According to B3LYP calculations with the 6-31+G(d) basis set, which contains diffuse functions for a better description of the (more diffuse in space) empty MOs, caffeine possesses a fairly large dipole moment: 4.0395 D in gas phase and 5.5151 D in water.

TD-B3LYP calculations with the 6-31+G(d) basis set were used to evaluate the electronically excited states of caffeine, in particular the energy of the HOMO-LUMO transition. In gas phase the energy of the HOMO-LUMO transition results to be 4.594 eV (corresponding to 270 nm), in good agreement with the experimental value (272 nm) measured in the UV spectrum in water [242]. Calculations which simulate the effect of water as a solvent were also performed with the the polarizable continuum model (PCM) [248]. The energy predicted for

the HOMO-LUMO transition was essentially identical to that supplied by the gas-phase calculations.

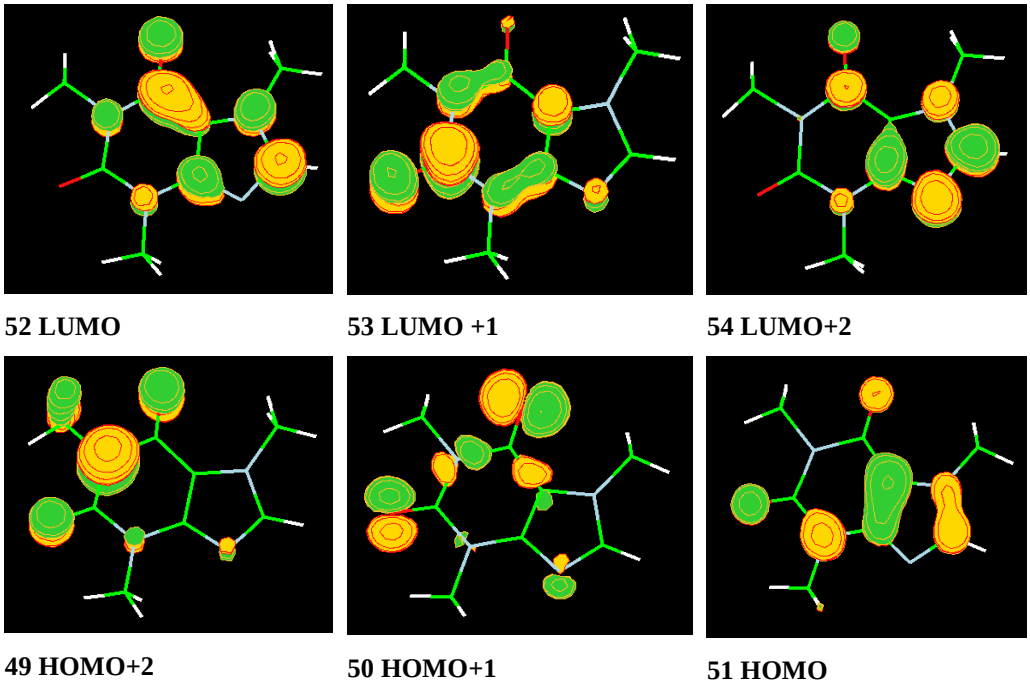

Figure 6.2. Representation of the frontier orbitals obtained with calculations B3LYP/6-31G(d)

7. CONCLUSIONS

The present thesis work is a study of the degradation of caffeine in water employing a photo-Fenton ($H_2O_2/Fe^{2+}/UV$) process, with the aim to evaluate the extent and rate of its elimination for possible applications to wastewater. Caffeine, as well as other organic compounds, is a contaminant of emerging concern (CEC). The removal of CECs from wastewater would contribute to reduce their increasing environmental impact. The process employed here to degrade caffeine is an advanced oxidation process (AOP) which takes advantage of a catalyst (Fe^{2+} ions), an oxidant (H_2O_2) and UV-visible radiation emitted by a mercury lamp.

A first aspect of the present study concerns the quality of water after exposition to this AOP. These analyses were carried out at the Faculty of Engineering of the University of Basque Country (UPV/EHU), in Vitoria-Gasteiz. In order to evaluate the effects of the two reagents on the water, two series of experiments were conducted on a caffeine water solution 0.592 10^{-3} M: one in which the concentration of the oxidant changes, keeping the catalyst dosage constants (Fe^{2+} 0.2 10^{-3} M), and another series in which the oxidant concentration is constant (H_2O_2 15.0 10^{-3} M), while the catalyst concentration changes. The parameters analysed to evaluate the quality of water at the end of the reaction are conductivity, turbidity, colour and aromaticity. They were measured before the start, then initially at intervals of about 1 minute and later of 10 minutes, for two hours.

The photo-Fenton reaction on the caffeine water solution produced a slight increase of conductivity, independently of the oxidant concentration. In contrast, as expected, conductivity was sizeably affected by the catalyst concentration, in agreement with the dissociation of iron sulphate into positive and negative ions. Indeed, a linear relationship between ferrous ion concentration and the average conductivity was observed. The application of the photo-Fenton process, under the current experimental conditions does not need further treatments to reduce the conductivity of the water, its value being lower than the limit fixed by the European Directives 75/440/EEC and 98/83/EC for drinking and surfaces water.

Colour (as measured by absorbance at 455 nm) and turbidity are strictly related. Both parameters increase during the reaction, then they reach a plateau. No evidence for a dependence on the oxidant concentrations was observed, while

both parameters increase with increasing concentration of catalyst, enhancing their initial and final values. Given that the ferrous ion in water undergoes oxidation to ferric ion, which can precipitate as $Fe(OH)_3$, the initial colour and turbidity are ascribed to this precipitate which causes a yellow-orange colour and cloudiness of the solution. Because of the strict dependence on the iron concentration, the increase of turbidity and colour during the reaction is plausibly not associated with degradation products of caffeine, but more likely with formation of Fe^{3+} derivatives. The application of the photo-Fenton process, under the current experimental conditions, would need further treatments to reduce turbidity and colour of water, given that they exceed the limits for drinking and surfaces water imposed by the European Directives 75/440/EEC and 98/83/EC.

Aromaticity was measured through the absorbance at 245 nm, but it was concluded that this method is not reliable for evaluating this parameter. Actually, absorption at 254 nm simply increases with increasing concentration of iron sulphate, whose extinction coefficient at this wavelength is fairly large.

An important aspect of the present study is concerned with the kinetics of degradation of caffeine, carried out at the Department of Chemistry G. Ciamician of the University of Bologna. The kinetics of degradation were followed through measurements of a physical property (absorbance at 272 nm) as a function of time. Absorbance is a suitable property, because it is proportional to concentration, provided the latter is sufficiently small that the Lambert-Beer law holds. TD-B3LYP calculations with the 6-31+G(d) basis set satisfactorily reproduce the maximum at 272 nm experimentally observed in the absorption spectrum of caffeine in water, ascribing the electronic transition to HOMO-LUMO excitation. Elaboration of the spectroscopic data demonstrated that the degradation of caffeine (carried out with an excess of oxidant) follows a first order rate law. Good linear plots were obtained reporting the natural logarithm of the difference between the absorbance at any time and that at the end of the reaction versus time. The slopes of these linear plots supplied the kinetic constants.

Two series of kinetics runs were carried out: one in which the concentration of the oxidant changes keeping the catalyst dosage constants (Fe^{2+} $0.2\ 10^{-4}$ M), and another in which the oxidant concentration is kept constant (H_2O_2 $2.0\ 10^{-3}$ M) while the catalyst concentration is changed. For both experimental series, the

absorption spectra of caffeine was recorded at time intervals in the range 0.5-5 minutes, according to the reaction rates.

The dependence of the reaction rate on the oxidant concentration was found to be small, although it is to be pointed out that even the smallest concentration of H_2O_2 employed was 16 times larger than that of caffeine. Future work would be necessary to investigate the effect of oxidant at lower concentrations.

The kinetic runs with constant oxidant concentration ($2.0\ 10^{-3}$ M) supplied clear evidence for the strong dependence of the reaction rate on the catalyst concentration. The relationship between kinetic constants and the corresponding Fe^{2+} concentrations indicated a nearly direct proportionality between the two variables.

The degradation rate of caffeine was evaluated also in the presence of only UV-visible radiation, and without one or both the two Fenton's reagents (H_2O_2 and Fe^{2+}). The results showed that UV-visible irradiation can degrade caffeine in water solution without Fenton's reagents, although the reaction would need a very long time. Addition of Fe^{2+} catalyst (without H_2O_2) somewhat increases the degradation rate, but a definitely higher rate is observed by adding H_2O_2 without Fe^{2+}. In the latter case, the measured reaction rate was as large as approximately 2/3 of that measured in the reaction with both Fenton's reagents. This finding indicates that the peroxidic O-O bond of H_2O_2 can be efficiently cleaved by the UV radiation to produce $OH^{\cdot}$ radicals. Each set of spectra recorded during the photo-Fenton processes shows an isosbestic point at about 300 nm, at least up to more than 50% completion of the reaction. This suggest that, as far as the isosbestic point is present, a single reaction takes place, implying that the products of degradation are not significantly further degraded.

Density functional B3LYP/6-31G(d) calculations show that the four most likely pathways promoted by enzymatic degradation of caffeine are strongly favoured on energetic grounds. According to the calculations 1,3,7-trimethyl uric acid is the most favoured product of the reaction between caffeine and hydrogen peroxide.

The present study serves as a window to the comprehension of the process of degradation of caffeine employing Fenton's reagents and UV-visible radiation. Future work should be aimed at identifying the products of degradation of this AOP. Coupling gas chromatography and mass spectrometry (GC/MS) it should

be possible to characterise these molecules, thus understanding if the process actually reduces the environmental impact or only shifts the problem producing other likely contaminants.

REFERENCES

[1] S. C. Anisfeld, Water Resource, Washington: Island Press, 2011, pp. 2-5.

[2] WHO and Unicef, Progress on Sanitation and Drinking Water: 2015 Update and MDG Assessment, Geneva, 2015.

[3] M. Petrovic, S. Gonzales and D. Barcelò, "Analysis and Removal of Emerging Contaminants in Wastewater and Drinking Water," *Trends in Analytical Chemistry,* vol. 22, no. 10, pp. 685-696, November 2003.

[4] T. P. Knepper, F. Sacher, F. T. Lange, J. H. Braunch, F. Karrenbrock, O. Roerden and K. Lindner, "Detection of Polar Organic Substances Relevant for Drinking Water," *Waste Management,* vol. 19, no. 1999, pp. 77-99, 1998.

[5] World Water Assessment Program and UNICEF, "The United Nations World Water Development Report 2017: Wastewater, the Untrapped Resource," Paris, 2017.

[6] R. U. Haden, "Introduction to Contaminants of Emerging Concern in the Environment: Ecological and Human Health Considerations," in *Contaminants of Emerging Concern in the Environment: Ecological and Human Health Considerations*, American Chemical Society, 2010, pp. 1-6.

[7] S. T. Glassmeyes, "U. S. Environmental Protection Agency and Emerging Contaminants," Cincinnati, 2009.

[8] D. Belhaj, R. Baccar, I. Jaabiri, J. Bouzid, M. Kallel, H. Ayadi and J. L. Zhou, "Fate of Selected Estrogenic Hormones in an Urban Sewage Treatment Plant in Tunisia (North Africa)," *Science of the Total Environment,* vol. 505, pp. 154-160, 2015.

[9] M. B. Ahmed, L. J. Zhou, H. Ngo and W. Guo, "Adsorptive Removal of Antibiotics from Water and Wastewater: Progress and Challenge," *Science of the Total Environment,* vol. 532, pp. 112-126, 2015.

[10] M. B. Ahmed, J. Zhou, H. Ngo, W. Guo, N. S. Thomaidis and J. Xu, "Progress in the Biological and Chemical Treatment Technologies for Emerging Contaminant Removal from Wastewater: A Critical Review," *Journal of Hazardous Material,* vol. 232, pp. 274-298, 5 February 2017.

[11] A. L. Lister and J. Van Der Kraak, "Endocrine Disruption: Why Is It so Complicated?," *Water Quality Research Journal,* vol. 36, no. 2, pp. 175-190, 2001.

[12] C. E. Stephen, D. I. Mount, D. J. Hansen, J. R. Gentile, G. A. Chapman and W. A. Brungs, “Guidelines for Deriving Numerical National Water Quality Criteria for the Protection of Aquatic Organisms and Their Uses,” 2016. [Online]. Available: https://www.epa.gov/sites/production/files/2016-02/documents/guidelines-water-quality-criteria.pdf.

[13] Chemical Safety Facts, “What Is a Flame Retardant,” 2019. [Online]. Available: https://www.chemicalsafetyfacts.org/flame-retardants/#. [Accessed 16 January 2019].

[14] Green Science Policy Institute, “Flame Retardants,” 2013. [Online]. Available: http://greensciencepolicy.org/topics/flame-retardants/.

[15] A. Pettigrew, “Halogenated Flame Retardants,” in *Othmer Encyclopedia of Chemical Technology*, New York, Wiley, 1994, pp. 654-76.

[16] BSEF, “Bromine Science and Environmental Forum,” 2000. [Online]. Available: t http://205.232.112.21/bsef/docs/Major_Brominated.doc;.

[17] M. Alaee, P. Arias, A. Sjodin and A. Bergman, “An Overview of Comercially Used Brominated Flame Retardants, Their Applications, Their Use Patterns in Differents Countries/Regions and Possible Mode of Release,” *Environmental International*, vol. 39, pp. 683-689, 2003.

[18] O. Segev, A. Kushumaro and A. Brenner, “Environmental Impact of Flame Retardants (Persistance and Biodegradability),” *International Journal of Environmental Research and Public Health,* vol. 6, no. 2, pp. 478-491, February 2009.

[19] C. A. DeWit, M. Alaee and D. C. G. Muir, “Levels and Trends of Brominated Flame Retardants in the Arctic,” vol. 64, pp. 209-233, 2006.

[20] I. Watanabe and S. I. Sakai, “Environmental Release and Behavior of Brominated Flame Retardants,” *Environmental International,* vol. 29, pp. 655-682, 2003.

[21] C. A. DeWit, “An Oveview of Brominated Flame Retardants in the Environment,” *Chemosphere,* vol. 46, pp. 583-624, 2002.

[22] J. De Boer, T. El-Sayed Aly, H. Fiedler, J. Leger, D. Muir, V. A. Nikiforov, G. T. Tomy and K. Tsunemi, The Handbook of Environmental Chemistry: Chlorinated Paraffins, vol. 10, Springer Science & Business Media, 2010.

[23] National Research Council, Toxicological Risks of Selected Flame-Retardant Chemicals, Washington (DC): National Academies Press (US), 2000.

[24] Chlorinated Paraffins Industry Association, *Letter to Darryl Arfsten (NRC), from Robert J.Fensterheim, Executive Director, CPIA, regarding chlorinated paraffins for use in furniture flame retardants.,* Washington DC: Chlorinated Paraffins Industry Association, 1999.

[25] IARC, "Some Flame Retardants and Textile Chemicals, and Exposures in the Textile Manufacturing Industry," *IARC Monographs on the Evaluation of Carcinogenic Risk to Human,* vol. 48, pp. 1-278, 1990.

[26] IARC, *IARC Monographs on the Evaluation of Carcinogenic Risk to Human,* no. 1, pp. 48-69, 1972.

[27] United State Code, "Title 7-Agricolture," 2012. [Online]. Available: https://www.govinfo.gov/content/pkg/USCODE-2012-title7/html/USCODE-2012-title7-chap6-subchapII-sec136.htm. [Accessed 16 January 2019].

[28] D. Pimentel and L. Levitan, "Pesticides: Amounts Applied and Amount Reaching Pests," *Bioscience,* vol. 36, no. 2, pp. 86-91, February 1986.

[29] M. Arias-Estevez, E. Lopez-Periago, E. Martinez-Carballo, J. Simal-Grandara, J. C. Mejuto and L. Garcia-Rio, "The Mobility and Degradation of Pesticides in Soils and the Pollution of Groundwater Resources," *Agricolture Ecosystem & Environment,* 2007.

[30] M. W. Aktar, D. Sengupta and A. Chowdhury, "Impact of Pesticides Use in Agriculture: Their Benefits and Hazards," *Interdisciplinary Toxicology,* vol. 2, no. 1, pp. 1-12, March 2009.

[31] M. I. Gurr, "Diet, Nutrition and the Prevention of Chronic Diseases (WHO, 1990)," *European Journal of Clinical Nutrition,* vol. 45, no. 12, pp. 619-623, 1991.

[32] Environews Forum, "Killer environment. Environ Health Perspect," *Environmental Health Perspectives,* vol. 107, no. 2, pp. A62-A63, February 1999.

[33] N. P. Cheremisinoff, Perfuolinated Chemicals (PCFs): Contaminants of Concern, Massachussetts: Jhon Wiley & Sons, 2016.

[34] EPA, "PFOA & PFOS Drinking Water Heath Advisories," EPA, 2016.

[35] F. Suja, B. K. Pramanik and S. Zain, “Contamination, Bioaccumulation and Toxic Effect of Perfluorinated Chemicals (PFCs) in the Water Environment: a Review Paper,” *Water Science & Technology,* pp. 1533-1544, 2009.

[36] EPA, “The Third Unregulated Contaminant Monitoring Rule (UCMR 3),” EPA, 2017.

[37] A. M. Calafat, Z. Kuklenyk, A. J. Reidy, S. P. Caudill, J. S. Tully and L. L. Needham, “Serum Concentration of 11 Polyfluoroalkyl Compounds in the U. S. Population: Data from the National Health and Nutrition Examination Survey (NHANES),” *Environmental Science & Technology,* vol. 41, no. 7, pp. 2237-2242, 1 April 2007.

[38] L. Maestri, S. Negri, M. Ferrari, S. Ghittori, F. Fabris, P. Danesino and M. Imbriani, “Determination of Perfluorooctanoic Acid and Perfuorooctanesulfonate in Human Tissue by Liquid Chromatography/Single Quadrupole Mass Specrtometry,” *Rapid Communication in Mass Specrometry: RCM,* vol. 20, no. 18, pp. 2728-2734, 2006.

[39] S. Catiglioni and E. Zuccato, “Illicit Drugs as Emerging Contaminants,” in *Contaminants of Emerging Concern in the Environment: Ecological and Human Health Considerations,* Milan, American Chemical Society, 2010, pp. 119-136.

[40] T. L. Jones-Lepp, D. A. Alvarez, J. D. Petty and J. N. Huckins, “Polar Organic Chemical Integrative Sampling and Liquid Cromatorgaphy-Electrospray/Ion-Trap Mass Spectrometry for Assessing Selected Prescription and Illicit Drugs in Treated Swage Effluents,” *Archives of Environmental Contamination and Toxicology,* vol. 47, no. 4, pp. 427-439, November 2004.

[41] N. Daglioglu, E. Y. Guzel and S. Kilercioglu, “Assessment of Illicit Drugs in Wastewater and Estimation of Drugs of Abuse in Adana Province, Turkey,” *Forensic Science International,* vol. 294, pp. 132-139, January 2019.

[42] J. Klaminder, T. Brodin, A. Sundelin, N. J. Andersn, J. Fahlman, M. Jonsson and J. Fick, “Long-Term Peristence of an Anxiolytic Drug (Oxazepam) in a Large Freshwater Lake,” *Environmental Science & Technology,* vol. 49, no. 17, pp. 10406-10412, 1 September 2015.

[43] E. Zuccato, S. Castiglioni, M. Tettamanti, R. Olandese, R. Bagnati, M. Melis and R. Fanelli, “Changes in Illicit Drug Consumpion Patterns in 2001 Detected by Wastewater Analysis,” *Drug and Alcohol Dependence,* vol. 118, no. 2-3, pp. 464-469, 1 November 2011.

[44] P. H. Liao, W. K. Yang, C. H. Yamg, C. H. Lin, C. C. Hwang and P. J. Chen, "Illicit Drug Ketamine Induces Adverse Effects From Behavioural Alteration and Oxidative Stress to P53-Regulated Apoptosis in Medaka Fish Under Environmentally Relevant Exposure," *Environmental Pollution,* vol. 237, pp. 1062-1071, June 2018.

[45] H. M. L. M. Lucia, A. N. Araujo, A. Fachini, A. Pena, C. Delerue-Matos and M. C. B. S. M. Montenegro, "Ecotoxicological Aspects Related to the Presence of Pharmaceuticals in the Aquatic Environment," *Journal of Hazardous Materials,* vol. 175, no. 1-3, pp. 45-95, March 2010.

[46] EEA, "Annual Report 2010 and Environmental Statement 2011," 2011.

[47] P. Verlicchi, M. Al Aukidy and E. Zambello, "Occurence of Pharmaceutical Compounds in Urban Wastewater: Removal, Mass Load and Environmental Risk After a Secondary Treatment - A Review," *Science of the Total Environment,* vol. 429, pp. 123-155, 1 July 2012.

[48] P. Verlicchi and E. Zambello, "How Efficient Are Constructed Wetlands in Removing Pharmaceuticals from Untreated and Treated Urban Wastewater? A Review," *Science of the Total Environment,* Vols. 470-471, pp. 1281-1306, 1 February 2014.

[49] M. Caraballa, F. Omil, A. C. Alder and J. M. Lema, "Comparison Between the Conventional Anaerobic Digestion (CAD) of Sewage Sludge and its Combination with a Chemical or Thermal Pre-Treatment Concerning the Removal of Pharmaceutical and Personal Care Products," *Water Science & Technology,* vol. 53, no. 8, pp. 109-117, 2006.

[50] K. Fent, A. A. Weston and D. Caminada, "Ecotoxicology of Human Pharmaceuticals," *Aquatic Toxicology,* vol. 78, no. 2, p. 207, June 2007.

[51] A. Sadezky, D. Loffer, M. Sclusenes, B. Roig and T. Ternes, "Real Situation: Occurrence of the Main Investigated PPs in Water Bodies," in *Pharmaceuticals in the Environment,* London, IWA Publishing, 2010, pp. 1-14.

[52] J. Hu, J. Zhou, S. Q. Zhou, P. Wu and Y. F. Tsang, "Occurence and Fate of Antibiotics in a Wastewater Treatment Plant and Their Biological Effects on Receiving Waters in Guizhou," *Process Safety and Environmental Protection,* vol. 113, pp. 483-490, January 2018.

[53] T. P. Van Boeckel and S. Gandra, “Global Antibiotic Consumption 2000 to 2010: an Analysis of National Pharmaceutical Sales Data,” *The Lancet Infectious Diseases,* vol. 18, no. 8, pp. 742-750, August 2014.

[54] OECD(a), “Health at a Glance,” 2015. [Online]. Available: http://www.oecd-ilibrary.org/sites/health_glance-2015-en/10/04/index.html?itemId=/content/chapter/health_glance-2015-68-en&mimeType=text/html.

[55] M. M. Schultz, E. T. Furlong, D. W. Kolpin, S. L. Werner, H. L. Schoenfuss, L. B. Barber, V. S. Blazer, D. O. Norris and A. M. Vajada, “Antidepressant Pharmaceuticals in Two U.S. Effluent-Impacted Streams: Occurrence and Fate in Water and Sediment, and Selective Uptake in Fish Neural Tissue,” *Environmental Science & Technology,* vol. 44, no. 6, pp. 1918-1925, February 2010.

[56] M. M. Painter, M. A. Burkley, M. L. Julius, A. M. Vajda, D. O. Norris, L. B. Barber, E. T. Furong, M. M. Schultz and H. L. Schoenfuss, “Antidepressants at Environmentally Relevant Concentrations Affect Predator Avoidance Behavior of Larval Fathead Minnows (Pimephales promelas),” *Environmental Toxicology and Chemistry,* December 2009.

[57] OECD(b), “Health Statistics,” 2015. [Online]. Available: http://dx.doi.org/10.1787/health-data-en.

[58] E. Felis and K. Miksch, “Removal of Analgesic Drugs from the Aquatic Environment Using Photochemical Methods,” *Water Science & Technology,* vol. 60, no. 9, pp. 2253-2259, 2009.

[59] P. Clot-Faybesse, F. Bertin-Hugault, C. Blochet, P. Denormandie, P. Rat, P. E. Hay and S. Bonin-Guillaume, “Analgesic Consumption in Nursing Homes: Observational Study about 99 Nursing Homes,” *Geriatrie et Psychologie Neuropsychiatrie du Vieillissement,* vol. 15, no. 1, pp. 25-34, March 2017.

[60] P. A. Hedin, Plant Resistance to Insect, vol. 208, American Chemical Society, 1983.

[61] J. A. Nathanson, “Caffeine and Related Methylxantines: Possible Naturally Occurring Pesticides,” *Science,* vol. 226, no. 4671, pp. 184-187, 1984.

[62] A. Nehlig and J. D. G. Daval, “Caffeine and the Central Nervous System: Mechanism of Action, Biochemical, Metabolic and Psycostimulant Effects,” *Brain Research Reviews,* vol. 17, pp. 193-170, 1992.

[63] Erowid, “Does Yerba Mate Contain Caffeine or Mateine?,” December 2003. [Online]. Available: https://erowid.org/plants/yerba_mate/yerba_mate_chemistry1.shtml.

[64] EFSA, «Scientific Opinion on the Safety of Caffeine - EFSA Panel on Dietetic Products, Nutrition and Allergies (NDA),» *EFSA Journal*, vol. 13, n. 5, p. 4102, 2015.

[65] Erowid, “Caffeine Content of Beverages, Food & Medications,” February 2015. [Online]. Available: https://www.erowid.org/chemicals/caffeine/caffeine_info1.shtml.

[66] M. B. Hicks, H. Hsieh and B. L. N. , “Tea Preparation and its Influence on Methylxanthine Concentration,” vol. 29, no. 3-4, pp. 325-330, 1996.

[67] V. R. Preedy, Caffeine: Chemistry, Analysis, Function and Effects, RSC Publishing, 2012.

[68] I. J. Buerge, T. Poiger, M. D. Muller and H. R. Buser, “Caffeine, an Anthtopogenic Marker for Wastewater Contamination of Surface Waters,” *Environmental Science & Technology*, vol. 37, no. 4, pp. 691-700, 2003.

[69] OECD, “High Production Volume Chemicals,” Paris, 2004.

[70] F. Magkos and S. A. Kavouras, “Caffeine Use in Sports, Pharmacokinetics in Man, and Cellular Mechanism of Action,” *Critical Review in Food Science and Nutrition*, vol. 45, no. 7-8, pp. 535-562, 1 October 2005.

[71] R. Pardo Lonzano, Y. Alvarez Garcia, D. Carral Tafalla and M. Farré Albaladejo, “Cafeina: un nutriente, un farmaco, o una droga de abuso.,” *Redalyc.org*, 2007.

[72] Human Metabolome Database (b), “Showing Metabocard for Theobromine (HMDB0002825),” [Online]. Available: http://www.hmdb.ca/metabolites/HMDB0002825. [Accessed 17 January 2019].

[73] J. Flores, J. A. Armijo and A. Mediavilla, Farmacologia Humana 3° Edicion, Barcellona: Masson, S. A., 2003.

[74] EFSA, “Scientific Opinion on Flavouring Group Evaluation 49, Revision 1 (FGE.49Rev1): Xanthine Alkaloids from the Triority List,” *EFSA Journal*, 2017.

[75] T. Giesbrecht, J. Rycrofts, M. J. Rowson and E. A. De Buin, “The Combination of L-theanine and Caffeine Improves Cognitive Performance and Increases Subjective Alertness,” *Nutritional Neurosciences*, vol. 13, pp. 283-290, 2010.

[76] Y. Dagan and J. T. Doljansky, “Cognitive Performance During Sustained Wakefulness: A Low Dose of Caffeine is Equally Effective as Modafinil in Alleviating the Nocturnal Decline,” *Chronobiology International,* vol. 23, pp. 973-983, 2006.

[77] S. C. Sigmon, R. I. Herning, W. Better, J. K. Cadet and R. R. Griffiths, “Caffeine Withdrawal, Acute Effects, Tolerance and Absence of Net Beneficial Effetcs of Chronic Administration: Celebral Blood Flow Velocity, Quantitative EEG and Subjective Effects,” *Psychopharmacology,* vol. 204, pp. 573-585, 2009.

[78] M. D. David Yew and S. Kim, “Medscape,” 2017. [Online]. Available: http://emedicine.medscape.com/article/821863-overview.

[79] N. Kristof, “Arsenic in Our Chicken?,” *The New York Time,* 4 April 2012.

[80] G. C. Ferraz, A. R. Teixeira-Neto, M. I. Mataqueiro, J. C. Lacerda-Neto and A. Queiroz-Neto, “Effects of Intravenous Administration of Caffeine on Physiologic Variables in Exercising Horses,” *American Journal of Veterinary Research,* vol. 69, no. 12, pp. 1670-1675, December 2008.

[81] C. U. Barcus, “Bees Buzzing on Caffeine,” *National Geographic News,* 2013.

[82] R. G. Hollingsworth, J. W. Armstrong and E. Campbell, “Caffeine As a Repellent for Slugs and Snalis,” *Nature,* vol. 417, pp. 915-917, 27 June 2002.

[83] University of Hawaii, “Control of Coqui Frog Populations in Hawaii,” 2002. [Online]. Available: https://portal.nifa.usda.gov/web/crisprojectpages/0194237-control-of-coqui-frog-populations-in-hawaii.html. [Accessed 24 June 2017].

[84] B. Gartrell and C. Reid, “Death by Chocolate: a Fatal Problem for an Inquisitive Wild Parrot,” *PubMed,* vol. 55, no. 3, pp. 149-151, June 2007.

[85] M. R. Burkhardt, P. P. Soliven, S. L. Werner e D. G. Vaught, «Determination of Submicrogram-Per-Liter Concentrations of Caffeine in Surface Water and Groundwater Samples by Solid-Phase Extraction and Liquid Chromatography,» *Journal of AOAC International,* vol. 82, pp. 191-166, 1999.

[86] R. L. Selier, S. D. Zaugg, J. M. Thomas and D. L. Howcroft, “Caffeine and Pharmaceutical as Indicators of Waste Water Contamination Wells,” *Ground Water,* vol. 37, pp. 405-410, 1999.

[87] C. Fernandez, M. Gonzalez-Doncel, J. Pro, G. Carbonell and J. V. Tarazona, “Occurrence of Pharmaceutically Active Compounds in Surface Water of the

Henares-Jarama-Tajo River System (Madrid, Spain) and a Potential Risk Characterization," *Science of the Total Environment,* vol. 408, no. 3, pp. 543-551, 1 January 2010.

[88] S. Zhang, Q. Zhang, S. Darisaw, O. Ehie and G. Wang, "Simultaneous Quantification of Polycyclic Aromatic Hydrocarbons (PAHs), Polychlorinated Piphenyls (PCBs), and Pharmaceuticals and Personal Care Products (PPCPs) in Mississippi River Water, in New Orleans Louisiana, USA," *Chemosphere,* vol. 66, no. 6, pp. 1057-1069, January 2007.

[89] Y. Vystavn, F. Huneau, V. Grynenko, Y. Vergeles, H. Celle-Jeaton, N. Tapie, H. Budzinski and P. Le Costumer, "Pharmaceuticals in Rivers of Two Regions with Contrasted Socio-Economic Conditions: Occurrence, Accumulation, and Comparison for Ukraine and France," *Water, Air, & Soil Pollution,* vol. 223, no. 5, pp. 2111-2124, June 2012.

[90] M. Kuster, D. A. Azevedo, M. Lopez de Alda, A. Neto and D. Barcelò, "Analysis of Phytoestrogens, Progestrogens and Estrogens in Environmental Waters from Rio de Janeiro (Brazil)," *Environmental Intenational,* vol. 35, no. 7, pp. 997-1003, October 2009.

[91] Y. Yoon, J. Ryu, J. Oh and B.-G. S. S. A. Choi, "Occurrence of Endocrine Disrupting Compounds, Pharmaceuticals, and Personal Care Products in the Han Rive (Seoul, South Korea)," *Science of the Total Environment,* vol. 408, no. 3, pp. 636-643, January 2010.

[92] X. Yang, F. Chen, F. Meng, Y. Xie, H. Chen, K. Young, W. Lou, T. Ye and W. Fu, "Occurrence and Fate of PPCPs and Correlation with Water Quality Parameters in Urban Riverine Waters if the Pearl River Delta, South China," *Environmental Science and Pollution Research,* vol. 20, no. 8, pp. 5864-5875, August 2013.

[93] Z. Luo, Y. Tu, H. Li, B. Qiu, Y. Liu and Z. Yang, "Endocrine-Disrupting Compounds in the Xiangjiang River of China: Spatio-Temporal Disruption, Source Apportionment and Risk Assessment," *Ecotoxicology and Environmental Safety,* vol. 167, pp. 476-484, 15 January 2019.

[94] M. Williams, R. S. Kookana, A. Mehta, S. K. Yadav, B. L. Tailor and B. Maheshwari, "Emerging Contaminants in a River Recieving Entreated Wastewater from an Indian Urban Center," *Science of the Total Environment,* vol. 647, pp. 1256-1265, 10 January 2019.

[95] S. Weigel, J. Kuhlmann and H. Huhnerfuss, “Drugs and Personal Care Products as Ubiquitous Pollutants: Occurence and Distribution of Clofibric Acid, Caffeine and DEET in the North Sea,” *Science of the Total Environment,* vol. 296, no. 1-3, pp. 131-141, 5 August 2004.

[96] R. Seigner and R. F. Chen, “Caffeine in Boston Harbor Seawater,” *Marine Pollution Bulletin Journal,* no. 44, pp. 383-387, 2002.

[97] L. Mijangos, H. Ziarrusta, O. Ros, L. Kortazar, L. A. Fernandez, M. Olivares, O. Zuloaga, A. Prieto and N. Etxebarria, “Occurence of Emerging Pollutants in Estuaries of the Basque Country: Analysis of Source and Distribution, and Assessment of the Environmental Risk,” *Water Research,* vol. 147, pp. 152-163, 15 December 2018.

[98] P. M. Ondarza, S. P. Haddad, E. Avigliano, K. S. Miglioranza and B. W. Brooks, “Pharmaceuticals, Illicit Drugs and Their Metabolites in Fish from Argentina: Implications for Protected Areas Influenced by Urbanization,” *Science of the Total Environment,* vol. 649, pp. 1029-1037, 1 February 2019.

[99] J. L. Rodriguez-Gil, N. Caceres, R. Dafouz and Y. Valcarcel, “Caffeine and Paraxanthine in Aquatic Systems: Global Exposure Distributions and Probabilistic Risk Assessment,” *Science of the Total Environment,* vol. 612, pp. 1058-1071, 15 January 2018.

[100] S. M. Cameron, R. Long, C. Essenberg and T. Dodge, “Caffeine Pathway Map,” 15 May 2006. [Online]. Available: http://eawag-bbd.ethz.ch/caf/caf_map.html.

[101] P. Mazzafera, «Catabolism of Caffeine in Plants and Microorganisms,» *Frontiers in Bioscience: a Journal and Virtual Library,* vol. 9, pp. 1348-59, 1 May 2004.

[102] Human Metabolome Database (a), “Showing metabocard for Paraxanthine (HMDB0001860),” [Online]. Available: http://www.hmdb.ca/metabolites/HMDB0001860. [Accessed 28 December 2018].

[103] K. Madyastha and G. R. Sridhar, “A Novel Pathway for the Metabolism of Caffeine by a Mixed Culture Consortium,” *Biochemical and Biophysical Research Communications,* vol. 249, no. 1, pp. 178-81, August 1998.

[104] N. Naddeo, V. Rizzo and V. Belgiorno, Water, Wastewater and Soil Treatment by Advanced Oxidation Processes, Fasciano (Italy): ASTER onlus Editore, 2010.

[105] W. H. Glaze, J. Kang and D. H. Chapin, “The Chemistry of Water Treatment Processes Involving Ozone, Hydrogen Peroxyde and Ultraviolet Radiation,” *Ozone Science & Engineering,* vol. 33, pp. 335-352, 1987.

[106] F. Mendez-Arriaga, S. Esplugas and J. Giménez, “Degradation of the Emerging Contaminant Ibuprofen in Water by Photo-Fenton,” *Water Research,* vol. 44, no. 2, pp. 589-595, 2010.

[107] N. Villota, J. M. Lomas and L. M. Camarero, “Kinetic Modelling of Water-Color Changes in a Photo-Fenton System,” *Journal of Photochemistry and Photobiology A: Chemistry,* p. 573–579, 2018.

[108] J. L. Zhou, M. B. Ahmed, H. H. Ngo, W. Guo, N. S. Thomaidis and J. Xu, “Progress in the Biological and Chemical Treatment Techologies for Emerging Contminant Removal from Wastewater: A Critical Review,” *Journal of Hazardous Material,* vol. 232, pp. 274-298, 5 February 2017.

[109] A. Berni, *Processi di Ossidazione Avanzata (AOPs) Promossi da Radiazione UV : Confronto di Prestazioni,* 2016.

[110] S. N. Aki and M. A. Abraham, “An Economic Evaluation of Catalytic Supercritical Water Oxidation: Comparison with Alternative Waste Treatment Technologies,” *Environmental Progress,* vol. 17, no. 4, pp. 246-255, 1998.

[111] E. M. Aieta, K. M. Reagan, J. S. Lang, L. McReynolds, J. Kang and W. H. Glaze, “Advanced Oxidation Processes for Treating Groundwater Contaminated with TCE and PCE: Pilot-Scale Evaluations,” *Journal (American Water Work Association),* vol. 80, no. 5, pp. 64-72, 1988.

[112] S. Sharma, J. P. Ruparelia and M. L. Patel, “A General Review on Advanced Oxidation Processes fot Waste Water Treatment,” in *International Conference on Current Trends in Technology, NUiCONE,* 2011.

[113] F. J. Beltran, Ozone Reaction Kinetics for Water and Wastewater System, CRC Press, 2003.

[114] S. K. Sharma, Green Chemistry for Dyes Removal from Waste Water: Research Trends and Applications, John Wiley & Sons, 2010.

[115] W. Huang, *Homogeneous and Heterogeneous Fenton and Photo-Fenton Processes: Impact of Iron Complexing Agent Ethylenediamine-N,N’-Disuccinic Acid (EDDS),* Wuhan, 2012.

[116] K. Scott, Sustainable and Green Electrochemical Science and Technology, Jhon Wiley & Sons, 2017.

[117] R. E. Heeks, L. P. Smith and P. M. Perry, “Oxidation Technologies for Groundwater Treatment,” *ACS Symposium Series,* vol. 46, no. 8, pp. 110-132, 1991.

[118] D. F. Bishop, G. Stern, M. Fleischman and L. S. Marshall, “Hydrogen Peroxide Catalytic Oxidation of Refractory Organics in Municipal Waste Waters,” *Industry & Engineering Chemistry Process Design and Development,* vol. 7, pp. 110-117, 1968.

[119] C. Walling, «Fenton's Reagent Revisited,» *Account of Chemical Research,* vol. 8, n. 4, pp. 125-131, 1975.

[120] Metcalf and Eddy Inc, Wastewater Engineering: Treatment, Disposal, Reuse, New Delhi: McGraw-Hiil, 2003.

[121] EPA, «Extremely Hazardous Substances (EHS) Chemical Profiles and Emergency First Aid Guides,» U.S. Government Printing Office, Washington D.C., 1998.

[122] B. Langlais, D. A. Reckhow and D. R. Brink, Ozone in Water Treatment: Application and Engineering, CRC Press, 1991.

[123] P. S. Bailey, Ozonation in Organic Chemistry V1 First Edition, Academic Press, 1978.

[124] H. Tomiyasu, H. Fukutomi and G. Gordon, “Kinetics and Mechanism of Ozone Decomposition in Basic Aqueous Solution,” *Inorganic Chemistry,* vol. 24, no. 19, pp. 2962-2966, September 1985.

[125] J. Weiss, “Investigation on the Radical HO_2 in Solution,” *Transaction of the Faraday Society,* pp. 668-681, 1935.

[126] E. Staehelin, R. E. Buelher and J. Hoigne, “Ozone Decomposition in Water Studied by Pulse Radiolysis. 2. Hydroxyl and Hydrogen Tetroxyde (HO_4) as Chain Intermediates,” *The Journal of Physical Chemisrty,* vol. 88, no. 24, pp. 5999-6004, November 1984.

[127] J. Prousek, “Advanced Oxidation Processes for Water Treatment. Photochemical Processes,” *Chemické Listy,* vol. 90, no. 5, pp. 307-315, 1996.

[128] T. Deed, *The Manifacture of Hydrogen Peroxide,* Heather Wansbrough, 2005.

[129] I. H. Suffet, J. Mallevialle and E. Kawczynski, Advances in Taste-and-Odor Treatment and Control, American Water Works Association, 1995.

[130] J. M. Joseph, H. Destaillats, H. Hung and M. R. Hoffman, “The Sonochemical Degradation of Azobenzene and Relates Azo Dyes: Rate Enhancements via Fenton's Reactions,” *The Journal of Physical Chemistry A,* vol. 104, no. 2, pp. 301-307, 2000.

[131] X. Pang, Water: Molecular Structure and Properties, World Scientific, 2014.

[132] M. R. Hoffman, I. Hua, R. Hochemer, D. Williberg, P. Lang and A. Krate, Chemistry Under Extreme Non-Classical Conditions, Rudi van Eldik and Colin D. Hubbard, 1997.

[133] Zimpro-Siemens Water Techonogies, “Wet Air Oxidation Systems: the Cleanest Way to Treat the Dirtiest Water,” 2013. [Online]. Available: https://www.siemens.com/content/dam/webassetpool/siemens/markets/water/water-solutions-rothschild-broussard/documents_ws/Zimpro%20Wet%20Air%20Oxidation.pdf. [Accessed 14 January 2019].

[134] S. T. Kolackowski, P. Plucisnski, F. J. Beltran, F. J. Rivas and D. B. McLurgh, “Wet Air Oxidation: a Review of Process Technologies and Aspects in Reactor Design,” *Chemical Engineering Journal,* vol. 73, no. 2, pp. 143-160, May 1999.

[135] V. S. Mishra, V. V. Mahajani and J. B. Joshi, “Wet Air Oxidation,” *Industrial & Engineering Chemistry Research,* vol. 34, pp. 2-48, 1995.

[136] F. C. Moreira, R. A. R. Boaventura, E. Brillas and V. J. P. Vilar, “Electrochemical Advanced Oxidation Processes: A Review on their Application to Synthetic and Real Wastewaters,” *Elsevier,* vol. 202, pp. 217-261, 2016.

[137] M. Panizza and G. Cerisola, “Direct and Mediater Anodic Oxidation of Organic Pollutants,” *Chemical Reviews,* vol. 109, no. 12, pp. 6541-6569, 6 August 2009.

[138] N. L. Weinberg and H. R. Weinberg, Electrochemical Oxidation of Organic Compounds, Stamford: Central Research Division, American Cyanamid Company, 1968.

[139] J. Belloni, M. Mostafavi, H. Remita, J. Marignier and M. Delcourt, “Radiation Induced Synthesis of Mono- and Multi- Metallic Clusters and Nanocolloids,” *New Journal of Chemistry,* vol. 22, no. 11, pp. 1239-1255, November 1998.

[140] S. P. Ramnani, S. Sabharwal and J. Vinod Kumar, “Advantage of Radiolysis Over Impregnation Method for the Synthesis of SiO_2 Supported Nano-Ag Catalyst for

Direct Decomposition of N2O," *Catalysis Communications,* vol. 9, no. 5, pp. 756-761, March 2008.

[141] J. Emspak, "Live Science," 5 May 2016. [Online]. Available: https://www.livescience.com/54652-plasma.html.

[142] M. Moreau, N. Orange and M. G. J. Feuilloley, "Non-Thermal Plasma Technologies: New Tools for Bio-Decontamination," *Biotechnology Advances,* vol. 26, no. 6, pp. 610-617, November-December 2008.

[143] S. Masuda, S. Hosokawa, X. Tu and Z. Wang, "Novel Plasma Chemical Technologies - PPCP and SPCP for Control of Gaseous Pollutants and Air Toxics," *Journal of Electrostatics,* vol. 34, no. 4, pp. 415-438, May 1995.

[144] D. Gerrity, B. D. Stanford, R. A. Trenholm and S. A. Snyder, "An Evaluation of a Pilot-Scale Nonthermal Plasma Advanced Oxidation Process for Organic Compound Degradation," *Water Research,* vol. 44, no. 2, pp. 493-504, January 2010.

[145] S. Lerouge, M. R. Wetheimer, R. Marchand, M. Tabrizian e L. Yahia, «Effect of Gas Composition on Spore Mortality and Etching During Low-Pressure Plasma Sterilization,» *Journal of Biomedical Materials Research,* vol. 51, n. 1, pp. 128-135, July 2000.

[146] CATC & EPA, "Using Non-Thermal Plasma to Control Air Pollutants," North Carolina, 2005.

[147] NESCAUM, "Status Report on NO_X: Control Technologies and Cost Effectiveness for Utility Boilers," June 1998. [Online]. Available: http://www.nescaum.org/documents/execsum_nox.pdf/view?searchterm=None. [Accessed 14 January 2019].

[148] BOC Process Gas Solution, "California Air Resources Board Innovative Clean Air Technology Grant ICAT 99-2," New Jersey, 2001.

[149] W. Gernjac, T. Krutzel, A. Glaser, S. Malato, J. Caceres, R. Bauer and A. R. Fernandez-Alba, "Photo-Fenton Treatment of Water Containing Natural Phenolic Pollutants," *Chemosphere,* vol. 50, no. 1, pp. 71-78, January 2003.

[150] A. M. Amat, A. Arques, F. Lopez and M. A. Miranda, "Solar Photo-Catalysis to Remove Paper Mill Wastewater Pollutants," *Solar Energy,* vol. 79, no. 4, pp. 393-401, October 2005.

[151] C. M. Sharpless and K. J. Linden, "UV Photolysis of Nitrate: Effects of Natural Organic Matter and Dissolved Inorganic Carbon and Implications for UV Water Disinfection," *Environmental Science & Techonolgy,* vol. 35, no. 14, pp. 2949-2955, 2001.

[152] M. Kito, H. Nguyen and J. Tram, "Hydrogen Peroxide & UV Treatment," in *ENVE 436 Course Project*, California, 1996.

[153] Water Research Institute, *New Concepts of UV/H_2O_2 Oxidation,* C.H.M. Hofman-Caris, E.F. Beerendonk, 2011.

[154] C. Maillard, C. Guillard and P. Pichat, "Comparative Effects of the TiO_2-UV, H_2O_2-UV, H_2O_2-Fe^{2+} Systems on the Disappearance Rate of Benzamide and 4-Hydroxybendamide in Water," *Chemosphere,* vol. 24, no. 8, pp. 1085-1094, April 1992.

[155] P. L. Yue, "Modeling of Kinetics and Reactor for Water Purification by Photooxidation," *Chemical Engineering Science,* vol. 48, no. 1, pp. 1-11, June 1993.

[156] T. Kopp, M. Kother, B. Bruckner and K. H. Radeke, "Removal of Phenol in an Aqueous Solution by Oxidation Using Ozone and Hydrogen Peroxide Under Ultraviolet Irradiation," *Chemische Technik,* vol. 45, no. 5, pp. 401-403, October 1993.

[157] F. L. Rosario-Ortiz, E. Wert and S. A. Sydney, "Evaluation of UV/H_2O_2 Treatment for the Oxidation of Pharmaceuticals in Wastewater," *Water Research,* vol. 44, no. 5, pp. 1440-1448, March 2010.

[158] F. Yuan, C. Hu, X. X. Hu, D. B. Wei, Y. Chen and J. H. Qu, "Photodegradaton and Toxicity Changes of Antibiotics in UV and UV/H_2O_2 Process," *Journal of Haxardous Material,* vol. 185, no. 2-3, pp. 1256-1263, 30 January 2011.

[159] N. De la Cruz, L. Esquius, D. Grandejean, A. Magnet, A. Tungler, L. F. De Alencastro and C. Pulgarin, "Degradation of Emergent Contaminants by UV, UV/H_2O_2 and Neutral Photo-Fenton as Pilot Scale in a Domestic Wastewater Treatment Plant," *Water Research,* vol. 45, no. 15, pp. 5839-5845, 1 October 2013.

[160] P. Van Aken, K. Van Eyck, J. Degreve, S. Liers and J. Luyten, "COD and AOX Removal and Biodegradability Assessment for Fenton and O_3/UV Oxidation Processes: A Case Study from a Graphical Industry Wastewater," *Ozone Science & Engineering,* vol. 35, no. 1, pp. 16-21, 1 January 2013.

[161] B. M. Souza, B. S. Souza, T. M. Guimaraes, T. F. S. Ribeiro, A. C. Cerqueira, G. L. Sant'Anna and M. Dezotti, “Removal of Recalcitrant Organic Matter Content in Wastewater by Means of AOPs Aiming Industrial Water Reuse,” *Environmental Science and Pollution Research,* vol. 23, no. 22, pp. 22947-22956, November 2016.

[162] N. N. Greenwood and A. Earnshaw, Chemistry of the Elements 2nd Edition, Oxford: Butterworth-Heinemann, 1997.

[163] A. Vogelpohl, “Applications of AOPs in Wastewater Treatment,” *Water Science & Technology,* vol. 55, no. 12, pp. 207-211, 2007.

[164] O. Carp, C. L. Huisman and A. Reller, “Photoinduced Reactivity of Titanium Dioxide,” *Progress in Solid State Chemistry,* vol. 32, no. 1-2, pp. 33-117, 2004.

[165] G. Raj, Organic Name Reactions and Molecular Rearrangements. Third Revised and Enlarged Edition, S. K. Rastogi for Krishna Prakashan Media (P) Ltd, 2008.

[166] H. J. H. Fenton, “Oxidation of Tartaric Acid in Presence of Iron,” *Journal of the Chemical Society,* vol. 65, pp. 899-901, 1894.

[167] P. Bigda, “Consider Fenton's Chemistry for Wastewater Treatment,” *Chemical American Photochemical Society Newsletter,* vol. 22, no. 2, pp. 62-66, December 1995.

[168] J. De Laat and H. Gallarad, “Catalytic Decomposition of Hydrogen Peroxyde by Fe(III) in Homgeneous Aqueous Solution: Mechanism and Kinetic Modeling,” *Environmental Science & Technology,* vol. 33, pp. 2726-2732, 1999.

[169] J. J. Lu, P. H. Lin, Q. Yao and C. Chen, “Chemical and Molecular Mechanisms of Antioxidants: Experimental Approaches and Model Systems,” *Journal of Cellular and Molecular Medicine,* vol. 14, no. 4, pp. 840-860, April 2010.

[170] A. J. Machulek, F. H. Quina, F. Gozzi, V. O. Silva, L. C. Frefrich and E. F. Moraes, “Fundamental Mechanistic Studies of the Photo-Fenton Reaction for the Degradation of Organic Pollutants,” in *Organic Pollutants Ten Years After the Stockholm Convention Environmental and Analytical Update,* Tomas Puzyn, 2012.

[171] E. Neyens and J. Baeyens, “A Review of Classic Fenton's Peroxidation as an Advanced Oxidation Technique,” *Journal of Hazardous Materials,* vol. 98, no. 1-3, pp. 33-50, 17 March 2003.

[172] H. R. Eisenhauer, “Oxidation of Phenolic Wastes: Oxidation whit Hydrogen Peroxide and a Ferrous Salt Reagent,” *Water Pollution Control Federation,* vol. 36, pp. 1116-1128, 1964.

[173] C. Walling and A. Goosen, “Mechanism of the Ferric Ion Catalyzed Decomposition of Hydrogen Peroxide. Effect of Organic Substrate,” *Journal of the American Chemical Society,* vol. 95, no. 9, pp. 2987-2991, May 1973.

[174] B. H. J. Bielski, D. E. Cabelli and R. L. Arudi, “Reactivity of HO_2/O_2- Radicals in Aqueous Solution,” *Journal of Physical and Chemical Reference,* vol. 14, no. 4, 1985.

[175] M. Kitis, C. D. Adams and G. T. Daigger, “The Effects of Fentons Reagent Pretratment on the Biodegradability of Nonionic Surfactants,” *Water Research,* vol. 33, no. 11, pp. 2561-2568, August 1999.

[176] J. Yoon, Y. Lee and S. Kim, “Investigation of the Reaction Pathway of OH Radicals Produced By Fenton Oxidation in the Conditions of Wastewater Treatment,” *Water Science & Technology,* vol. 44, no. 5, pp. 15-21, 2001.

[177] C. Walling and S. Kato, “The Oxidation of Alcohols by Fenton's Reagent: the Effect of Copper Ion,” *Journal of American Chemistry Society,* vol. 93, pp. 4275-4281, 1971.

[178] R. Venkatadri and R. W. Peters, “Chemical Oxidation Technologies: Ultraviolet Light/Hydrogen Peroxide, Fenton's Reagent and Titanium Dioxide-Assisted Photocatalysis,” *Hazardous Waste and Hazardous Materials,* vol. 10, pp. 107-149, 1993.

[179] H. S. Lin and C. C. Lo, “Fenton Process for Treatment of Desizing Wastewater,” *Water Reseasch,* vol. 31, no. 8, pp. 2050-2056, 1997.

[180] P. Maletzky and R. Bauer, “Immobilisaton of Iron Ionf of Nafion (R) and its Applicability to the Photo-Fenton,” *Chemosphere,* vol. 38, no. 10, pp. 2315-2352, 1999.

[181] E. E. Ebrahiem, M. N. Al-Maghrabi and A. R. Mobarki, “Removal of Organic Pollutants from Industrial Wastewater by Applying Photo-Fenton Oxidation Technology,” *Arabian Journal of Chemistry,* vol. 10, pp. S1674-S1679, 2017.

[182] D. A. D. A. Aljuboury, P. Palaniandy, H. B. A. Aziz, H. B. Abdul and S. Ferroz, “Degradation of Total Organic Carbon (TOC) and Chemical Oxygn Demand (COD)

in Petroleum Wastewater by Solar Photo-Fenton," *Global Nest Journal*, vol. 19, no. 3, pp. 430-438, November 2017.

[183] K. Zhao, X. Quan, S. Chen, H. T. Yu, Y. B. Zhang and H. M. Zhao, "Enhanced Electro-Fenton Performance by Fluorine-Dopes Popous Carbon for Removal Organic Pollutants in Wastewater," *Chemical Engineering Journal*, vol. 354, pp. 606-615, 15 December 2018.

[184] H. G. Kim, Y. J. Ko, S. Lee, S. W. Hong, W. S. Lee and J. W. Choi, "Degradation of Organic Compounds in Actual Wastewater by Electro-Fenton Process and Evalutation of Energy Consumption," *Water Air and Soil Pollution,* vol. 229, no. 10, p. 335, October 2018.

[185] E. Chamarro, A. Marco and S. Esplugas, "Use of Fenton Reagent to Improve Organic Chemical Biodegradability," *Water Research,* vol. 35, no. 4, pp. 1047-1051, 2001.

[186] T. L. Brown, H. E. Le May Jr, B. E. Bursten, C. Murphy, P. Woodward, S. Langfrd, D. Sagatys and A. George, Chemistry: The Central Science, Pearson Higher Education, 2013.

[187] H. J. Benkelberg and P. Warneck, "Photodecomposition of Iron(III) Hydroxo and Sulfate Complexes in Aqueous Solution: Wavelenght Dependence of OH an SO_4^- Quantum Yelds," *Journal of Physical Chemistry,* vol. 99, no. 14, pp. 5214-5221, 1995.

[188] Y. Lee, J. Jeong, C. Lee, S. Kim and J. Yoon, "Influence of Various Reaction Parameters on 2,4-D Removal in Photo/Ferroxilate/H_2O_2 Process.," *Chemosphere,* vol. 51, no. 9, pp. 901-912, 2003.

[189] B. Morgan and O. Lahav, "The Effect of pH on the Kinetics of Spontaneous Fe(II) Oby O_2 in Aqueous Solution – Basic Principles and a Simple Heuristic Description," *Chemosphere,* vol. 68, pp. 2080-2084, November 2006.

[190] E. Lipczynska-Kochany, "Degradation of Aqueous Nitrophenols and Nitrobenzene by Means of the Fenton Reaction," *Chemosphere,* vol. 22, no. 5-6, pp. 529-536, 1991.

[191] M. G. Alam and A. Tawfik, "Fenton and Solar Photo-Fenton Oxidation of Industrial Wastewater Containing Pesticides," in *Seventeenth International Water Technology Conference*, Instanbul, 2013.

[192] E. Brillas, I. Sirés and M. A. Oturan, “Electro-Fenton Process and Related Electrochemical Technologies Based on Fenton's Reaction Chemistry,” *International Journal of Advanced Research in Engineering, Science & Management,* vol. 109, pp. 6570-6631, 2009.

[193] J. J. Aaron and M. A. Oturan, “New Photochemical and Electrochemical Methods for the Degradation of Pesticides in Aqueous Media. Envitonmental Application,” *Turkish Journal of Chemistry,* vol. 25, no. 4, pp. 209-520, 2001.

[194] P. C. Foller and R. T. Bombard, “Processes for the Production of Mixture of Caustic Soda and Hydrogen Peroxide Via the Reduction of Oxygen,” *Journal of Applied Electrochemistry,* vol. 25, no. 7, pp. 613-627, July 1995.

[195] M. Panizza, P. A. Michaud, G. Cerisola and C. Comninellis, “Anodic Oxidation of 2-Naphthol at Boron-Doped Diamond Electrodes,” *Journal of Electroanalytical Chemistry,* vol. 507, no. 1-2, pp. 206-214, July 2001.

[196] P. V. Nidhees and R. Gandhimathi, “Trends in Electro-Fenton Process for Water and Wastewater Treatment: An Overview,” *Desalination,* pp. 1-15, 1 August 2012.

[197] A. G. Vlyssides, P. K. Karlis and A. A. Zorpas, “Electrochemical Oxidation of Noncyanide Strippers Wastes,” *Environment International,* vol. 25, no. 5, pp. 663-670, July 1999.

[198] D. Arapoglou, A. Vlyssides, C. Israilides, A. Zorpas and P. Karlis, “Detoxification of Methyl-Parathion Pesticide in Aqueous Solutions by Electrochemical Oxidation,” *Journal of Hazardous Materials,* vol. 98, no. 1-3, pp. 191-199, 17 March 2003.

[199] N. Daneshvar, A. Oladegaragoze and N. Djafarzadeh, “Decolorization of Basic Dye Solutions by Electrocoagulation: An Investigation on the Effect of Operational Prameters,” *Journal of Hazardous Materials,* vol. 129, no. 1-3, pp. 116-122, 28 February 2006.

[200] Y. Yavuz and A. S. Koparal, “Electrochemical Oxidation of Phenol in a Parallel Plate Reactor Using Rutheium Mixed Metal Oxide Electrode,” *Journal of Hazardous Materials,* vol. 136, no. 2, pp. 296-302, 21 August 2006.

[201] U. Kurt, O. Apaydin and M. T. Gonullu, “Reduction of COD in Wastewater from a Organized Tannery Industrial Region by Electro-Fenton Process,” *Journal of Hazardous Material,* vol. 143, pp. 33-40, 2007.

[202] T. J. Mason and J. P. Lorimer, “An Introduction to Sonochemistry,” *Endeavour*, vol. 13, no. 3, pp. 123-128, 1989.

[203] A. Adityosulindro, L. Barthe, U. Haza, K. Gonzales-Labrada, H. Delmas and C. Julcour, “Sonolysis and Sono-Fenton Oxidation for Removal of Ibuprofen in (Waste)Water,” *Ultrasonic Chemistry,* vol. 39, pp. 889-896, 2017.

[204] J. L. Wang and L. J. Xu, “Advanced Oxidation Processes for Wastewater Treatment: Formation of Hydroxil Radical and Application,” *Environmental Science & Technology,* vol. 42, pp. 251-325, 2012.

[205] Y. T. Shah, A. B. Pandit and V. S. Moholkar, Cavitation Reaction Engineering, New York: Plenum Press/Kluwer Academic, 1999.

[206] B. D. Storey and A. J. Szeri, “Water Vapor, Sonoluminescence and Sonochemistry,” *Proceeding of the Royal Society A*, vol. 456, pp. 1685-1709, 2000.

[207] E. Hart and A. Henglein, “Sonochemistry of Aqeuous Solutions: Hydrogen-Oxygen Combustion in Cavitation Bubbles,” *Journal of Physical Chemistry,* vol. 91, pp. 3654-3656, 1987.

[208] J. Liang, S. H. N. Komarov and E. Kasai, “Improvement in Sonochemical Degradation of 4-Chlorophenol by Combined Use of Fenton-Like Reagents,” *Ultrasonics Sonochemistry,* vol. 14, no. 2, pp. 201-207, February 2007.

[209] J. Lin and Y. Ma, “Oxidation of 2-Chlorophenol in Water by Ultrasound/Fenton Method,” *Journal of Environmental Engineering,* vol. 126, no. 2, pp. 130-137, February 2000.

[210] M. V. Bagal and P. R. Gogate, “Wastewater Treatment Using Hybrid Treatment Schemes Based on Cavitation and Fenton Chemistry: A Review,” *Ultrasonics Sonochemistry,* vol. 21, no. 1, pp. 1-14, January 2014.

[211] M. Siddigue, R. Faroog and G. J. Price, “Synergistic Effects of Comining Ultrasound With the Fenton Process in the Degradation of Reactive Blue 19,” *Ultrasonics Sonochemistry,* vol. 21, no. 3, pp. 1206-1212, May 2014.

[212] G. Cruz-Gonzales, K. Gonzalez-Labrada, Y. Milian-Rodriguez, I. Quesada-Penate, J. A. Colin-Luna, J. Ramirez-Munoz and U. J. Jauregui-Haza, “Enhancement of Paracetamol Degradation by Sono-Fenton Process,” *International Journal of Chemical, Material and Environmental Research,* vol. 2, no. 4, pp. 37-45, 2015.

[213] M. P. Rayaroth, U. K. Aravind and C. T. Aravindakumar, “Deradation of Pharmaceuticals by Ultrasound-Based Advanced Oxidation Process,” *Environmental Chemistry Letters,* vol. 14, no. 3, pp. 259-290, September 2016.

[214] J. J. Pignatello, D. Liu e P. Huston, «Evidence for an Additional Oxidant in the Photoassisted Fenton Reaction,» *Environmental Science & Technology,* vol. 33, n. 11, pp. 1832-1839, 1999.

[215] J. J. Pignatello, E. Oliveros and A. Mackay, “Advanced Oxidation Processes for Organic Contaminant Destruction Based on the Fenton Reaction and Related Chemistry,” *Critical Reviews in Environmental Science & Technology,* vol. 36, no. 1, pp. 1-84, 2006.

[216] J. P. Hunt and H. Taube, “The Photochemical Decomposition of Hydrogen Peroxide. Quantum, Yelds, Tracer and Fractionation Effects,” *Journal of the American Chemical Society,* vol. 74, pp. 5999-6002, 5 December 1952.

[217] I. N. Martyanov, E. N. Savinov and V. N. Parmon, “A Comparative Study of Efficency of Photooxidation of Organic Contaminants in Water Solution in Various Photochemical and Photocatalytic Systems. 1. Phenol Photooxidation Promoted by Hydrogen Peroxide in a Flow Reactor,” *Journal of Photochemistry and Photobiology A: Chemistry,* vol. 107, pp. 227-231, 1997.

[218] M. Perez, F. Torrades, J. A. Garcia-Hortal, X. Domenech and J. Peral, “Removal of Organic Contaminants in Paper Pulp Treatment Effluents Under Fenton and Photo-Fenton Conditions,” *Applyed Catalysis B: Environmental,* vol. 36, pp. 63-74, 2002.

[219] S. M. Kim and A. Vogelpohl, “Degradation of Organic Pollutants by the Photo-Fenton Process,” *Chemical Engineering Technology,* vol. 21, no. 2, pp. 187-191, 1998.

[220] A. Duran, J. M. Monteagudo and I. S. Martin, “Operation Costs of the Solar Photo-Catalytic Degradation of Pharmaceuticals in Water: A Mini-Review,” *Chemosphere,* vol. 211, pp. 482-488, November 2018.

[221] J. J. Pignatello, “Dark and Photoassisted Fe3+-Catalyzed Degradation of Chlorophenoxy Herbicides by Hydrogen Peroxide,” *Environmental Science & Technology,* vol. 26, pp. 944-951, 1992.

[222] J. Kiwi, A. Lopez and V. Nadtochenko, “Mechanism and Kinetics of the OH-Radical Intervention During Fenton Oxidation in Presence of a Significant Amount of

Radical Scavenger," *Environmental Science & Technology,* vol. 34, no. 11, pp. 2162-2168, 2000.

[223] J. E. F. Moraes, F. H. Quina, C. A. O. Nascimiento, D. N. Silva and O. Chiavone-Filho, "Treatment of Saline Wastewater Contaminated with Hydrocarbons by the Photo-Fenton Process," *Environmental Science & Technology,* vol. 38, no. 4, pp. 1183-1187, 2004.

[224] J. De Laat and T. G. Le, "Effects of Chloride Ions on the Iron(III)-Catalyzed Decomposition of Hydrogen Peroxide and on the Efficiency of the Fenton-Like Oxidation Process," *Applied Catalysis B: Envronmental,* vol. 66, no. 1-2, pp. 137-146, June 2006.

[225] W. Gernjac, T. Krutzel, A. Glaser, S. Malato, J. Caceres, R. Bauer and A. R. Fernandez-Alba, "Photo-Fenton Treatment of Water Containing Natural Phenolic Pollutants," *Chemosphere,* vol. 50, no. 1, pp. 71-78, January 2003.

[226] A. M. Amat, A. Arques, F. Lopez and M. A. Miranda, "Solar Photo-Catalysis to Remove Paper Mill Wastewater Pollutants," *Solar Energy,* vol. 79, no. 4, pp. 393-401, October 2005.

[227] A. M. Braun, L. Jacob and E. Oliveros, "Up-Scaling Photochemical Reactions," in *Advances in Photochemistry,* vol. 36, Jhon Wiley & Sons, 2009.

[228] M. Anpo, "Utilisation of TiO_2 Photocatalysts in Green Chemistry," *Pure and Applied Chemistry,* vol. 72, no. 7, pp. 1265-1270, 2000.

[229] W. J. Lough and I. W. Wainer, High Performance Liquid Chromatography: Fundamental Principles and Practice, Blackie Acedemic & Professional, 1995.

[230] S. Lindsay and J. Barnes, High Performance Liquid Chormatography, John Wiley & Sons, 1992.

[231] J. Ritter, Water Quality. Principles and Practices of Water Supply Operation, American Water Works Association, 2003.

[232] C. E. Boyd, Quality Water: An Introduction, Springer Science+Business Media, New York, 2000.

[233] A. W. W. A. W. E. F. American Public Health Association, «Standard Methods for the Examination of Water and Wastewater,» 1999.

[234] A. Hazen, «The Measurement of the Colors in Natural Waters,» *Journal of the American Chemical Society,* 1896.

[235] A. Bricaud, A. Morel and L. Preour, “Absorption by Dissolved Organic Matter of the Sea (Yellow Substance) in the UV and Visible Domanis,” *Limnology and Oceanography*, vol. 26, no. 1, pp. 43-53, 1981.

[236] M. G. Gore, Spectrophotometry and Spectrofluometry: a Practical Approach, Oxford University Press, 2000.

[237] ISO 2211, *Liquid Chemical products — Measurement of Colour in Hazen Units (Platinum-Cobalt Scale),* 1973.

[238] Swedish University of Agricolutural Science, “Absorbance, ABS420/5,” 4 Semptember 2018. [Online]. Available: https://www.slu.se/en/departments/aquatic-sciences-assessment/laboratories/vattenlabb2/detaljerade-metodbeskrivningar/absorbance-abs4205/.

[239] G. M. Badger, The Structure & Reaction of the Aromatic Compounds, Cambridge: 1954, 1954.

[240] G. M. Badger, Aromatic Character and Aromaticity, Cambridge: Cambridge University Press, 1969.

[241] G. Korshing, C. W. Chow, R. Fabris and M. Drikas, “Absorbance Spectroscopy-Based Examination of Effects of Coagulation on the Reactivity of Fractions of Natural Organic Matter with Varying Apparent Molecular Weight,” *Water Researh,* vol. 43, no. 6, pp. 1541-1548, April 2009.

[242] T. Atomssa and A. V. Gholap, “Characterization of Caffeine and Determination of Caffeine in Tea Leaves Using UV-Visible Spectrometer,” *Africal Journal of Pure and Applied Chemistry*, vol. 5, no. 1, pp. 1-8, January 2011.

[243] J. W. Moore and R. G. Pearson, Kinetics and Mechanism, Jhon Wiley & Sons, 1981.

[244] W. G. Zijlstra, A. Buursma e O. W. van Assendelft, Visible and Near Infrared Absorpion Spectra of Human and Animal Haemoglobin. Determination and Application, VSP, 2000.

[245] M. J. Frisch, G. W. Trucks, H. B. Schlegel, G. E. Scuseria, M. A. Robb, J. R. Cheeseman, G. Scalmani, V. Barone, B. Mennucci and G. A. Petersson, *Gaussian 09, Revision A.02,* Wallingford CT: Gaussian Inc., 2009.

[246] A. D. Becke, “Density Functional Thermochemistry III. The Role of Exact Exchange,” *Journal of Chemical Physics,* vol. 89, no. 5648, pp. 1-5, 1993.

[247] R. E. Stratmann, G. E. Scuseria and M. J. Frisch, “An Efficient Implementation of Time-Dependent Density-Functional Theory for the Calculation of Excitation Energies of Large Molecules,” *Journal of Chemical Physics,* vol. 109, pp. 8218-8224, 1998.

[248] J. Tomasi, B. Mennuci and R. Cammi, “Quantum Mechanical Continuum Solvation Models,” *Chemical Reviews,* vol. 105, pp. 2999-3094, 2005.

[249] N. Lazaroff, W. Sigal e A. Wasserman, «Iron Oxidation and Precipitation of Ferric Hydroxilsulfates by Resisting Thiobacillur Ferrooxidans Cells,» *Applied and Environmental Microbiology,* pp. 942-938, April 1982.

[250] S. Inagaki, Orbitals in Chemistry, Springer Science & Business Media, 2009.

[251] T. L. Gilchrist and R. C. Storr, Organic Reactions and Orbital Symmetry, CUP Archive, 1979.

[252] Varian Inc, “Advantage Note Number 6 - Varian Cary 50 UV Vis,” November 2006. [Online]. Available: http://photos.labwrench.com/equipmentManuals/1052-1504.pdf. [Accessed 26 February 2019].